Max Planck Graduate Center
mit der Johannes Gutenberg-Universität Mainz

JG|U

Folding and assembly of the major light-harvesting chlorophyll protein (LHCII) of the photosynthetic apparatus in plants: The chlorophyll a - containing intermediate

Dissertation

zur Erlangung des Grades

"Doktor der Naturwissenschaften"

an der Johannes Gutenberg-Universität Mainz

von

Lei Jiang

Aus Hubei, China

Mainz, 2015

Table of Contents

1. Introduction

1.1. Photosythesis

Photosynthesis is the physico-chemical process by which plants, algae and photosynthetic bacteria use light energy to drive the synthesis of organic compounds. In plants, algae and certain types of bacteria, the photosynthetic process results in the release of molecular oxygen and the removal of carbon dioxide from the atmosphere that is used to synthesize carbohydrates (oxygenic photosynthesis). Other types of bacteria use light energy to create organic compounds but do not produce oxygen (anoxygenic photosynthesis). The overall equation for photosynthesis is deceptively simple:

$$6CO_2 + 6H_2O \xrightarrow{\text{light}} C_6H_{12}O_6 + 6O_2 \quad (1)$$

In fact, a complex set of physical and chemical reactions must occur in a coordinated manner for the synthesis of carbohydrates. To produce a sugar molecule such as sucrose, plants require nearly 30 distinct proteins that work within a complicated membrane structure (Whitmarsh et al, 1999).

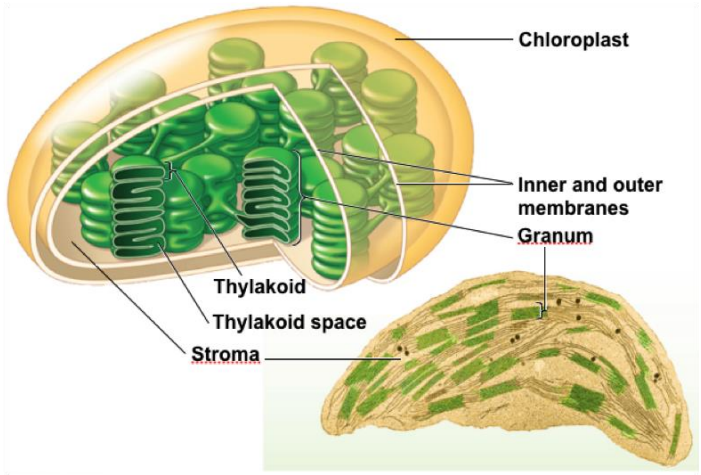

Fig.1.1. Structure of chloroplast. Figure cited from www.studyblue.com/notes/note/n/exsc-223-study-guide-2011-12-thompson/deck/9733919

The photosynthetic process in plants and algae occurs in small organelles known as chloroplasts (Fig.1.1) that are located inside cells. The photosynthetic reactions are traditionally divided into two stages - the "light reactions," which absorbs the light energy to produce organic energy molecules (ATP

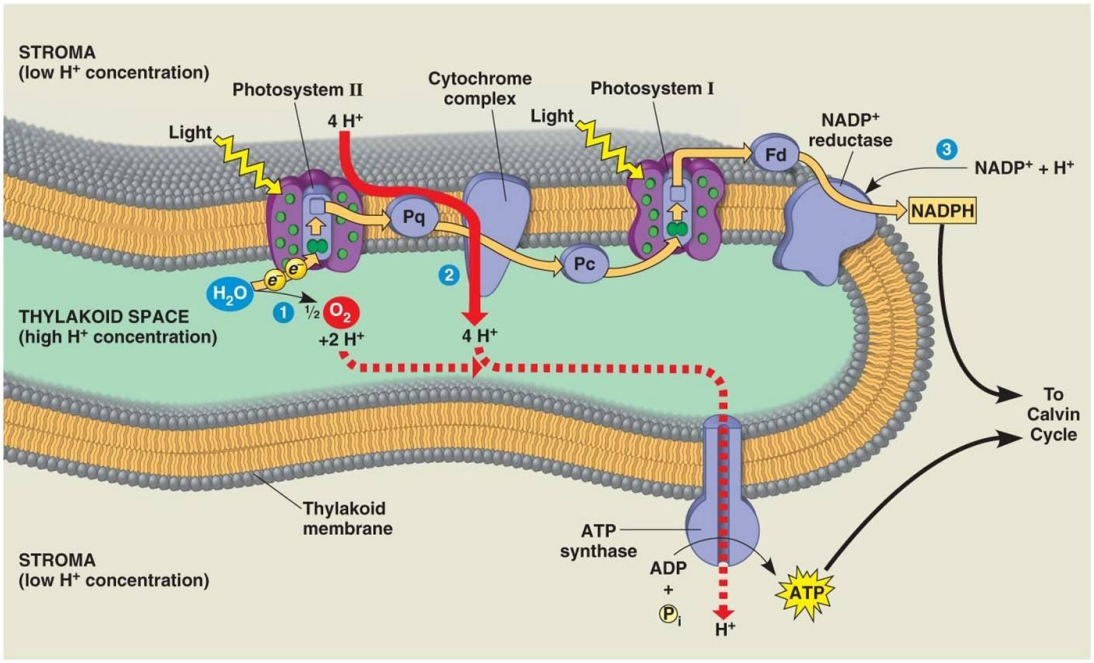

Fig.1.2. Light reaction and structure of thylakoid membrane consisting of photosynthetic apparatus.

Figure cited from http://galleryhip.com/thylakoid-membrane-structure.html

and NADPH) and the "dark reactions," which uses ATP and NADPH generated from the light reaction to fix carbon dioxide (CO_2) into carbohydrates. The light reactions occur in a complex membrane system (thylakoid membrane) that is made up of protein complexes, electron carriers, and lipid molecules. In membranes, the lipid molecules arrange themselves in a bilayer, with the polar head toward the water phase and the fatty acid chains aligned inside the membrane forming a hydrophobic core. The protein complexes embedded in the thylakoid membrane have a unique orientation with respect to the inner and outer space, the asymmetrical arrangement of protein complexes allows some of the energy released of during electron transport to create an electrochemical gradient of proton across the thylakoid membrane (Fig.1.2) (Agarwal, 2005).

Photosynthesis is initiated by the absorption of photons by the antenna complexes of photosystem II (PS II). Light, primarily visible light (wavelengths from 400 to 700 nm), is collected by 200-300 pigment molecules of chlorophyll a (Chl *a*) and b (Chl *b*) and carotenoids) that are bound to light-harvesting protein complexes (LHCII) located in the thylakoid membrane. These light-harvesting complexes which surround the reaction centers serve as an antenna and transfer energy to the reaction center. PS II then uses light energy to drive two chemical reactions -- the oxidation of water and the reduction of plastoquinone (Raghavendra, 1998). PS II is large multisubunit chlorophyll (Chl)-protein complex that consists of more than

30 proteins. At the center of this complex is the reaction center, which is composed of a D1/D2 heterodimer and a few intrinsic low molecular weight polypeptides, such as Cyt b559 and PsbI, PsbT and PsbW (Minagawa et al, 2004). Surrounding reaction center are other subunits to form the "core" complex, which includes the core antenna composed of Chl *a*-binding proteins, CP43 and CP47, which mediate excitation energy to reaction center, and several chlorophyll *a/b*-binding proteins, of which the most abundant is the LHCII (Boekema et al, 1995).

1.2. LHCII

The major LHCII protein is one of the most abundant membrane proteins on Earth, accounting for roughly 30% of all proteins in plant thylakoid membranes. It binds about half of the total Chls in chloroplasts (Peter et al, 1991). The complex was discovered by Philip Thornber in 1965 (Thornber, 1995). The major antenna complex, LHCII, is organized in heterotrimers composed of the products of the *Lhcb1-3* genes (Caffarri et al, 2004) and various pigment molecules (Kouřil et al, 2012).

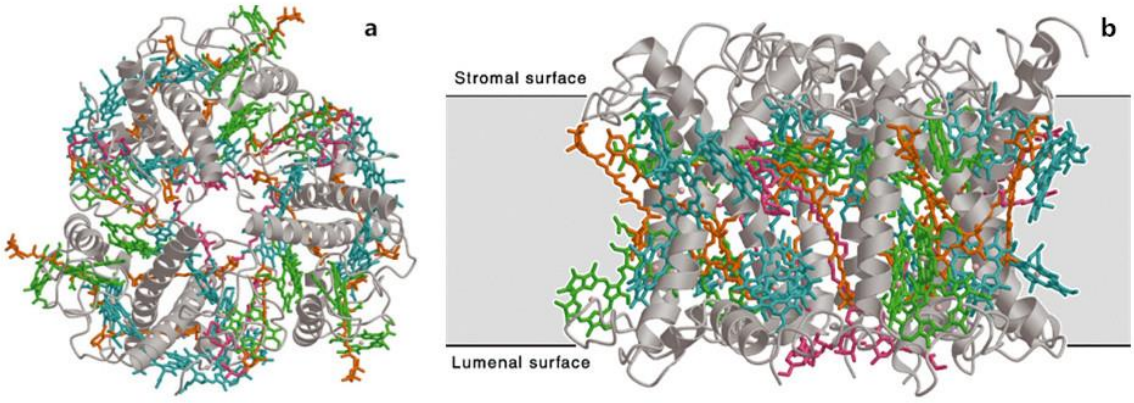

Fig.1.3. Three dimensional structure of pea LHCII trimer a) top view from stromal side; b) side view. LHCII protrudes from a 35 Å lipid bilayer (black lines) by 13 Å on the stromal side and by 8 Å on the lumenal side. Grey, polypeptide; cyan, Chl *a*; green, Chl *b*; orange, carotenoids; pink, lipids. Figure revised by Standfuss (2005).

1.2.1 Molecular structure of LHCII

In 1994, an initial structure of pea LHCII was obtained at 3.4 Å resolution from electron diffraction of two-dimensional (2-D) crystals by Kühlbrandt and coworkers (Kühlbrandt et al, 1994). This provided a general description of LHCII, which contains three transmembrane *a*-helices and a short amphipathic helix, as well as several pigment binding sites. In 2004, the first X-ray structure of LHCII was reported and a three-dimensional (3-D) structure of spinach LHCII was obtained at 2.7 Å resolution (Liu et al, 2004). The 2.5 Å structure of pea LHCII, which was determined by X−ray crystallography by Kühlbrandt's group (Standfuss et al, 2005) and had 94% of the 232 amino acids resolved, shows how membranes interact to form chloroplast grana, and revealed the mutual arrangement of 42 chlorophylls *a* and *b*, 12 carotenoids and six lipids in the LHCII trimer (Fig.1.3). The secondary structure model of spinach LHCII is similar to the electron crystallographic model of LHCII from pea. Apart from three transmembrane helices which were already complete in 3.4 Å electron microscopy (EM) structure, two short amphipathic helices on the lumenal side (helices 2 (H2) and 5 (H5)), linking helix 1(H1) to helix 3 (H3) and helix 4 (H4) to the C-terminus, were resolved. The two central H 1 and H 4 are interlocked by a symmetrical pair of salt bridges, making this part of the complex particularly rigid. Both crystal structures from Liu and Standfuss revealed that these 14 Chls in each monomer can be unambiguously distinguished as 8 Chl *a* and 6 Chl *b* molecules. Assignment of the orientation of the transition dipole moment of each Chl has been achieved; most Chl *a* molecules are bound to the intertwined transmembrane helices H1 and H4. Five Chl *a* and three Chl *b* molecules are found in the stromal layer; the other three Chl *a* and three Chl *b* are located in the lumenal layer. The center-to-center distances between neighboring Chls fall within a narrow range of 10 Å to 13 Å. In the LHCII trimer, the 6 Chl *b* molecules (Chls 9 to 14) form a cluster around the neoxanthin (Neo) binding pocket near the monomer interface (Fig.1.4). The resulting Chl *a/b* molar ratio of 1.33 is consistent with the value determined by earlier biochemical analyses (Ruban et al, 1999). The pair of lutein (lut) molecules occupies a central location in the interior of the LHCII monomer, forms a network, and supports the

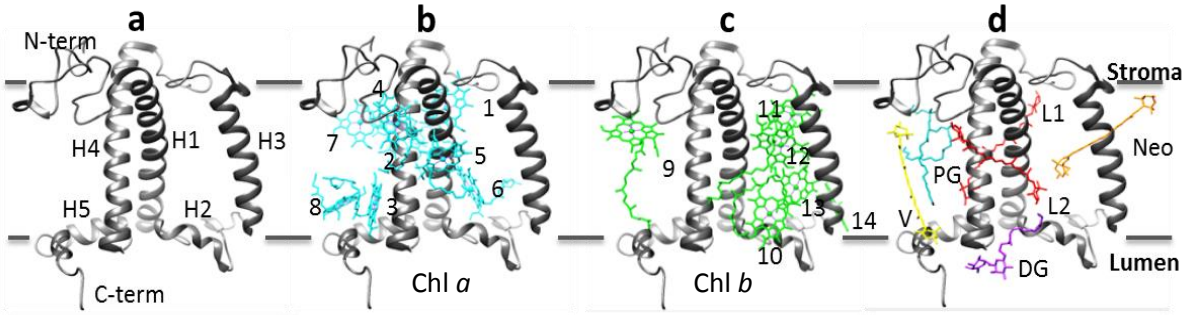

Fig.1.4. Side view of the LHCII monomeric structure. a) Three transmembrane α-helices (H1, H3, H4) and the amphipathic helices H1 and H3 (H2), H4 and the C-terminus (H5); b) 8 Chl *a* bindings; c) 6 Chl *b* bindings; d) 4 carotenoids and lipids bindings. Figure was constructed with pdb viewer (entry 2BHW; Standfuss, 2005). Dark grey: polypeptides; cyan: Chl *a*; green: Chl *b*; red: lutein; orange: neoxanthin; yellow: violaxanthin; blue: PG; purple: DGDG.

linkage between H1 and H4 (Barros et al, 2009). Neo in LHCII is present almost exclusively as the 9′-*cis* stereoisomer, whereas the other three bound carotenoids are in the all-trans conformation. (Takaichi et al, 1998). The location of violaxanthin at the monomer-monomer interface would make it easy to exchange this carotenoid for zeaxanthin in the xanthophyll cycle (Yamamoto et al, 1962 and 1985)

In addition to the polypeptide and pigments, two different lipids complete the LHCII structure. Phosphatidyl glycerol (PG) is involved in the formation of trimer, and cannot be removed by non-ionic detergent treatment (Trémolières et al, 1981). Digalactosyl diacyl glycerol (DGDG), one the other hand, presumably binds at the periphery of the trimers to maintain the structural integrity of the complex and to facilitate crystal formation (Nussberger et al, 1993).

1.2.2 Functions and regulation processes of LHCII

The primary function of LHCII is to make the photosynthetic process in green plants more effective by absorbing solar photons and delivering their excitation energy to the reaction center. The energy stores in electronic excited states of the chromophores (Scholes et al, 2005). At temperatures near room temperature the fastest Chl *b* to Chl *a* transfer seems to occur with a lifetime of approximately 150−200 femtosecond (fs). Further components have life times of approximately 500−600 fs and 5−7 picoseconds (ps). Energy transfer among the Chl *a*

molecules occurs on a timescale of typically 1 ps and longer (Connelly et al, 1997; Trinkunas et al, 1997; Kleima et al, 1997; Gradinaru et al, 1998; Visser et al, 1996). The energy transfer between pigments is not slow redox processes but excitonic energy transfer (Linnanto et al, 2006). The arrangement of the chromophores enables a perfect energy transfer from the light harvesting antennas to the core complexes.

Besides the major role of harvesting light, LHCII also has three other important functions, one in the regulation of thylakoid membrane structure, i.e., grana stacking, another one in the

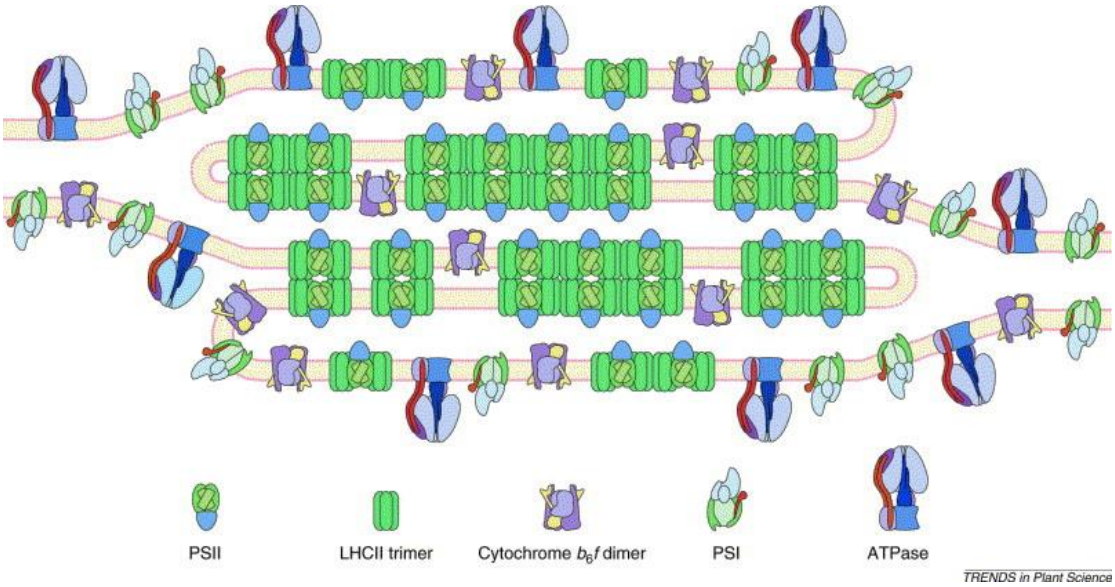

Fig.1.5. Structure of thylakoid membrane. Figure revised by Allen and Forsberg (2001)

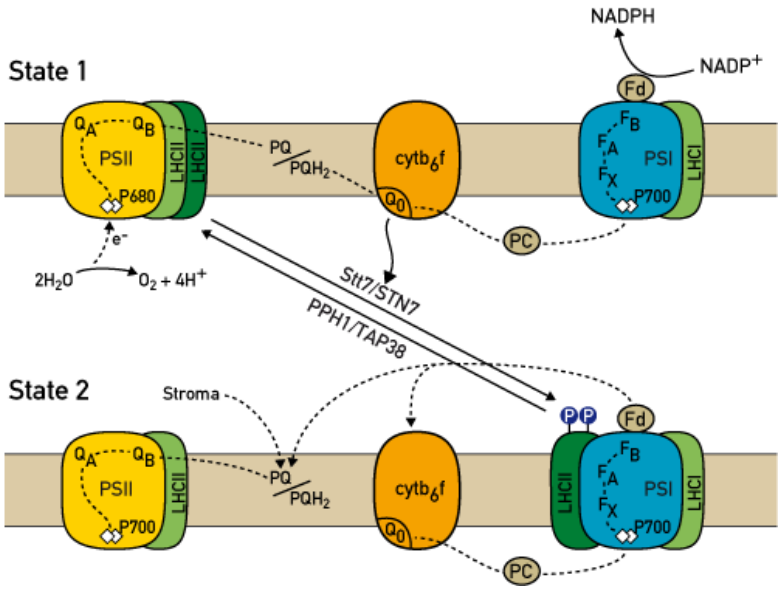

Fig.1.6. Scheme of state transition. Figure revised by Rochaix (2011)

regulation of the distribution of excitation energy between the two photosystems, and the third one involving in dissipation of excess excitation energy by non-photochemical quenching (NPQ). LHCII is apparently essential for grana stacking. In the

developing chloroplasts, the formation of grana stacks directly coincides with the appearance of LHCII (Fig.1.5). Studies on Chl *b*-deficient mutant from Arabidopsis (Murray et al, 1990) showed that not only LHCII level was highly reduced in the absence of Chl *b* but also less stacked thylakoid membranes existed in the deficient mutant. It is thought that thylakoid membrane appression is maintained primarily by the balance of van der Waals' attractive interactions between the many Chl *a/b*-proteins which surround PS II core complexes and, to a lesser extent, by the screening of repulsive negative charges by positive-charged cations (Chow et. al, 1991; Anderson et. al, 1994, Daum et. al, 2010). The Kühlbrandt group suggested that the positive and negative charges on the stromal membrane surface of LHCII trimers showed a 'velcro'-like, nonspecific interaction and this interaction is likely to play a major role in the cohesion of thylakoid grana (Standfuss, et al. 2005).

In oxygen-evolving photosynthesis, the two photosystems--PS I and PS II--function in parallel, and their excitation levels must be balanced to maintain an optimal photosynthetic rate under natural light conditions. State transitions in photosynthetic organisms balance the absorbed light energy between the two photosystems by relocating light-harvesting complex II proteins (Minagawa, 2011) (Fig.1.6). It has been demonstrated that state transition is a long-term acclimation to various natural light conditions in higher plants and that a part of LHCII is phosphorylated and behaves as an effective PS I antenna. State transition is triggered by changes in the redox state of the plastoquinone (PQ) pool. Reduction of PQ activates LHCII phosphorylation, which initiates the subsequent migration of LHCII to PS I (state 1 to state 2 transition). Thus, various environmental stressors in higher plants, including heat stress, tend to affect state transition through a change in energy distribution between the photosystems. Moderate heat stress induces increased energy transfer to PS I at the expense of PS II and migration of phosphorylated LHCII from grana stack to stroma lamellae, suggesting a state 1 to state 2 transition, with LHCIIs migrating from PS II to PS I (Wientjes et. al, 2013; Nellaepalli et. al, 2011; Ducruet et. al 2007; Mohanty et. al 2002).

Besides adjusting light absorption, algae and plants have ways of getting rid of excess light energy that has already been absorbed. Regulation of light harvesting to balance the absorption and utilization of light energy will focus on protective non-photochemical mechanisms that

quench singlet-excited Chl and harmlessly dissipate excess excitation energy as heat. These NPQ processes occur in almost all photosynthetic eukaryotes, and they help to regulate and protect photosynthesis in environments in which light energy absorption exceeds the capacity for light utilization (Müller et. al, 2001; Horton et. al (1991; 2005)) proposed that in excess light the decrease in the thylakoid lumen pH causes an increase in aggregation of LHCII resulting in formation of an efficient pathway for non-radiative dissipation of excitation energy.

Xanthophylls in LHCII also play an important role in protecting photosynthetic apparatus against high light condition. When Chl absorbs light, it is excited from its ground state to its singlet excited state, ^{1}Chl*. From there it can relax back to ground state via fluorescence, photochemistry or NPQ. ^{1}Chl* can also, by intersystem crossing, produce triplet excited state ^{3}Chl*, which in turn is able to produce singlet oxygen $^1O_2$*, a very reactive oxygen species, which is very harmful to photosynthetic apparatus. Efficient quenching of ^{3}Chl by carotenoids has been proven in studies on isolated and recombinant LHCII (Dall'Osto et al, 2006; Peterman et al, 1995 and 1997; Mozzo et al, 2008) and minor PSII antenna complexes (Mozzo et al, 2008). These latter studies confirmed that efficient ^{3}Chl quenching is related to the action of Lutein (Lut) at binding sites L1 and L2, and that Violaxanthin (Vx) and Neoxanthin (Nx) are much less efficient or not involved in these processes. Replacement of Lut at L1 and/or at L2 by Vx resulted in less efficient ^{3}Chl quenching (Dall'Osto et al, 2006), strongly increased photoinhibition (*i.e.* long-lasting depression of the PSII efficiency) and degradation of LHCII under light stress (Kalituho et al, 2007) underlining the important specific role of Lut in photoprotection *via* ^{3}Chl quenching (Jahns and Holzwarth, 2012). Niyogi (Niyogi, et al. 1998) has proved that xanthophyll pigments in the LHCs also appeared to have a critical role in NPQ. The extent of NPQ in plants is strongly correlated with the levels of zeaxanthin and antheraxanthin that are formed from violaxanthin *via* the xanthophyll cycle.

1.2.3. LHCII biogenesis

The LHC apoproteins are the products of the Lhc super-gene family, which comprises at least 30 homologous genes in Arabidopsis (Jansson, 1999). The family contains not only the three main polypeptide components of the major LHCII, Lhcb1, Lhcb2 and Lhcb3, but also the so-called "minor" antenna complexes of photosystem II, referred to as CP24, CP26 and CP29 (Camm & Green, 2004), which originate from the gene products Lhcb6, Lhcb5 and Lhcb4, respectively (Jansson et al, 1992). Other members are the antenna complexes of PS I Lhca1, Lhca2, Lhca3 and Lhca4 and the related and more recently identified Lhca5 and Lhca6 (Jansson, 1999), as well as photoprotective stress-response proteins (Meyer et al, 1984; Adamska, 1997) and the PsbS protein (Wedel et al, 1992; Kim et al, 1992).

LHCII is nuclear-encoded protein (Kung et. al, 1972). The LHCII cDNA was first isolated (Broglie et. al, 1981) and sequenced (Coruzzi et. al, 1983) in the early 1980s by Cashmore (Cashmore, 1984). Native LHCII isolated from plant tissue consists of three isoforms, Lhcb1, Lhcb2 and Lhcb3 in a ratio of about 8:3:1 (Jansson, 1994). The amino acid sequences of all three isoforms are highly conservative in different species, with more than 75% similarity for the same isoform (Zhang et. al, 2008). Lhcb1 and Lhcb2 are very similar in polypeptide sequence and pigment content, while Lhcb3 is different from the other two, as it lacks an N-terminal phosphorylation site and has a higher chlorophyll *a/b* ratio, suggesting the absence of one Chl *b* (Standfuss et. al, 2004).

The LHCII apoprotein, light harvesting *a/b* binding protein (LHCP), is considered being transported and inserting into thylakoid membrane via SRP-mediated protein delivery (High et. al, 1997) (Fig.1.7). LHCP is synthesized in the cytosol and the protein is post-translationally targeted to the chloroplast envelope (CE) through an amino-terminal transit peptide (TP), forming an Lhcb precursor (pLhcb). pLhcb passes through the chloroplast outer and inner envelope via the TOC/TIC import machinery (Soll et. al, 2004; Kessler et. al.,2009). TP-cleaved, mature LHCP forms a delivery complex with the chloroplast signal recognition particle (cpSRP) through the binding of the polypeptide to both cpSRP54 and cpSRP43 subunits (Stengel et. al, 2008). cpSRP-LHCP transit complex then binds to the membrane and

forms a four-subunit complex with cpFtsY. With both cpFtsY and cpSRP54 in the GTP-bound state, this large complex slides along the membrane until it reaches an open translocase containing ALB3 and/or possibly unknown components. The substrate is released for integration, and GTP is hydrolyzed to release cpSRP and cpFtsY for further rounds of targeting (Pool, 2005; Schünemann, 2004; Moore et. al., 2003).

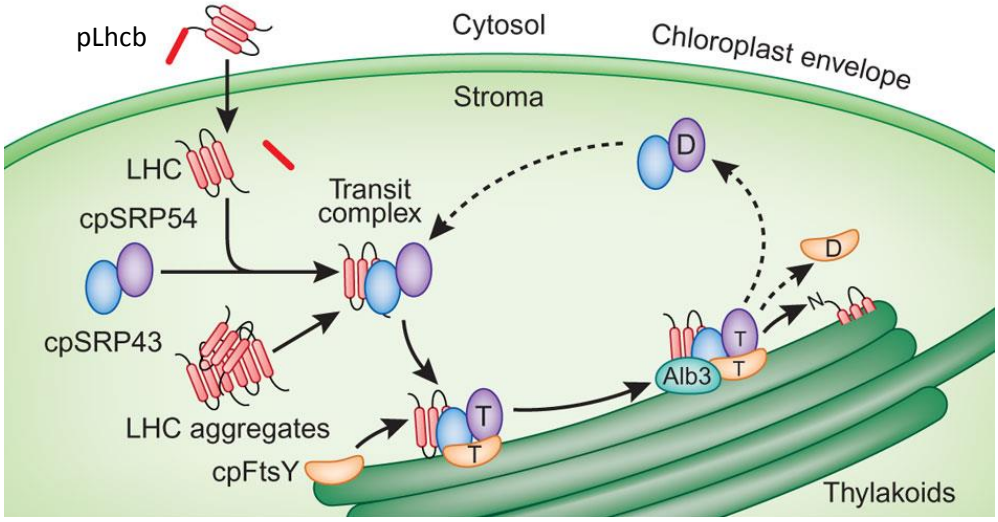

Fig.1.7. The mode of LHCP being transported and inserting into thylakoid membranes via SRP-pathway. Figure revised by Henry (2010).

Both Hoober and Tanaka believed that LHCII assembled in the chloroplast envelope (Hoober et. al, 2001; Tanaka et. al, 2007). It is hypothesized that the LHC apoprotein binds chlorophyllide *a* after removal of TP, chlorophyllide *a* oxygenase (CAO) on the inner envelope membrane interacts with translocons and LHC, and converts chlorophyllide *a* into chlorophyllide *b*. They proposed that CAO would also play a role in the transport of LHCP. However, neither is there any evidence showing LHCII were found on the inner envelope, nor is there any direct proof of existence of LHCP-CAO complex. Furthermore, it has been proved that LHCP is transported to thylakoid membrane by forming a transit complex with cpSRP, and cpSRP so far hasn't showed that it binds also CAO enzyme. Although CAO was found on the inner envelope and at thylakoid membranes, the enzyme chlorophyll synthase, which catalyzes the last step of chlorophyll biosynthesis, was found primarily located in thylakoid membranes (Soll et. al, 1983; Rüdiger, 1987). After being transported to thylakoid membrane, how LHCP

assemble with pigments and how folded LHCII integrated into membrane are still unclear. Little is known about what enzymes or proteins are involved in LHCII assembly *in vivo*.

1.2.4. LHCII reconstitution *in vitro*

Membrane protein structural biology is still a largely unconquered area, given that approximately 25% of all proteins are membrane proteins and yet less than 150 unique structures are available. Membrane proteins have proven to be difficult to study. Their surface is relatively hydrophobic and they can only be extracted from the cell membrane with detergents. They are also often flexible and unstable. This leads to challenges at all levels, including expression, solubilization, purification, crystallization, data collection and structure solution (Carpenter et al, 2008). Detergents have played significant roles in understanding of the structure and function of membrane proteins. They serve as tools to isolate, solubilize, and manipulate membrane proteins for subsequent biochemical and physical characterization. Detergents solubilize membrane proteins by creating a mimic of the natural lipid bilayer environment without interference by other membrane components (Seddon et. al, 2004; Garavito et. al, 2001).

LHCII and related Chl *a/b* binding proteins are able to spontaneously self-assemble in detergent, yielding complexes biochemically and spectroscopically similar to the native complexes isolated from thylakoid membranes. Early LHCII reconstitution experiments used apoproteins and pigments that were both extracted from thylakoids (Plumley et. al, 1987). A few years later a method was developed to refold LHCII from isolated pigments and recombinant protein overexpressed in *Escherichia coli* (*E.coli*) (Paulsen et. al, 1990). This allows us to create various mutants for different research purposes. Also, the crystal structure of LHCII is known. These advantages make LHCII an interesting model system to learn more about membrane protein function and folding in general.

LHCII self-organization can be triggered by simply mixing the apoprotein solubilized in the ionic detergent dodecyl sulfate with a non-ionic detergent solution of the pigments. The assembly process can then easily be monitored for kinetic studies by time-resolved fluorescence

spectroscopy using the Chls as built-in fluorescence labels and by time-resolved circular dichroism (CD) in the far-UV range observing a-helix content changes at 222 nm. Such experiments showed that protein folding is dependent on the binding of pigments, and both pigment assembly and secondary structure formation are tightly coupled. LHCII formation *in vitro* occurred in at least two apparent phases, a faster one in the range of 10 s to 1 min and a slower one taking several minutes (Fig.1.8). The faster step could be assigned to the binding of mostly Chl *a* by forming an unstable intermediate containing only LHCP, Chl *a* and xanthophylls; whereas the slower one represents irreversible Chl *b*, perhaps also some Chl *a*, binding (Booth et al, 1996; Horn et al, 2002, 2004 and 2007). It has been revealed that most of Chl *a* molecules were able to be replaced by Chl *b*, which adopted similar orientations as the Chl *a* that they replaced (Kleima, 1999). One Chl *a* molecule is required to form the trimer (Kleima et.al, 1998). This indicated that the Chl *a* binding sites more or less prefer Chl *a* but are also able to bind Chl *b*. The 5 Chl *b* binding sites, on the other hand, are exclusively to bind Chl *b* and an additional one exhibits a slight preference for Chl *b* versus Chl *a* (Hobe et al., 2003). Chl *a* binding to their binding sites appears to be weak and reversible as long as the Chl *b* binding sites are not filled, while of Chl *b* binding to its exclusive binding sites is largely irreversible.

Reconstituted LHCII monomer can be trimerized in the presence of lipids; monomers and trimers can be separated by sucrose density centrifugation (Hobe et.al, 1994).

1.3. Spectroscopic methods applied on LHCII study

Simple spectroscopic techniques such as absorption and fluorescence spectroscopy in the visible range were also used to investigate the LHCII function. As LHCII naturally contains fluorophores, steady-state fluorescence measurements were used both qualitative and quantitatively for analyzing Förster energy transfer between Chl *b* to *a*, Chl to introduced fluorescent dye, or LHCII to other energy acceptor, i.e. Quantum Dots (Gundlach et. Al., 2009;

Werwie et. al, 2012). Time-resolved fluorescence measurements, as mentioned before, were used for kinetic studies. Another valuable technique used in LHCII studies is CD measurement, as the spectra in the far-UV range provide information about the secondary structure of proteins. CD spectra can be readily used to estimate the fraction of a molecule that is in the *a*-helix conformation, the ß-sheet conformation, the ß-turn conformation, or some other (e.g. random coil) conformation (Whitmore et. al, 2008). LHCII CD spectra in the visible range give overall conformational information about pigment–protein interactions and interactions between pigments in different monomeric subunits (Georgakopoulou, et. al. 2007). Fluorescence and CD spectroscopies are unable to give detailed structural information among different domains.

Among all the spectroscopies applied in membrane protein studies, X-ray crystallography is currently the most favored technique to monitor the three dimensional structure of proteins. Well-ordered crystals are a prerequisite for determining the precise atomic structure of any protein, and hence for understanding the exact molecular mechanisms and modes of action. However, most membrane proteins are notoriously difficult to crystallize; furthermore monitored conformations might not always represent the catalytic or functional state (Fanucci et. al, 2003). Flexible subunits are always missing in the crystal structure due to inherent disorder. Unstable proteins are also not available for X-ray. NMR spectroscopy can provide

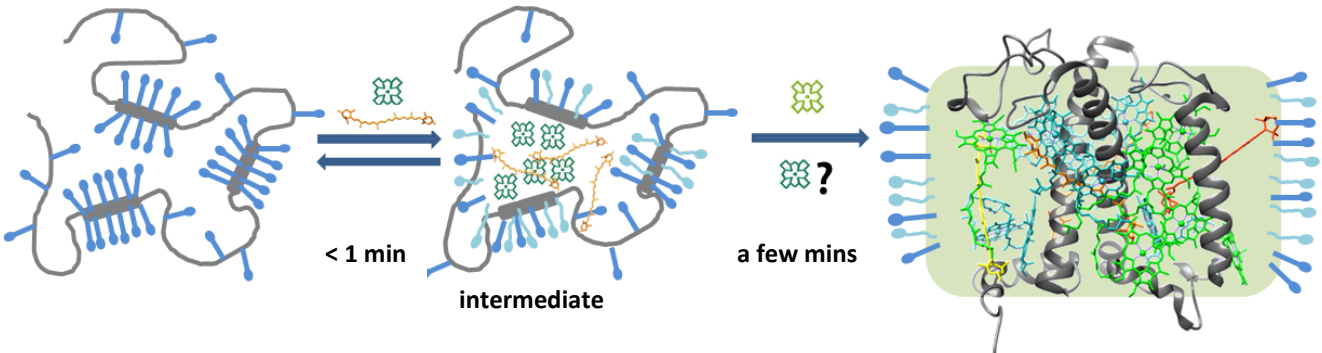

Fig.1.8. Two-step scheme of LHCII assembly. The apoprotein (grey) dissolved in SDS (blue) already containing some a-helices binds Chl *a* (dark green) and caroteinoids (orange) in a reversible fast step and then binds Chl *b* (light green), perhaps also some Chl *a* in the slower step. Pigments were dissolved in buffer containing OG (light blue) before added to the protein. Folded LHCII figure was constructed with pdb viewer (entry 2BHW; Standfuss, 2005). Dark grey: polypeptides; cyan: Chl *a*; green: Chl *b*; orange: lutein; orange red: neoxanthin; yellow: violaxanthin;

information about the structure and dynamics of membrane proteins, but liquid NMR spectroscopy is limited to molecules below 25-30 kDa and therefore, not suited for the LHCII. Solid-state NMR can be used for larger proteins but requires a careful choice of the detergent, elaborated stable isotope labelling schemes to overcome signal overlaps and to collect distance restraints (Montaville et al, 2010). Attempt on LHCII showed further problems caused by the necessary protein concentration and therefore, aggregation problems (Dietz, 2008).

As an alternative, electron paramagnetic resonance (EPR) spectroscopy, which is more sensitive, offers the possibility to study macromolecular structure and function because EPR signals are generated only by unpaired electrons, which are fairly rare in biological systems (Biswas, 2001). This technique, especially site-directed spin labeling EPR (SDSL-EPR), is used in the determination of secondary, tertiary and quaternary protein structure and associated conformational changes. Protein dynamics and the relative orientation of protein components in ordered systems can also be measured. Spin labels are nitroxides which are stable free radicals in the general form $O\text{-}NR^1R^2$ with a functional group for specific attachment to the protein (covalently binding or as a ligand). The most popular covalent sites are cysteine residues, which, if necessary, can be introduced into the protein structure using molecular biology techniques. Nitroxide spin labels are small and have been shown to have minimal effects on protein structures. From EPR experiments with spin labels, four primary parameters are obtained: (1) side chain mobility, (2) distances to other paramagnetic centers, e.g., a second spin label or a metal ion within the very same or another molecule, (3) solvent and oxygen accessibility, and (4) a measure for polarity of the environment of the spin-label (Drescher, 2012).

The recombinant LHCP can be modified by site-directed mutagenesis to attach spin labels to engineered cysteine residues replacing other amino acids without a functional impact. This makes LHCII a good candidate for EPR analyses. Two popular EPR-techniques have been applied on LHCII in the last decade in order to study the protein dynamics are double electron resonance (DEER) and electron spin echo envelopment (ESEEM). DEER spectroscopy allows the measurement of distances between two spin-labeled residues in the range of 2–8 nm (Jeschke et. al, 2007). The distance distribution also reveals the rigidity or flexibility of the

measured positions. ESEEM provides additional information about the water accessibility of singly spin-labeled protein domains. A lot of information about the terminal domains, the rigid core and loop regions in a monomeric and trimeric assembly of the LHCII in aqueous solution were collected. Measurements of inter-spin distance distributions between two spin pairs labelled indicated the core of LHCII in solution had a structure very similar or identical to the one seen in crystallized LHCII trimers; while the intra molecular distances measured at the lumenal loop domain showed broader distance distributions, indicating some mobility of this loop structure (Dockter et. al, 2012). In kinetic EPR measurements of LHCII protein folding, the positioning of the spin pair spanning the hydrophobic core of LHCII preceded the juxtaposition of the spin pair on the luminal side of the complex, implying that superhelix formation of helices 1 and 4 is a late step in LHCII assembly (Dockter et al, 2009). ESEEM measurements of singly spin-labelled LHCII showed some residues exhibit identical water accessibility in monomers and trimers, revealing them being in similar environments; while some residues of monomers showed slightly but significantly enhanced water accessibility as compared with their trimeric equivalents (Volkov et al, 2009).

1.4. Aims of this work

Tanaka et al.(1993) also found that LHCII apoproteins in etiolated tissues began to accumulate immediately after a pulse light in parallel with the formation of Chl *a*, in the absence of any accumulation of Chl *b*; but the level of the apoprotein decreased during the subsequent dark incubation, when Chl *b* accumulation kept at a low level. Both *in vivo* and *in vitro* study suggested that during LHCII assembly, an unstable intermediate was formed containing Chl *a* and carotenoids bound to the apoprotein, subsequently the binding of Chl *b* stabilized the complex. However, little is known about this intermediate.

Therefore in this work we wish to collect more information about this intermediate and try to understand how protein molecule organizes itself. This information will help us better understand how LHCII assembles *in vivo*.

To aim this, three questions would be answer:

1. **How can we analyze this Chl *a*-containing intermediate?** Chl *a*-containing intermediate was unstable and not able to be separated from unfold LHCP. Samples from any preparation would end up a mixture. Any contaminants which might interfere analysis must be got rid of before adding pigments. Optimizing purification of apoprotein took an important part in this work.

2. **How many Chl *a* molecules are able to bind to the protein in the absence of Chl *b*?** The strategy for addressing this question was to use fluorescent dye as a monitor to observe Chl *a* binding. Measurements were designed based on Förster resonance energy transfer (FRET). Fluorescent dyes were carefully chosen according to the Förster distance between donor and acceptor.

3. **What does this intermediate look like?** DEER and UV-CD spectroscopies were the main tools to address this question. Results collected from several techniques were compared with unfolded LHCP and fully folded LHCII for mapping the picture of this intermediate.

2. Material and methods

2.1. Equipment

Adsorption Spectrometer

UV-2101 PC	Shimadzu Corporation, Japan
V-550	Jasco labor and data technique GmbH, Groß-Umstadt
Software: Spectra Manager	
Eppendorf photometer	Eppendorf Vetrieb Germany GmbH, Wessling-Berzdorf

Autoclave

Varioclave Typ 500 H+P	Labor technique GmbH, Munich

Camera

Canon Power Shot A710IS digital	Canon Germany GmbH, Krefeld

CD Spectrometer

J-810-S	Jasco labor and data technique GmbH, Groß-Umstadt
Pelletier element:	Modell CDF-426S/426L
Software:	Spectra Manager

Cell disruption

French Pressure Cell Press	SLM Aminco, SLM Instruments
Ultrasonic cell disruptor	
Probe: V1A, V9906	Sonics & Materials Inc., Danburry,

	Conetticut, USA
Controller: Vibra Cell,	Sonic and Materials Inc., Danburry, Conetticut, USA

Centrifuges

Cooling centrifuges

J2HS	Beckmann Instruments, Munich
Rotors: JLA-10500, JA-20.50	
Mikro 22 R	Hettich Zentrifugen, Tuttlingen
Rotors: 1015, 1016 and 1195	
Rotina 38 R	Hettich Zentrifugen, Tuttlingen
Rotors: 1792 und 1789-L	

Table centrifuges

Mikro 12-29	Hettich Zentrifugen, Tuttlingen
Rotor: 2029	

Ultra centrifuges

Optima XL-100K, XL-90K and XL-80K	Beckmann Instruments, Munich
Rotors: SW60Ti, SW41Ti, SW40Ti	

Cycler/Rotator

Culture cycler type rotator	Bachofer GmbH, Reutlingen

EPR Spectrometer

cw-EPR:

Benchtop Miniscope MS 300	Magnettech GmbH, Berlin
5340A Frequency Counter	Hewlett-Packard Company, USA
Software: MiniScope Control version2.5.1	Magnettech GmbH, Berlin

DEER:

Spectrometer: Elexsys EX 580	Bruker BioSpin GmbH, Rheinstetten
Resonator: Split Ring ER4118X-MS3	
Resonator Q-Band	Self-construction AG Jeschke, ETH Zurich, switzerland
Amplifier: high-power TWT (150 W)	
Temperature control: Oxford CF935	Oxford Instruments, UK
Cryostat, ITC4 temperature controller	
Software:	DEER Analysis 2013 http://www.epr.ethz.ch/software

Fluorescence Spectrometer

Fluoromax 2 and Fluoromax-3	ISA SPEX Jobin Yvon, Grasbrunn
Cooling: Ministat Compatible Control	Huber Kältemaschinenbau GmbH, Offenburg
Software:	Datamax Software, version 2.24 Table Curve 2D version 4.0

Gel electrophoresis

Analytical gel electrophoresis:	
Gel gating system: Midget system	Pharmacia LKB Biotechnology, Piscataway
Voltage source	Bio-Rad Power-Pac 3000, USA
Cooling: Haake G, Haake D1, Modell Fisons	Firma Haake Messtechnik GmbH, Karlsruhe
Gel dryer: 2003 Slab Gel Dryer	LKB Bromma
Preparative gel electrophoresis:	
Model 491 Prep cell	BioRad, Munich

Gel tube 13 cm high, 37 mm inner diameter

Voltage source — Bio-Rad Power-Pac 3000, USA

Pump

Fraction Collector, Model 2128

Gel documentation

VersaDoc™ Imaging System 3000 — Bio-Rad, Munich

Software: Quantity One

Heating cabinet

Memmert — Memmert, Schwalbach

HPLC

Analytical HPLC:

Mixer: LG-1580-04 Quaternay Gradient Unit — Jasco labor and data technique GmbH, Groß-Umstadt

Pump: PU-1580 Intelligent

Detector: Diode Array Detector MD-1515

Column: Chromolith Speed ROD, RP 18e

Software: Jasco-PDA, BROWIN, Version 1.5

Preparative HPLC:

Pumps: PU-2080 Intelligent Pump

Detectors: Absorption: SP-6V; — Gynothek GmbH, Gemering; Shimadzu

Fluorescence: RF 535 — Corporation, Kyoto, Japan

Column: Waters Bondapak C18; 125 Å; 10µm; 30 x 300 mm

Software: Jasco-PDA, BROWIN, Version 1.5

Incubator

Certomat	H/B, Braun Biotech International, Melsungen
Laminar flow	
Laminar flow	SLEE Semiconductor Technik GmbH, Mainz
Magnetic stirrer	
Heidolph MR 3001 K8	HeidolphElektro, Kelheim
IKAMAG KMO2 basic	IKA, Labortechnik, Staufen
Mixer	
Heavy Duty Blendor	BlendorWaring, USA
PCR-Cycler	
Primus 25 Legal PCR-System	MWG-Biotech, Ebersberg
Modell 5524	
pH-Meter	
INOLab pH Level 2	WTW GmbH, Weilheim
Rotary evaporator	
Heidolph VV 2000	Heidolph Elektro, Kelkheim
Vacuum pump: CVC 2000,	Vacuubrand GmbH und Co, Wertheim
Cooling: Minichiller,	Huber, Offenburg
Shaker	
Certomat	H/B. Braun Biotech International, Melsungen
Phero Shaker,	Biotec Fischer, Reiskirchen
Ultrasonicator	
SONOREX Super	Bandelin, Berlin

Vibra Cell high intensity ultrasonic processor VC600	Sonics and Materials, Danbury, USA
Vortex	
IKA MS2 Minishaker	IKA Labortechnik, Staufen
Water bath	
Thermomix MM	H/B, Braun Biotech International, Melsungen
Water boiler	
HB4 basic	IKA, Labortechnik Staufen
Weighing machine	
BP 2100S	Sartorius AG, Göttingen
Analytik A200S	Sartorius AG, Göttingen

2.2. Chemicals

All used chemicals (p.A. quality) were purchased from companies: Amersham Pharmacia Biotech (Freiburg); Agilent Technologies (Waldbronn); Alfa Aesar (Karlsruhe); Avanti Polar-Lipids (Hamburg); Biomol (Hamburg); BioRad Laboratories (Munich); Boehringer (Mannheim); Macherey-Nagel (Düren); Merck KGaA (Darmstadt); MobiTec (Göttingen); New England BioLabs Inc. (Schwalbach); PeqLAB Biotechnologie GmbH (Erlangen); Riedel de Häen (Hannover); Roth GmbH (Karlsruhe); Serva (Heidelberg); Sigma-Aldrich (Deisenhofen) and Widmann Gas (Gase Center Herbarth, Budenheim)

Diethyl ether was distilled over KOH before use. Water free acetone was prepared from technical acetone or acetone waste from HPLC runs by single or double distillation, respectively.

2.3. Protein standard

For denaturing gel electrophoresis, protein test mixture 6 (Serva) was used and standard proteins were dissolved in a buffer consisting of 125 mmol/l Tris/HCl pH 6.8, 2 % SDS ,15 % glycerol, 10 mmol/l DTT, 0.025 % bromophenol blue, 0.025 % Orange G.

Table 2.1: Composition and molecular weights of the protein test mixture 6.

Molecular weight	Protein
97.4 kDa	Phosphorylase B
67.0 kDa	Albumin bovine
45.0 kDa	Albumin egg
29.0 kDa	Carbonic anhydrase bovine
21.0 kDa	Trypsin inhibitor soybean
12.5 kDa	Cytochrome C
6.5 kDa	Trypsin inhibitor, bovine lung

2.4. Labels

2.4.1. Fluorescence label

Parameters and specifications of dye labels were obtained from official websites of producers.

DY731-maleimide (DYOMICS, USA)

Specifications: $C_{44}H_{53}N_4O_{10}S_2Na$; molecular weight: 885.05 g/mol; max. absorption (ethanol): 736 nm; max. emission (ethanol): 760 nm; molar extinction-coefficient: 240000 [$cm^{-1} \cdot M^{-1}$]; soluble in water, methanol, DMF, DMSO; light sensitive.

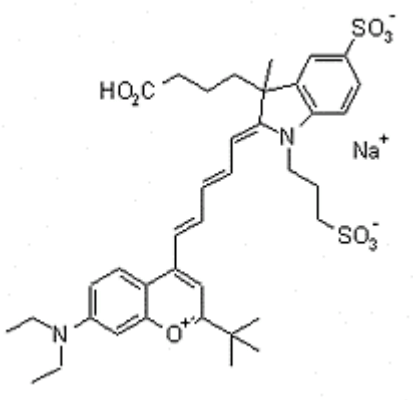

Figure 2.1. Structural formula of DY731.

DY634-maleimide (DYOMICS, USA)

Specifications: $C_{44}H_{53}N_4O_{16}S_4Na_3$; molecular weight: 1091.16 g/mol; max. absorption (ethanol): 635 nm; max. emission (ethanol): 658 nm; molar extinction-coefficient: 200000 [$cm^{-1} \cdot M^{-1}$]; soluble in water, methanol, DMF, DMSO; quantum yield in ethanol: 0.202.

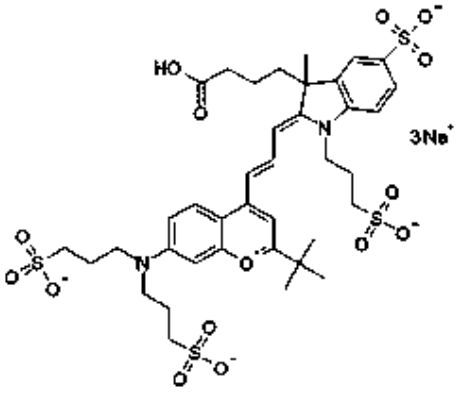

Figure 2.2. Structural formula of DY634.

DY615-maleimide (DYOMICS, USA)

Specifications: $C_{38}H_{44}N_4O_7S$; molecular weight: 700.86 g/mol; max. absorption (ethanol): 621 nm; max. emission (ethanol): 641 nm; molar extinction-coefficient: 200000 [$cm^{-1} \cdot M^{-1}$]; soluble in methanol, ethanol, DMF, DMSO, quantum yield in ethanol: 0.037

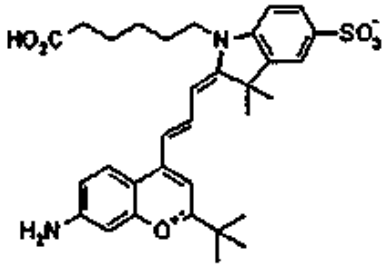

Figure 2.3. Structural formula of DY615

Rhodamine Red® C_2 maleimide (Invitrogen, USA)

Specifications: $C_{33}H_{36}N_4O_8S_2$; molecular weight: 680.79 g/mol; max. absorption (methanol): 560 nm; max. emission (methanol): 580 nm; molar extinction-coefficient: 119000 [$cm^{-1} \cdot M^{-1}$]; soluble in methanol, ethanol, DMSO, quantum yield in water: 0.5 (Grundlach, 2009)

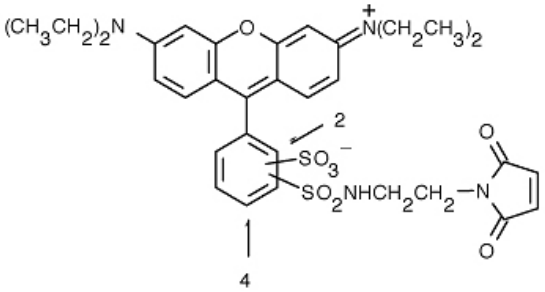

Figure 2.4. Structural formula of Rhodamine Red® C_2 maleimide

2.4.2. EPR label

3-(2-Iodoacetamido)-PROXYL, free radical - PROXYL-IAA (Sigma-Aldrich)
Specifications: $C_{10}H_{18}IN_2O_2$; molecular weight: 325.17 g/mol; soluble in DMSO, DMF, water, ethanol; light sensitive.

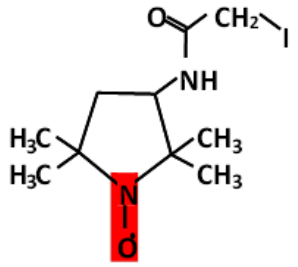

Figure 2.5. Structural formula of PROXYL-IAA.

2.5. Bacteria strains

2.5.1. JM101

Most of Lhcb1 clones were transformed in *E. coli* expression strain JM101 (purchased from NEB (Bad Schwalbach)) and stored as glycerol stocks.

2.5.2. XL10- Gold

XL10-Gold Ultracompetent cells of *E. coli* were part of "QuikChange Lightning Site-Directed Mutagenesis Kit" and purchased from Agilent Technologies (USA). All cells were thawed on ice, divided into aliquots, and stored at -80 ℃. Aliquots were thawed on ice directly before using.

2.6. Vectors

All constructed mutants used in this work are derivatives of the *Lhcb1* gene (*Lhcb1*2* AB80; Cashmore, 1984) from pea (*Pisum sativum*). The overexpression of different LHCII variants was carried out with the expression vector pDS12-RBSII vector (Fig. 2.6), which contains *Lhcb1* gene in the multiple cloning sites.

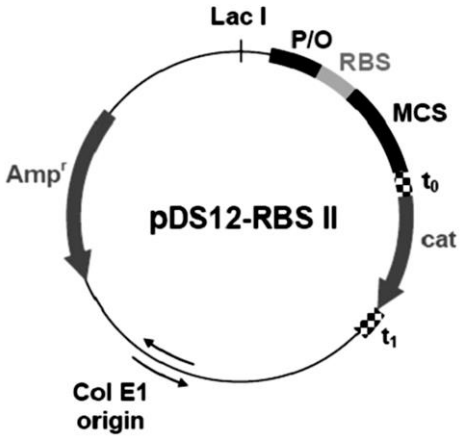

Figure 2.6. Schematic overview of the expression vector pDS12-RBSII. Col E1: origin of replication; Ampr: ß-lactamase gene for ampicillin resistance; Lac I: Lac repressor gene; P: T5 promotor PN25, O: *E. coli* lac operator; RBS: ribosome binding-site; MCS: multiple cloning-site; t0 and t1: terminators; cat: gene for chloramphenicol acetyltransferase for chloramphenicol resistance. Modified figure after Heinemann (1999).

For newly constructed mutants, the plasmid of suitable clones was isolated. QuikChange Lightning Site-Directed Mutagenesis Kit (Agilent Technologies, USA) was used for replacing amino acids. New mutants were sequenced and stored as glycerol stocks.

2.6.1 Plasmid isolation

Material:

peqGOLD plasmid miniprep kit II (PeqLAB Biotechnologie, Erlangen)

Liquid Luria-Bertani (LB) medium: 1 % Tryptone
0.5 % Yeast
1 % NaCl (pH 7.5)
pH adjusted to 7.5 by NaOH

LB-amp agar plate: LB media
1.5 % Agar
100 µg/ml Ampicillin

Method:

Bacteria of *E.coli* strain JM101 was separated on LB-amp agar plate at 37 ℃ overnight. 15 ml LB medium containing 100 mg/ml ampicillin were inoculated with a single bacterial colony picked from agar plate and incubated at 37 ℃ overnight with vigorous shaking. The plasmid DNA was isolated by using peqGOLD plasmid miniprep kit II. Purified DNA was eluted by 50 µl sterile aqua dest.

2.6.2 DNA quantification

The DNA concentration was measured the absorption at 260nm, 280nm and 320 nm by Eppendorf-Biophotometer.

DNA concentration was calculated as follow: c (DNA) [ng/µl] = (E_{260}-E_{320}) x dilution factor ng/µl

The purity was indicated by the ratio of E_{260}/E_{280}. A value of 1.8 indicates >90% purity. The value should not lower than 1.65.

2.6.3 Mutagenesis by using "QuikChange Lightning Site-Directed Mutagenesis Kit"

Material:

Isolated plasmid-DNA; QuikChange Lightning Site-Directed Mutagenesis Kit; primers containing the desired mutations (sense and antisense) ; LB-amp agar plate; LB medium

NZY^+ Broth: 1% (w/v) casein hydrolysate
0.5% (w/v) yeast extract
0.5% (w/v) NaCl
pH 7.5
supplemented with 12.5 mmol/l $MgCl_2$, 12.5 mmol/l MgSO4 and 0.4% (w/v) glucose

Methods:

Table 2.1: List of all used primers and their specifications

Name	Sequence	length	Description
S160Cfw	5'-CCA CTT TAC CCA GGT GGA TGC TTT GAT CCA TTG GGC TTA GCT G-3'	43nt	Replacement S160C
S160Crv	5'-CAG CTA AGC CCA ATG GAT CAA AGC ATC CAC CTG GGT AAA GTG G-3'	43nt	Replacement S160C

Due to the fact that almost all mutagenesis preparations had very good yields, half volumes of the protocol manual were used; reaction samples were prepared as follow, all ingredients excluding the enzyme were mixed on ice, enzyme was carefully adding before PCR:

Table 2.2: Composition of PCR mixture

Material	Amount
10x reaction buffer	2.5 µM
dsDNA template	~50 ng
Primer	~60 ng sense + ~60 ng antisense
dNTP mix	0.5 µl
QuikSolution reagent	0.75 µl
QuikChange Lighning Enzyme	0.5 µl
ddH_2O steril	25 µl

According to the manual instruction, both sense and antisense prime are between 25 and 45 bases in length, with a melting temperature (T_m) ≥78°C. The mutation was located in the middle of each primer; highly expressed codons of replacing amino acids were preferred. The polymerase chain reaction (PCR) was done as Table 2.3 described.

Table 2.3: PCR program for mutagenesis reaction

Cycles	Temperature	Time	Description
-	110 ℃	-	Preheating the lid
1x	95 ℃	2 min	Activation
18x	95 ℃	20 sec	Denaturing
	60 ℃	30 sec	Annealing
	68 ℃	3 min	Elongation
1x	65 ℃	5 min	Final elongation
-	4 ℃	-	Storage

1 µl restriction enzyme *Dpn* I was gently added after PCR and the mixture was immediately incubated at 37 ℃ for 5 min to digest the parental supercoiled dsDNA. XL10-Gold ultracompetent cell aliquots were gently thawed on ice and 1.5 µl ß-ME was added. Incubated cells on ice for 2 min and transfer 1.5 µl *Dpn* I-treated DNA to XL10-Gold cells. The mixtures were incubated on ice for 30 minutes. In the next step, NZY^+ broth was preheated in 42 ℃ water bath; the mixture was heat shocked for 30 sec at 42 ℃ in water bath, incubated on ice for 2 min and 250 µl NZY^+ broth was added; then incubated at 37 ℃ for 1 hour. In the end, mixture was plated on LB-amp plates and incubated overnight at 37 ℃. The other day, single colony was picked and overnight grown in 15 ml liquid LB-medium at 37 ℃ containing 100 mg/ml ampicillin to isolate plasmid (2.6.1). Whether mutagenesis is successful or not is checked by DNA sequencing (2.6.4).

2.6.4 DNA Sequencing

Material:

400 ng DNA; 1 µl sequencing primer

Methods:

A mixture containing ~400 ng DNA, 1 µl sequencing primer and ddH_2O steril was prepared and analyzed by GENterprise company (Mainz). The sequencing primer used in this work was Ds340 (-).

DS340-	5'-CTT TAC GAT GCC ATT GGG-3'	18nt length	Binds 340 bp downstream the stopp codon (reverse primer)

2.6.5. Glycerol stocks

Material:

400 µl *E. coli* XL10-Gold overnight culture; 600 µl 80 % glycerol

Method:

New mutants were stored as glycerol stocks, 400 µl *E. coli* XL10-Gold overnight cultures were mixed with 600 µl 80 % glycerol and frosted at -80 ℃.

2.7 Preparative biochemical methods

2.7.1 Extraction of pigments (Total extract)

Material:

Leaves of pea (*Pisum sativum)*; acetone; distilled diethyl ether; 5 mol/l NaCl; Nitrogen 5.0

Extraction buffer: 1 mol/l Tris/HCl pH 7.8
1 mmol/l DTT
330 mmol/l sorbitol

Method:

Seeds were incubated in water bubbled with air for 1-2 days, put under moistened vermiculite and grown under 16 hours light and 8 hours dark condition for 2 weeks. Plant leaves were cut and ground with extraction buffer (800 ml per 550 g leaves) and then filtrated through three layers cotton and one layer gaze. The filtrate was centrifuged at 4 ℃, 8000 rpm (Beckmann cooling centrifuge; rotor: JLA-10500) for 5 min. The green pellet was suspended in acetone (400 ml per 550 g leaves). After second centrifugation, the green supernatant was transferred to into a separating funnel. Slowly added distilled diethyl ether in to the funnel and carefully mixed by very gently moving and inverting to avoid emulsion. Release the pressure by opening the stopcock. 5 mol/l NaCl was added to transfer pigments into ether phase, slowly decreased salt concentration and acetone was gradually extracted into water phase.

Repeated these steps until pigments were all transferred to ether phase, acetone all moved to water phase and water phase contained no salt.

Pigment ether solution was stored at -20 ℃ overnight to get rid of residual water. Ice crystals were removed by Buchner funnel and pigments were dried in rotary evaporator. Pigment concentration and composition was analyzed by dissolving in water-free acetone and measured by HPLC. Pigments extract was stored at -20 ℃, kept in dark and under N_2 atmosphere.

2.7.2 Extraction of single pigments

Material:

1, 4-dioxane, acetone, distilled diethyl ether, ethanol, 60% KOH (w/v), 4 mol/l NaCl, Nitrogen 5.0

Method:

Pigment total extract was dissolved in acetone, cooled on ice by stirring and 0.15 volume 1, 4-dioxane was slowly added from a dropping funnel. Subsequently, 0.32 volume water was added; stopped stirring and precipitated chlorophylls on ice for 1 hour. After that, mixture was centrifuged (15 min, 4 ℃, 8000 rpm, Beckmann, rotor JLA10.500). The chlorophylls were in the pellet while the supernatant contained the xanthophylls.

The chlorophyll pellet was dissolved in distilled diethyl ether and water soluble substances were extracted by water in a separating funnel. Carefully removed water phase and repeated one time. The ether phase was stored at -20 ℃ overnight; ice was removed and pigments were dried in rotary evaporator.

The xanthophyll solution was transferred to a separating funnel and extracted most pigments by ether. After that, ether was removed by rotary evaporator; ethanol and 60% KOH were added and incubated the mixture at 30 ℃ overnight to saponify the remaining chlorophylls and lipids. The xanthophylls were extracted into ether phase followed the same procedure as the extraction of pigment total extract. Chlorophyllids were removed in this step. The dried pigments were stored in a N_2-atmosphere at -20 ℃ until preparative HPLC was ready.

Separation of the chlorophylls and xanthophylls by using the preparative HPLC

Material:

RP-HPLC with Waters Bondapak column (C18; 125 Å; 10 μm; 30 x 300 mm); pigments; acetone, distilled diethyl ether; buffered water
(0.1 mmol/l HEPES pH 7.0)

Detectors Gynkotek	Shimadzu RF 535
Detect wavelength 440 nm	Excitation 435 nm
Absorption 0.04	Emission 680 nm
Response Standard	Response Medium
	Range 2
	Sensitivity high

Program:

All programs for controlling the pump, the composition of the mobile phase, flow rate and time were set before running.

Table 2.4: Program for preparative HPLC

	Program name	Time (min)	Description
Chlorophyll	CHLEQUIL	600	Column equilibration
	CHLSUPERLOOP	42	Sample loaded on the column
	CHLPREP	305	Preparative run for chlorophylls
Xanthophyll	XANEQUIL	600	Column equilibration
	XANSUPERLOOP	42	Sample loaded on the column
	XANPREP	132	Preparative run for xanthophylls

Table 2.5: Program of the acetone/water gradient in order to separate chlorophylls. Flow 5 ml/min

Acetone (%)	Water (%)	Time (min)	Timepoint (min)
85	15	0	0
85	15	240	240
87	13	60	300
100	0	5	305

Table 2.6: Program of the acetone/water gradient in order to separate xanthophylls. Flow 5 ml/min

Acetone (%)	Water (%)	Time (min)	Timepoint (min)
76	24	0	0
76	24	100	100
100	0	32	132

Method:

The column was equilibrated one day before preparative running. The column was first cleaned by 100% acetone for 1 hour at flow rate 3 ml/ min, and then equilibrated for 540 min at flow rate 0.3 ml/min. For

chlorophyll separation, the column was calibrated by 85% acetone and 76% acetone was used for xanthophylls preparative run. The dried pigments were solubilized in 80% Acetone and centrifuged at room temperature (10 min, 8000 rpm, Beckmann, JA25.50 rotor). The supernatant containing pigments was loaded into the sample loop and started PREP program for separation after samples were completely loaded. All eluted fractions were analyzed by analytical HPLC to check the purity.

All separated pigments were mixed with diethyl ether in a separating funnel, washed with water, and dried in a rotary evaporator. The amount of pigments was checked by analytic HPLC. Subsequently pigment aliquots were prepared.

2.7.3 Pigment concentration

Material:

80% acetone; water free acetone

Method:

The dried pigments were dissolved in water free acetone, and then a defined volume of pigment solution was mixed with 80 % acetone and the absorption measured at 750, 663.6, 646.6,440 nm. The pigment concentration was calculated after Porra *et al*. (1989) and Davies (1976):

Chl *a* = 12.3 * A663.6 – 2.55 * A646.6 = [µg/ml] * dilution factor

Chl *b* = 20.3 * A646.6 – 4.9 * A663.6 = [µg/ml] * dilution factor

Xan = 4.17 * A440 = [µg/ml] * dilution factor

2.7.4. Pigment composition analyzed by analytical HPLC

Material:

RP-HPLC with column (Chromolith Speed ROD, RP 18e); 100 % acetone (filtrated and degased); buffered water (degased, 0.2 mmol/l Tris/HCl pH 7.0)

Table 2.7: Program of the acetone/water gradient Flow 1 ml/min

Acetone (%)	Water (%)	Time (min)	Timepoint (min)
70	30	0	0

100	0	3.5	3.5
70	30	3	6.5

Method:

The composition of the isolated pigments was monitored by using the reversed phase high performance chromatography (RP-HPLC) either after pigment extraction or pigment separation. The separation was based on two phases: a nonpolar surfaced modified silica stationary phase and a polar acetone/water mixture mobile phase. After calibrating column with two runs of 80% acetone, pigments were separated due to their hydrophobicity for hydrophobic pigments had a longer retention time on the column. The separation effect was controlled by varying the composition of the mobile phase. Eluted molecules were detected by UV-Vis spectroscopy and the pigment concentration was calculated by integration of the peak area.

2.7.5. Preparation of pigment aliquots

Material:

Isolated pigments; 100% water free acetone; nitrogen 5.0

Method:

After analyzing the pigment composition (2.7.4) and concentration (2.7.3), the isolated pigments were dissolved in 100 % water free acetone. Pipetting required amount in aliquots and dried pigments under a continuously nitrogen flow. All prepared aliquots were stored in screw cap micro tubes with O-ring seal at -20 ℃ in the dark.

2.7.6. Overexpression and isolation of LHCP from *E. coli* as inclusion bodies

Material:

Liquid LB medium; LB-amp agar plate; 1 mg/ml Ampicillin; 1 mol/l IPTG; 70% ethanol

Lysis buffer:	0.8 mg/ml DTT 4 µg/ml DNaseI	Tris buffer:	50 mmol/l Tris/HCl pH 8.0 1 mmol/l EDTA
Detergent buffer:	1 % Desoxycholacid (w/v)	Triton buffer:	0.5 % Triton X-100 (w/v)

1 % Triton X-100 (Tx) (w/v)	20 mmol/l Tris/HCl pH 7.5
200 mmol/l NaCl	1 mmol/l EDTA
20 mmol/l Tris/HCl pH7.5	
2 mmol/l EDTA	
10 mmol/l ß-me	

Method:

Glycerol stocks (2.6.5) of concerned mutants were plated on LB-amp plates and incubated for overnight at 37 ℃. 0.1% Ampicillin was added into LB medium; isolated bacterial culture was picked by a pipette tip which was cleaned with 70 % ethanol before and dropped the tip into the LB medium, then incubated at 37 ℃ and 175 rpm on an incubation shaker overnight. After that, isopropyl-ß-thiogalactoside (IPTG) was added to induce the production of protein. After 4 hour incubation, the bacterial culture was centrifuged (10 min., 8000 rpm, 4 ℃; Beckmann, rotor JLA10.500) and the pellet was suspended in lysis buffer.

Bacteria cells were broken mechanically in the French press or by using ultrasonication. In French press procedure, the bacteria-lysis mixture was put into the French press apparatus, and pressed through the French press for at least 2 times. In the ultrasonic procedure, the mixture in lysis buffer was filled into glass test tube and put in ice bath; ultrasonic probe was inserted into mixture for at least 1cm deep and the mixture was ultrasonic-treated for 5 min (duty cycle 50%, intensity 5). After breaking cells, the lysate was centrifuged (5 min., 8000 rpm, 4 ℃; Beckmann, rotor JA25.50) and resuspended in 15 ml detergent buffer. The solution was centrifuged (5 min., 8000 rpm, 4 ℃; Beckmann, rotor JA25.50) again and the white pellet was suspended in 8 ml triton buffer and incubated by spinning over at 4 ℃ overnight. The solution was centrifuged (5 min., 8000 rpm, 4 ℃; Beckmann, rotor JA25.50) the other day and the pellet was washed by 8 ml tris buffer. After another centrifugation (5 min., 8000 rpm, 4 ℃; Beckmann, rotor JA25.50), the pellet was resuspended in 4 ml tris buffer and the protein concentration was measured photometrically.

2.7.7. Analysis of protein concentration

Material:

A_{280} buffer	10 mmol/l	Tris/HCl pH 6.8
	2 %	Sodiumdodecylsulfate (SDS)
	1 mmol/l	ß-me

Method:

The protein solution was diluted by A_{280} buffer as 10 µl protein solution and 990 µl A_{280} buffer. ß-me was added as a fresh solution and the protein was denatured at 100 ℃ water bath for 1 min. absorption of these protein solutions was measured photometrically at 280 nm. The concentration was defined as:

$$C\ [mg/ml] = \frac{A_{280} * f * 530[\mu g/ml]}{1000 * d}$$

A_{280} = Absorption at 280 nm, f = diluting factor, d = path length [cm]

2.7.8. Protein purification by SDS polyacrylamide gel electrophoresis (SDS-PAGE)

Material:

Midget gel chamber; glass plates; aluminum oxide plates; 1.5 mm spacer; combs

LDS running buffer	25 mmol/l Tris	Sparmix	4% SDS (w/v)
	192 mmol/l glycine	without colour	24% glycerol (v/v)
	0.1 % LDS (w/v)		1.4 mmol/l ß-ME
	0.5 mmol/l EDTA		100 mmol/l Tris/HCl, pH 7.0

Table 2.9: Composition of the acrylamide solutions

Stock solutions	Separating gel 10%	Separating gel 15%	Stacking gel 4.5%
30 % acrylamide / 1 % bisacrylamide	18 ml	27.4 ml	6 ml
1 mol/l Tris/HCl pH 8.8	22.6 ml	22.6 ml	-
1 mol/l Tris/HCl pH 6.8	-	-	5.2 ml
80 % glycerol	3.4 ml	3.4 ml	5 ml
Aqua dest.	11.2 ml	1.8 ml	23.4 ml
10 % APS	400 µl	400 µl	200 µl
TEMED	26 µl	26 µl	26 µl

Method:

Electrophoretic separation of proteins was carried out under denaturing conditions (i.e., in the presence of SDS) in discontinuous gel system after Laemmli(1970). SDS-PAGE separates proteins according to their molecular weight, based on their differential rates of migration through a sieving matrix (a gel) under the influence of an applied electrical field. Gels (1.5 mm thick) were prepared in a midget gel

chamber and consisted of a 4.5 % stacking gel and a 10 % or 15 % separating gel. The components of the separating gel were mixed and degassed by water jet pump. After adding the radical donator ammonium per sulfate (APS) and the catalysator N, N, N, N-tetramethylethylendiamin (TEMED), the mixture was carefully poured into the gel chamber and filled it to about ¾, and then each gel was covered by 200 µl dest. water to get a smooth surface. After 1 hour polymerization, water was removed and the stacking gel solution was added and filled the rest of the chamber. A comb was inserted into each gel to form sample loading pocket. One hour later, the chamber was placed at 4 ℃ for more than 1.5 hour to have gel fully polymerized.

Proteins were mixed with ¼ volumn of sparmix and boiled 2 min at 100 ℃ water bath to be denatured. Gels were placed at an electric gel chamber and covered with LDS running buffer. Each gel page was able to load up to about 150 µg protein. Fluorescent dye labelled protein was loaded on the very left lane as a reference indicating where the target protein was. The separation was initiated by an electric voltage of 80 volt to have all proteins loaded on the stacking gel and then the voltage was increased to 150 volt to have further separation. After gel running, gel band containing LHCP was cut and inserted into a 14 KDa dialysis tubing filled with running buffer. The tubing was placed in a horizontal gel electrophoresis apparatus like western blot chamber filled with LDS running buffer. After 1 hour 30 min at 15 V electroelution, all the proteins were eluted from gel slices. During the whole procedure, the gel chamber as well as the electroelution chamber was connected to a cooling water cycle to keep the gel under 4 ℃.

2.7.9. Protein purification by preparative gel electrophoresis

Material:

Acrylamide/Bisacrylamide 37.5:1 (40% w/v); 1.5 mol/L Tris/HCl pH 8.8; 0.5 mol/L Tris/HCl pH 6.8; 10% APS; TEMED; water-saturated 2-butanol

10x Electrode (Running) Buffer	0.25 mol/l	Tris
	1.92 mol/l	glycine
	1%	Lithium dodecyl sulfate (LDS) (w/v)
	pH 8.3	
Sample Buffer (LDS-reducing buffer)	0.06 mol/l	Tris/HCl, pH 6.8
	2%	LDS (w/v)
	5%	ß-ME (v/V)
	10%	glycerol (v/v)
	0.025%	bromophenol blue

Table 2.8: Composition of the acrylamide solutions

	Separating Gel		Stacking Gel	
	volumn	End concentration	volumn	End concentration
Acrylamide/Bisacrylamide 37.5:1 (40% w/v)	40 ml	15%	3.25 ml	5.2%
1.5 M Tris/HCl pH 8.8	26.7 ml	375 mM	-	-
0.5 M Tris/HCl pH 6.8	-	-	6.25 ml	125 mM
dH_2O	40 ml		15.5 ml	
10% APS	266.7 µl	0.025%	125 µl	0.05%
TEMED	26.7 µl	0.025%	25 µl	0.1%

Method:

The preparative gel electrophoresis was performed on Model 491 Prep Cell purchased from Bio-rad, Munich. During a run, proteins are electrophoresed through a polyacrylamide(PA) cylindrical gel. As molecules migrate through the gel matrix, they separate into disk-shaped bands. Individual bands migrate off the bottom of the gel where they pass directly into the elution chamber for collection. Preparative PA-gel column was prepared following the manual provided by Bio-rad company (Bio-rad Model 491 Prep cell manual (http://www.bio-rad.com/webroot/web/pdf/lsr/literature/M1702925.pdf). About 10 cm high separating gel was prepared in 37 mm (internal diameter) gel tube; the monomer mixture of separating gel was degassed before pouring into the gel tube; about 1 cm high water-saturated 2-butanol was carefully overlaid by using a glass dropping pipette and liquid was slowly released against the inner wall of the gel tube. The gel was kept overnight in refrigerator with a water cycling through the cooling core for complete polymerization. The other day, the butanol overlay was discarded and the gel column surface was washed by distilled water for several times; about 2 cm high stacking gel monomer solution was added above the separating gel as soon as 10% APS and TEMED are added. The stacking gel monomer was overlaid with water-saturated 2-butanol and polymerized for 4-5 hours.

The apparatus was assembled followed the manual; the protein solution was diluted at least 1:4 with sample buffer, and heated at 95 ℃ for 4 min. The sample was carefully loaded on the surface of stacking gel. The gel electrophoresis was performed in 1x Electrode (Running) Buffer and the purified protein was also eluted in the same buffer with a flow rate of 0.16 ml/min. Fractions were automatically collected as 1.5 ml per fraction and the collection was started after the dye front was eluted. An electric voltage of 300 volt was used as the running.

To determine which fractions contain purified LHCP, every eighth fraction after the dye front was analyzed by 15% denaturing SDS-PAGE gel. When the region with LHCP was identified, every fraction within that region was analyzed to determine the level of contamination. Fractions containing the purified protein were precipitated (2.7.9.3) and concentrated as required for further experiments.

2.7.10. Labeling of LHCP

2.7.10.1. Labeling with SH-reactive fluorescence dye

Material:

LHCP; 1 % LDS; 100 mmol/l sodium phosphate buffer pH 7.0; 100 mmol/l triscyanoethylphosphine (TCyEP) in dimethylformamide (DMF); DMSO; fluorescence dye (2.4.1).

Method:

The labeling of LHCP with fluorescence dye was done followed the method described in Gundlach *et. al.* (2009)

2.7.10.2. Labeling with SH-reactive spin labels

Material:

LHCP; 0.5 % LDS (w/v); 100 mmol/l sodium phosphate buffer pH 7.0; 100 mmol/l TCyEP in DMF; 10 mg/ml PROXYL-IAA in DMSO.

Method:

The labeling of LHCP with spin label was done followed the method described in Volkov *et. al.* (2009)

2.7.10.3. Protein precipitation

Material:

Labeled LHCP; 100 mmol/l acetic acid; 100 % acetone; 70 % ethanol

Method:

Labeled protein was precipitated using acidified acetone by adding 1/10 volume of 100 mmol/l acetic acid and 2.3 fold volume of acetone. This mixture was incubated at -20 ℃ for 3 hours and then centrifuged (14000 rpm, 4 ℃; 10 min., Hettich, rotor 1195). The protein pellet was washed with ice cold

70 % ethanol; the precipitated protein was dissolved in LDS solution and the concentration was analyzed (2.7.7). All labeled samples were stored in the dark at -20 ℃.

2.7.11. Protein reconstitution by using the detergent-exchange method

Material:

2x Solubilization buffer	200 mmol/l	Tris/HCl pH 9.0
	4 %	LDS (w/v)
	10 mmol/l	ε-aminocapronic acid
	2 mmol/l	benzamidine

1 mol/l ß-me; ethanol p.A.; pigment total extract; 10 % octylglucoside (OG); 2 mol/l KCl

Method:

LHCP was dissolved in 1x solubilization buffer with a protein concentration 0.4 mg/ml. The protein was denatured in 100 ℃ water bath for 2 min and after cooled down, 11 mmol/l ß-ME was added to reduce thiol group. About 4 fold molecular excess of pigments (14 Chl molecules per LHCP) were dissolved in ethanol p.A by mixing and in the sonic bath. The pigment solution was added, thoroughly vortexed for 30 s and incubated for 10 min at room temperature. After that 1% OG was added, well mixed and incubated at room temperature for another 10 min. Later 0.2 mol/l KCl was added and incubated on ice for 15 min. The insoluble KDS was precipitated and the refolded LHCII was forced to move to OG micelle. The insoluble KDS was removed by centrifugation (14000 rpm, 4 ℃; 15 min., Hettich, rotor 1195) and refolded monomers could be either purified by ultracentrifugation or used for a trimerization.

2.7.12. Protein reconstitution by using the detergent-diluting method

2.7.12.1. SDS-denatured reconstitution

Material:

0.2 µg/µl (7.8 µM) LHCP; 1% SDS (w/v); 1 mol/l Dithiothreitol (DTT); 10% OG (w/v) and 0.4% phosphatidylglycerol (PG) (w/v), 0.25 µg/µl (280 µmol/l) Chl molecules (Chl *a:b* ratio=3) corresponding to about 3 fold molecular excess of pigment over LHCII, 0.058 µg/µl (114 µmol/l)

carotenoids corresponding to about 4 molecular excess of pigment over LHCII (assuming 4 xanthophyll molecules per LHCII)

In Chl *a* reconstitution 0.19 µg/µl (213 µmol/l) Chl *a* and 0.058 µg/µl (114 µmol/l) carotenoids were used instead of Chl *a*, Chl *b* and carotenoids mixture. The molecular excesses of pigment over protein were 3 and 4, respectively, assuming 8 Chl *a* molecules and 4 xanthophylls per protein.

2x Reconstitution buffer	25%	sucrose
	200 mmol/l	Li-Borate pH 9.0

Method:

The reconstitution was followed the method described in Horn et al (2007).

In order to have less pigment aggregation and keep Chls longer time in aqueous solution, the detergent concentration was adjusted to 0.26% SDS in protein solution and 2.6% OG and 0.104% PG in pigment solution.

2.7.12.2. Guanidine hydrochloride (GuCl)-denatured reconstitution

Material:

4 µg/µl (157 µmol/l) LHCP; 6 mol/l GuCl; 2% OG (w/v); 0.08% PG (w/v); 100 mmol/l lithium borate (pH 9.0), 12.5% sucrose (w/v); 10 mmol/l DTT; 0.22 µg/µl (244 µmol/l) Chl (Chl *a:b* ratio=3); 0.09 µg/µl (171 µmol/l) carotenoids; 0.17 µg/µl (188 µmol/l) Chl *a*

Method:

The reconstitution was followed the method described in Yang et al (2003).

Pigment solution contained either Chl *a*/carotenoids, or Chl *a*/Chl *b*/carotenoids. The reconstitution was initiated by manually mixing the pigment solution and GuCl-denatured protein solution at a ratio of 10:1 at room temperature. After 10 min incubation, solution was centrifuged and the supernatant was taken for further measurements.

2.7.13 Trimerization of his-tagged LHCII by using Ni^{2+}-chelating Sepharose fast flow column

Material:

Reconstituted LHCII (2.7.10) (the apoprotein contains a C-terminal hexahistidyl tag); Ni^{2+}-chelating Sepharose fast flow column (0.8 cm x 4 cm) (Bio-Rad, Hercules, CA); Chelating Sepharose Fast Flow (GE Healthcare, Schweden); 0.3 mol/l $NiCl_2$; 50 mmol/l Tris/HCl pH 7.5; 2 % SDS; 0.4 mol/l imidazole; 0.1 mol/l EDTA; 20 % ethanol

OG buffer	1 % OG (w/v)	Tx buffer	0.05 % Tx (w/v)
	0.1 mol/l Tris/HCl pH 9.0		0.1 mol/l Tris/HCl pH 7.5
	12.5 % sucrose (w/v)		0.1 mg/ml PG
Elution buffer	0.05 % Tx (w/v)		
	0.1 mol/l Tris/HCl pH 7.5		
	0.1 mg/ml PG (w/v)		
	0.3 mol/l imidazole		

Method:

The trimerization of LHCII monomers was done like described in Yang (2003) and the regeneration of the column material was done as described in Dockter (2009).

2.7.14. Sucrose density gradient ultracentrifugation

Material:

Ultracentrifugation Beckmann Optima 100/90/80; rotors SW60, SW40/41; sucrose (0.6 mol/l for SW60, 0.3 mol/l for SW40/41); 50 mmol/l sodium phosphate pH 8.5; 0.15 % n-dodecyl-ß-D-maltoside (LM).

Method:

Refolded monomers and trimers were purified by using ultracentrifugation. The defined sucrose solution containing buffered solution and 0.15% LM was filled into Beckmann ultracentrifugation tubes and frozen at -20 ℃. Gradients were formed during defrosting. The top layer was removed and LHCII samples were carefully loaded at the top the gradient. All tubes were balanced and centrifuged under vacuum at 4 ℃ for 16-17 hours. After the ultracentrifugation, free pigments, monomers, trimers, and aggregates were separated and formed bands among the gradient. Monomers or trimers were collected by using a syringe, stored on ice in the dark, and analyzed.

2.7.15. Quantification of the LHCII concentration

The concentration of LHCII monomers and trimers was defined photometrically at 670 nm with a molar extinction coefficient ($\varepsilon_{monomeric\ LHCII} = 5.46 * 10^5$ [$cm^{-1} * M^{-1}$]) (Kühlbrandt 1988).

2.7.16. Preparation of EPR samples

Material:

80 % Deuterium glycerol (glycerol-d8, 98 atom % D, Isotec USA); deuterium oxide (D_2O); 2 mol/ LiOH
Both protein and pigment solutions were prepared in D_2O as described below:

Protein solution:	90 µmol/l spin-labelled LHCP
	1% LDS (w/v)
	100 mmol/l Li-Borate, pH 8.1
	12.5% sucrose (w/v)
Pigment solution:	5% OG (w/v)
	1.5% Tx (v/v)
	0.16% PG (w/v)
	0.02% Sodium deoxycholate (w/v)
	62.5 mmol/l Li-Borate, pH 8.1
	7.8% sucrose (w/v)
	16% pigments dissolved in ethanol p.A. (v/v)

Methods:

The EPR sample preparation was modified from Dockter's (2009) work. For cw-EPR measurements, about 90 µmol/l LHCP solution was prepared as well as the reference PROXYL-IAA spin label was dissolved in the same buffer with different concentrations. Samples were loaded on 50 µl capillary and about 2 cm high (~2 µl) sample was loaded via capillary action. Measurements were taken at room temperature on Bench-top (Modulation 1.5 gauss, sweep 150 gauss, time 60 s, microwave attenuation 16).

For DEER measurements, the pigment solution contained 1.5 µg/µl (1.68 mmol/l) Chl *a* corresponding to a stoichiometric excess over protein of 2.33 (assuming 8 Chl *a* per LHCII) and 0.6 µg/µl (1.17 mmol/l) carotenoids (lutein:neoxanthin:violaxanthin=3:1:1) corresponding to a stoichiometric excess of lutein over protein of about 3.26 (assuming 2 lutein molecules per LHCII). Chl *a* and carotenoids were mixed

in ethanol, after a few seconds in ultrasonic bath, solution was quickly centrifuged at room temperature. If there was no pellet forming, solution was quickly given to the pigment buffer and roughly vortexed. The protein and pigment solutions were 1:1 mixed and incubated in dark for 5 min. 80% glycerol was added to have a glycerol final concentration 32% (v/v). Sample was quickly transferred to EPR quartz tube and frozen in liquid N_2. All samples were stored in liquid N_2 before DEER measurements were taken.

2.8. Analytic methods

2.8.1 Gel electrophoresis

2.8.1.1. Analytical SDS-PAGE

Material:

SDS running buffer	25 mmol/l Tris	Sparmix	4% SDS (w/v)
(Laemmli running buffer)	192 mmol/l glycine		24% glycerol (v/v)
	0.1 % SDS (w/v)		1.4 mmol/l ß-ME
	0.5 mmol/l EDTA		100 mmol/l Tris/HCl, pH 7.0
			20 mmol/l bromphenol blue

Method:

Gel (0.75 mm thick) preparation and experiment setting were the same as 2.7.8 described.

Each gel pocket was able to load up to 5 µg protein. The protein standard was usually loaded on the very left lane as a reference.

2.8.1.2. Low denaturing gel electrophoresis (green gel)

Material:

Deriphat buffer	0.15 % deriphat (w/v)
	12 mmol/l Tris
	48 mmol glycine

Method:

The low denaturing gel electrophoresis allows us to separate refolded LHCII samples under mild conditions without being destroyed. In the contrast to SDS-PAGE, 10 % PA gels were used instead of 15 % PA in SDS gel electrophoresis and Deriphat buffer was used for running buffer. The voltage was reduced to 40 volt to load samples on stacking gel and 80 volt was used for separation. During the procedure, the samples were kept dark and the gel chamber was connected to a cooling water cycle to keep the gel under 4 ℃.

2.8.1.3. Coomassie brilliant blue staining

Material:

Coomassie solution	0.25% Coomassie brilliant blue G-250 (w/v)				
	40% ethanol (v/v)				
	7% acetic acid (v/v)				
Discolor solution 1	10 % ethanol (v/v)		Discolor solution 2	10 %	acetic acid (v/v)
	7 ml acetic acid (v/v)				

Method:

After gel electrophoresis, protein bands could be stained by a triphenylmethane dye Coomassie Brilliant Blue G-250 to visualize proteins. The gels were incubated for 20-30 min in Coomassie solution. Later the gels were put in discolor solution 1 for 1 hour and then in discolor solution 2 until staining was limited to protein bands. After staining, the gels were imaged and analyzed by VersaDoc (Bio-Rad).

2.8.1.4. Densitometric analysis of PA gels using Versa Doc

Material:

VersaDoc (BioRad); Software: Quantity one (BioRad); protein gel

Method:

The VersaDoc was used to analyze the protein amount of each protein band. To record fluorescence images of PA gels, gels were placed directly on the VersaDoc Fluorescent Reference Plate without coomassie staining, fluorescence dye labeled proteins were excited by UV-light and exposed to light for 10-60 sec to get proper images. Coomassie stained gels were placed on White Light Conversion Screen

and the images taken with 0.5-5 sec exposure time. A defined amount of bovines serum albumin (BSA) was used as a protein standard for quantification. All analyses were done using the software Quantity One.

2.8.2. Spectroscopy

2.8.2.1. Ultraviolet–visible spectroscopy (UV/Vis)

UV/Vis spectroscopy, refers to absorption spectroscopy, is a spectroscopic technique which measures the absorption of radiation, as a function of frequency or wavelength, due to its interaction with a sample using light in the visible and adjacent (near-UV and near-infrared [NIR]) ranges. Monochromatic light passes through the sample cell, the transmission of light is detected. The concentration of sample is determined based on Beer–Lambert law:

$$A = -\log (I/I_0) = \varepsilon * c * l$$

where A is the measured absorbance, I_0 is the intensity of the incident light at a given wavelength, I is the transmitted intensity, ε is the extinction coefficient, c is the concentration of the sample, l is the path length through the sample (usually is the length of the sample cell).

Absorption spectroscopy was used to determine the protein (2.7.7) as well as pigment concentration, fluorescence dye concentration and the concentration of the LHCII complex (2.7.14).

2.8.2.2. Fluorescence emission spectroscopy

Parameters:

All measurements were taken under front face setting with detector sensitivity level 3 and correction S/R.

Measurements of refolded non-labeled LHCII

Excitation wavelength: 470 nm	**Scan: 600-850 nm**
Time increment: 1.0 nm	Integration: 0.5 s
Excitation band width: 0.5 nm	Emission band width: 5 nm

Measurements using Rhodamine-labeled LHCP

Excitation wavelength: 550 nm	**Scan: 560-750 nm**
Time increment: 1.0 nm	Integration: 0.2 s
Excitation band width: 1 nm	Emission band width: 5 nm

Measurements using DY 731-labeled LHCP

Excitation wavelength: 420 nm	**Scan: 600-850 nm**
Time increment: 1.0 nm	Integration: 0.2 s
Excitation band width: 0.5 nm	Emission band width: 5 nm

Method:

Due to the fact of high Chl concentration, 1 mm cuvette was used and front face technique was used to avoid distorted fluorescence signals causing by reabsorption of the emitting light.

In the measurements of refolded LHCII using non-labeled LHCP or spin-labeled LHCP, samples were excited at 470 nm where the Chl *b* molecules absorbed light. If all pigments were correctly bound to the LHCII, all exciting energy was transferred to Chl *a* and emitted as Chl *a* fluorescence at 680 nm. In the measurements of using dye labeled LHCP, samples were excited at the wavelength where the energy donor absorbed most light and the acceptor absorbed little light.

2.8.2.2. Time-resolved fluorescence measurement

Parameters:

Non-labeled LHCP:	DY 731 labeled LHCP:
Experiment Typ: Multigroup	Experiment Typ: Multigroup
Total time: 700 s	Total time: 700 s
Excitation: 470 nm	Excitation: 420 nm
Emission: 660 and 680 nm	Emission: 680 and 760 nm
Time increment: 1.0 s	Time increment: 2.0 s
Time integration: 0.1 s	Time integration: 0.15 s
Excitation band width: 0.5 nm	Excitation band width: 0.8 nm
Emission band width: 1 nm	Emission band width: 8 nm
Signal: S/R	Signal: S/R

Method:

Time-resolved fluorescence measurements were performed using a stopped-flow device (RX- 2000 Rapid Kintetics Accessory (Applied Photophysics Limited, UK)) at 20 ℃. The assembly was initiated by mixing equal volumes of recombinant protein and pigment solutions. Protein and pigment solutions were prepared as 2.7.11.1 described. 1.5 fold molecular excess of Chl *a* (8 Chl *a* per protein) was used in the measurement without Chl *b*. After proteins had been denatured and pigments were freshly added to its buffer solution, protein and pigment solutions were put in two syringes before measurements; 150 µl of either solution were taken, rapidly injected and mixed in a fluorescence cuvette, which was already fixed in the fluorescence spectrometer. However, due to the dead volume of rapid mixing device, each

1.5 ml protein solution could only have 3-4 injections after a steady state flow is reached. For each injection, syringe plugs were pushed to mix two solutions ca. 3s after recording signals. All measurements were taken under front face setting.

Kinetic traces were fitted to a sum of two exponentials by using the software Table Curve (version 2D 4.0, SPSS Inc., Chicago). In most cases, a biexponential function with the following equation can be used:

Decrease of the signal:

$Y = A + B * \exp(- XC) + D * \exp(- XE)$

Increase the signal:

$Y = A + B * (1-\exp(- XC)) + D * (1 - \exp(- XE))$

Characterize the individual steps by the reaction constants C and E, which are the reciprocals of the reaction times τ_1 and τ_2 results with the unit [sec]. The accompanying amplitudes B and D are the respective proportion of the step in the total signal change (Horn, 2004).

2.8.2.3. Circular dichroism (CD) spectroscopy

Parameters

CD spectra for analysing refolded LHCII monomer and trimer

Scan: 400-750 nm	Sensitivity: Standard
Data Pitch: 1 nm	Response: 2 s
Band width: 4 nm	Scanning Speed: 100 nm/min
Temperature: 4 ℃	

Time-resolved CD measurement

Wavelength: 700 nm	Measurement time: 1 hour
Data Pitch: 1 nm	Response: 1 s
Band width: 4 nm	Temperature: 24 ℃

UV-CD spectra for analysing protein secondary structure

Scan: 190-300 nm	Sensitivity: Standard
Data Pitch: 1 nm	Response: 2 s
Band width: 4 nm	Scanning Speed: 50 nm/min
Temperature: 23 ℃	

Method:

Circular dichroism (CD) is an absorption spectroscopy method based on the differential absorption of left and right circularly polarized light. Optically active chiral molecules will preferentially absorb one direction of the circularly polarized light. The difference in absorption of the left and right circularly

polarized light can be measured and quantified. UV-CD is used to investigate the secondary structure of proteins. Vibrational CD, IR-CD, is used to study the structure of small organic molecules, proteins and DNA. UV/Vis CD investigates charge transfer transitions in metal-protein complexes. CD is usually expressed as the differential absorbance of left and right circularly polarized light, $\Delta\varepsilon \equiv \varepsilon_L - \varepsilon_R$, or in degrees ellipticity (θ). Here, ε_L and ε_R are the molar extinction coefficients for left circularly polarized (LCP) and right circularly polarized (RCP) light. The degree of ellipticity (θ) is defined as the tangent of the ratio of the minor to major elliptical axis; linear polarized light has 0 degrees of ellipticity (θ), while fully LCP or RCP will have + or - 45 degrees respectively. Molar ellipticity [θ] is circular dichroism corrected for concentration, and molar circular dichroism and molar ellipticity can be converted directly by equation (Greenfield, *Nat Protoc*. 2006):

$$\Delta\varepsilon = [\theta]/3298.2 \quad \text{deg.cm}^2.\text{dmol}^{-1}$$

The LHCII contains a lot of chromophores, Chls and carotenoids. A close electronic coupling between the pigments and the protein backbone leads to an increase or decrease of the electronic levels, which are visible as a clear positive / negative peak in the CD spectrum. If the Chls are tightly located, their π electron-cloud can affect each other and the energy transfer results in either signal amplification or excitonic split. The experimentally observed negative CD bands around 470 and 490 nm upon monomerization/trimerization due to interactions between pigments in different monomeric subunits (Georgakopoulou et al, 2007) were used for detecting whether LHCII were correctly folded.

In proteins, absorption in the region 240 nm and below is due principally to the peptide bond; the different types of regular secondary structure found in proteins give rise to characteristic CD spectra in the far UV. Fitting the data from far UV-CD spectra in different algorithms can provide an estimation of the secondary structure composition of proteins (Kelly, et al. 2005).

2.8.2.4. Electron paramagnetic resonance spectroscopy

Theoretical background:

Electron Paramagnetic Resonance (EPR), also called Electron Spin Resonance (ESR), is a branch of magnetic resonance spectroscopy which utilizes microwave radiation to probe species with an odd number of electrons, such as radicals, radical cations and anions and certain transition metals in the presence of a static magnetic field. An electron is a negatively charged particle with certain mass, it mainly has two kinds of movements. The first one is spinning around the nucleus, which brings orbital magnetic moment. The other is spinning around its own axis, which brings spin magnetic moment. Magnetic moment of the molecule is primarily contributed by unpaired electron's spin magnetic moment.

This magnetic moment interacts with the applied magnetic field. For single unpaired electron, there will be two possible energy states, this effect is called Zeeman splitting.

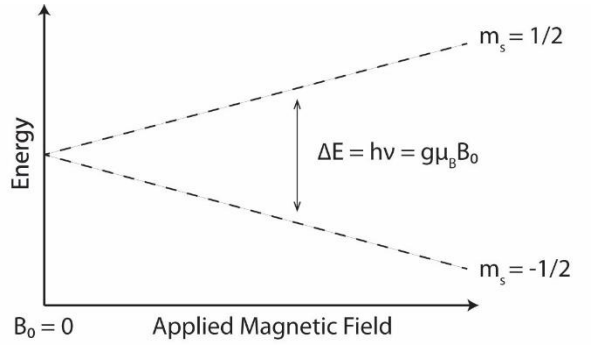

In the presence of external magnetic field, with absorption of radiation, the difference between the two energy states can be written as:

$$\Delta E = E(m_s=1/2) - E(m_s=-1/2) = h\nu = g\mu_B B$$

(g is the free electron factor with a value of 2.0023; μ_B is the magnet moment; B is the applied magnetic field)

With the intensity of the applied magnetic field increasing, the energy difference between the energy levels widens until it matches with the microwave radiation, and results in absorption of photons (Weil J. and Bolton J. *Electron Paramagnetic Resonance: Elementary Theory and Practical Applications.* Second Edition. Wiley-Interscience; 2007).

Experimental settings:

Proteins tagged with paramagnetic groups (usually nitroxide) can be easily detected by EPR. Pairs of nitroxide labels were introduced into recombinant LHCP via covalently binding on Cys residue at certain positions of protein backbone (2.7.15). Labeling efficiency was measured by X-band (9.5 GHz) continues wave EPR (cw-EPR) spectrometer benchtop MiniScope MS 300 (Magnettech GmbH, Germany) at Max Planck Institute of Polymer Research Mainz and working group of Prof. Dr. Katja Heinze (Institute of Inorganic and Analytical Chemistry, Johannes Gutenberg University-Mainz). The distance between two spins was analyzed by using double electron-electron resonance (DEER) technique. Four-pulse DEER measurements were measured on a home-built apparatus by Dr. Yevhen Polyhach at the ETH Zürich (working group of Prof. Dr. Gunnar Jeschke). The temperature was constant at 50 K. Measurements were done in a modified Q-band spectrometer (34 GHz). Further detailed information to the EPR specifications, and DEER measurements are described in Dockter *et al*. (2012). DEER data were analyzed using the "Deer Analysis 2013" program (http://www.epr.ethz.ch/software).

3. Results

This work aims at characterizing intermediate complex during LHCII assembly, containing Chl *a* and carotenoids but without Chl *b*. Unlike the fully pigmented complex that is stable and can be separated from unfold apoprotein LHCP (the light-harvesting chlorophyll *a/b*-binding protein) by partially denaturing gel electrophoresis (so called "green gel") (Paulsen, 1990), weakly bound Chl *a* molecules would dissociate from the protein during gel electrophoresis (Fig.3.1). Therefore it was unlikely to have furthermore purification steps to get purer intermediate complex after mixing LHCP, Chl *a* and carotenoids; protein labels, which could allow us to observe protein and protein folding, were highly required in this work. In native LHCII complex, there is only one cysteine (Cys) residue and can be replaced by serine (Ser) residue without disturbing protein folding (Grundlach et al, 2009). Thus maleimide protein labels that can be covalently bound to SH group of Cys residue were chosen as markers and introduced site-specifically into LHCP. That fluorescent labels serve as energy donor or acceptor to Chl molecules based on Förster resonance energy transfer (FRET) enables us to monitor whether Chl molecules have been bound or not; pairs of nitroxide labels allow us to investigate whether and how protein structure changes *via* site-directed spin labelling (SDSL).

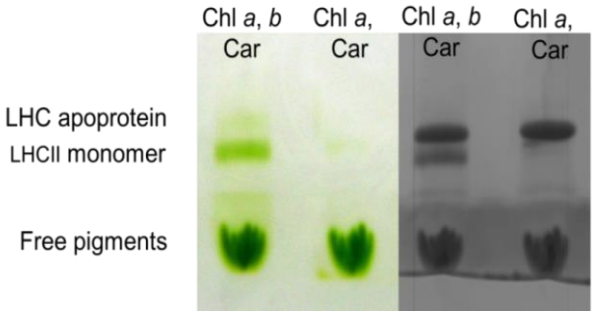

Fig.3.1. Partially denaturing gel electrophoresis of LHCII monomer and Chl *a* only containing intermediate, green gel (left-hand panel) and gel after coomassie staining (right-hand panel).

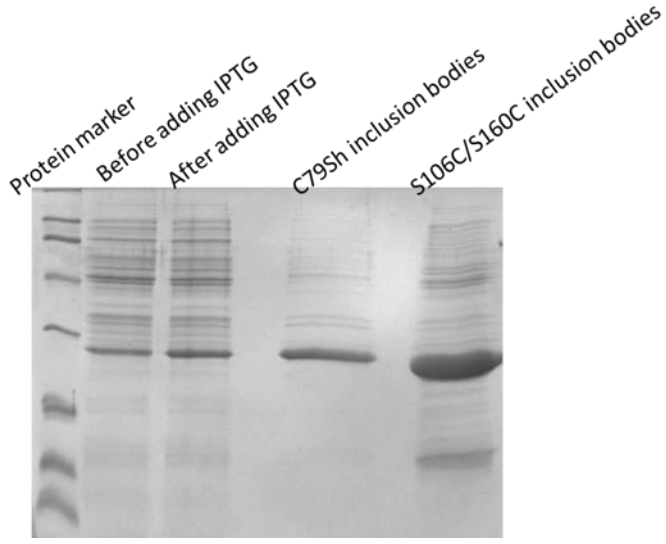

Fig.3.2. Coomassie stained 15 % denaturing SDS glycerol gel of C79Sh and S106C/S160C inclusion bodies. The second and third lanes were C79Sh bacterial cultures before and after adding IPTG inductor. The fourth lane was C79Sh IBs after washing steps. The fifth lane was S106C/S160C IBs after washing steps.

3.1. Purification of LHCP

As LHCP was overexpressed from bacterial cells, the inclusion bodies (IB) after overexpression contain not only target protein LHCP but also bacterial proteins after disruption process. Most of

the bacterial proteins were got rid of during the washing step, a few of them left as foreign proteins. The purity of bacterial LHCP could be checked on a denaturing SDS gel (Fig.3.2). The LHCP formed a distinct band at 26 kDa. Lane 2 and 3 showed a lot of foreign proteins were together with our target protein LHCP before washing step. The amount of foreign proteins differed, depending on the clone and disruption process. It is unclear what these foreign proteins were. In order to see how much foreign proteins can be labelled, two different fluorescent dyes were chosen, a hydrophobic dye Rhodamine Red® C2 maleimide and a hydrophilic dye DY-634 maleimide; a Cys free mutant C79Sh was used as a

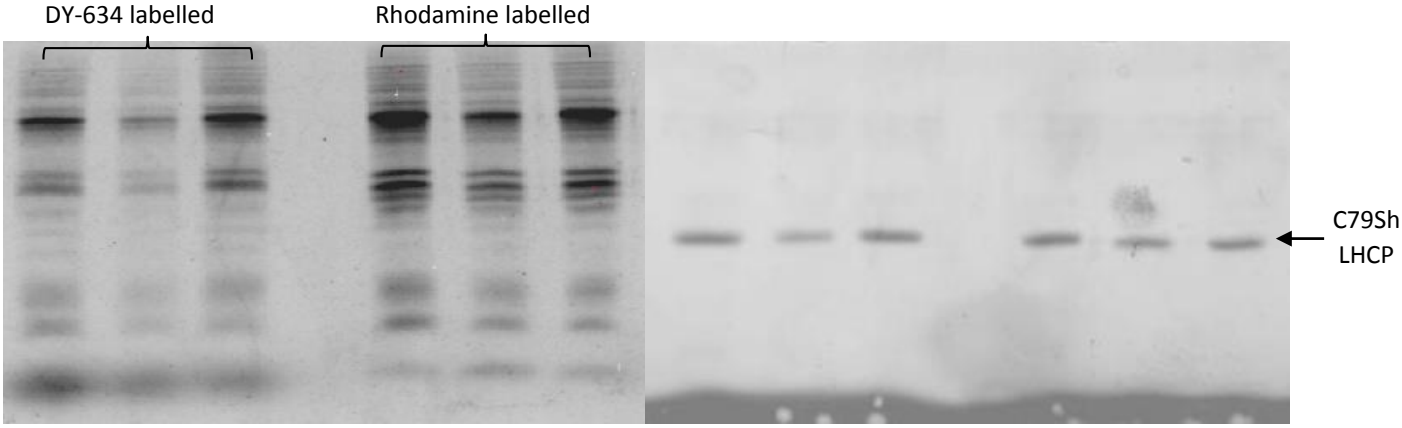

Fig.3.3. Fluorescence image (left-hand panel) of denaturing gel and coomassie stained gel (right-hand panel) of dye labelled C79Sh after different precipitation methods. All re-precipitated proteins were re-dissolved in SDS and analyzed by denaturing gel. For each dye, the first lane was sample from acidic acetone precipitation method; the second lane was sample from ethanol precipitation method; the third lane was using ethanol and NaCl to precipitate proteins.

control. Three methods were applied to check how much protein would be re-precipitated after labelling. Although these foreign proteins were hardly seen after coomasssie staining (Fig.3.3 right-hand panel), quite a few of them had noticeable fluorescence emission and nearly spread among the whole lane, from small molecules to big ones (Fig.3.3 left-hand panel). According to lane 4 in Fig.3.2 and right-hand panel of Fig.3.3, the foreign proteins only took a very small portion before and after labelling; therefore, the percentage of foreign proteins was assumed very low, and the absorption at 280 nm was taken and calculated as LHCP concentration. How efficiently those foreign proteins were labelled was calculated as apparent labelling yield:

$$\text{Apparent labelling yield (\%)} = \frac{dye\ concentration\ (\mu mol/l)}{protein\ concentration\ (\mu mol/l)} * 100\%$$

The yield of how many proteins re-precipitated after labeling procedure was calculated as:

$$\text{Protein yield (\%)} = \frac{amount\ of\ precipitated\ protein\ (\mu g)}{amount\ of\ protein\ used\ (\mu g)} * 100\%$$

As Table 3.1 shown, these foreign proteins had quite high apparent labelling efficiency: more than 30% apparent labelling yield for DY-634 and nearly 50% for Rhodamine. In all three precipitation methods, acidic acetone had highest precipitation yield; nearly 70% proteins were able to precipitate, however,

Table 3.1 Yields of protein after re-precipitation and apparent labelling yield of foreign

	Precipitation Method	Protein yield	Apparent labelling yield
DY-634	HAc+Aceton	69.42%	31.70%
	ethanol	39.22%	29.06%
	ethanol+NaCl	56.71%	34.04%
Rhodamine	HAc+Aceton	79.50%	48.72%
	ethanol	48.50%	47.63%
	ethanol+NaCl	63.07%	50.51%

Acidic acetone precipitation was followed by the method described in method chapter 2.7.9.1; ethanol precipitation was done by using ethanol to precipitate proteins with ethanol at 80% end concentration; ethanol + NaCl precipitation was based on ethanol precipitation and additionally added 0.5 mol/l NaCl. After precipitation, samples were centrifuged and pellets were washed by 70% ethanol. After re-dissolved in SDS, re-precipitated protein concentration and fluorescent dye concentration were analysed by absorption spectra.

these three re-precipitation methods had almost the same dye apparent labelling yield. Therefore it is very important to get rid of these foreign proteins because these foreign proteins would also be labelled by spin label for EPR and cause bigger noise in DEER measurements.

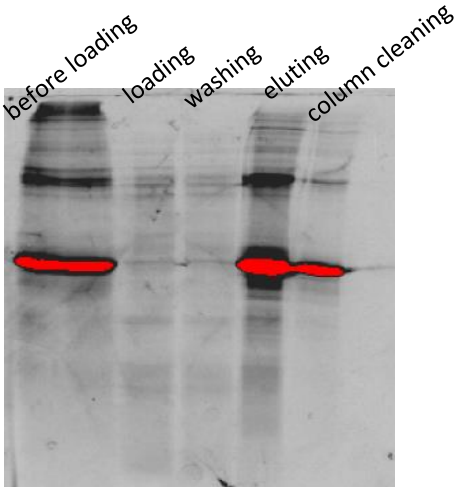

Fig.3.4. Fluorescence image of denaturing gel of dye labelled LHCP loading and purification on Ni-column. The first lane was the sample before loaded on Ni- column. The rest lanes were elutes collected at each step. Proteins were eluted from Ni-column by 0.3%SDS/0.3mol/l imidazole solution. To obtain fluorescence bands from the contaminants, long exposure time was used, and dye labelled LHCP always saturated during imaging and showed red bands

Many LHC mutants have His-tag at C-terminus; Ni-sepharose column were applied to try to get rid of contaminants in the inclusion bodies. The resin usually exhibits high affinity and selectivity for 6xHis-tagged recombinant fusion proteins. It was possible to get rid of nonspecific binding protein in the washing step. We used dye-labelled protein, and dissolved in urea. As Fig.3.4 showed, most proteins were able to bind to Ni^{2+} and eluted from column in the eluting step. Only a few were left after eluting. However, the purification was not significant; foreign proteins were eluted together with target protein. We tried to use more washing steps with increased imidazole concentration step by step to get rid of

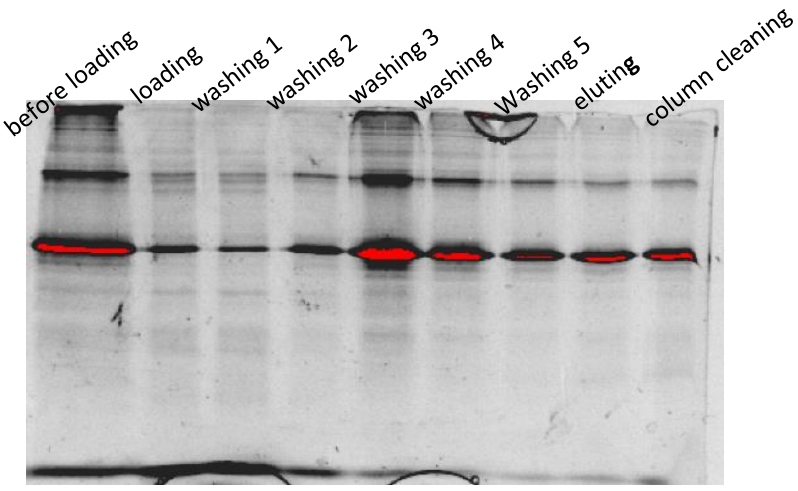

Fig.3.5. Increased imidazole concentration in the washing steps of Ni-column purification from washing step 1 to step 5, the imidazole concentration was increased gradually from 10 mmol/l to 50 mmol/l

non-specific bound foreign proteins. When imidazole concentration reached 30 mmol/l, quite a lot of target protein was eluted from column (Fig.3.5). Also we noticed that most free dye was separated but most foreign proteins were still left. The Ni-sepharose column had almost no effect on purifying LHCP. Based on good separation of proteins on analytical SDS-PAGE, first attempt was tried on 1.5 mm thick gel, which enabled us to load up to 150 µg protein on one gel; electroelution was used for eluting protein from gel bands followed by the method describe by S á-Pereira (S á-Pereira, 2000). Dye labelled protein was loaded on the very left lane and used as a marker. Gel slices must carefully be inserted into dialysis-tubing. Overlapping of gel slices caused loss of protein elution. Electroelution was able to recover up to 80% protein from gel. The protein was further concentrated in 10 KDa Amicon Ultra Centrifugal Filters. However, this approach always resulted in a very high LDS concentration, more than 12%, after Amicon centrifugation step. Too high LDS concentration caused very low LHCII reconstitution yield and we could hardly re-precipitate LHCP from the solution. Taking advantage of the lower solubility of free potassium dodecyl sulfate (KDS) vs micellar KDS even at neutral pH, KCl with final concentration from 10 to 50 mmol/l was additional added to protein solubilized in 0.5% LDS (Carraro et al, 1994; Suzuki and Terada, 1988); Suzuki (1988) found that when SDS concentration was 0.5%, the lowest concentrations of potassium salt to remove DS was around 20 mmol/l and this concentration was sufficient enough to get rid of most of the DS. Similar results were found in LHCP. When KCl final concentration was 10 mmol/l, nearly no protein co-precipitated with KDS; at 20 mmol/, some KDS precipitated and formed a small pellet, about 97% protein remained in the supernatant. Increased KCl final concentration resulted in not only more KDS precipitation but also loss of the protein. When KCl final concentration reached 50 mmol/l, only about 62% protein left in aqueous solution. Using KCl with a final concentration of 20 mmol/, KDS precipitation method was applied on protein solution collected from electroelution. After the first precipitation, more than half of dodecyl sulfate (DS) was removed; another half of DS was got rid of after repeating precipitation step. Third trial of precipitation failed. Protein was concentrated to 90 µmol/l and LDS ended up at a concentration more than 3%, which was triple as much as that in protein buffer solution for EPR rapid-mixing method.

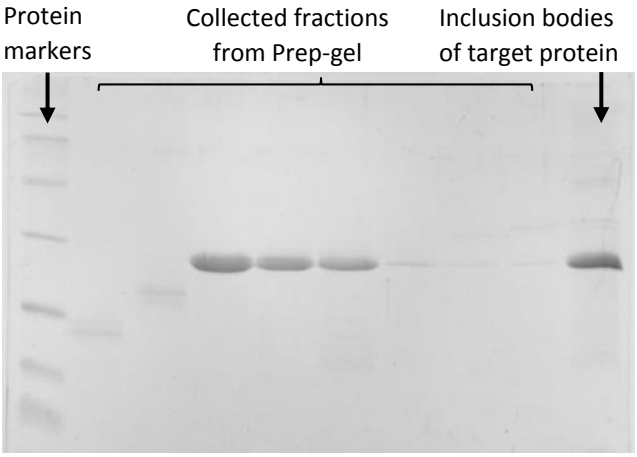

Fig.3.6. Every 8 aliquots of collected fractions from preparative gel electrophoresis were analyzed by 15% denaturing SDS-PAGE gel to determine in which range the fractions contain target protein.

Finally, preparative gel electrophoresis (Prep-gel) was adopted. Prep-gel enabled us to load 50 mg total protein. Fractions containing target proteins were directly eluted and collected after running through a cylindric 15% polyacrylamide gel. Analytical gel electrophoresis was used to determine which collecting fractions of Prep-gel contained the target protein. We first loaded every 8 aliquots to find out in which range aliquots contained purified target protein (Fig.3.6). Later, all collected fractions in this range were analyzed again on gel (Fig.3.7) to determine which aliquots would be used to precipitate purified LHCP and perform further measurements. All fractions were continually collected; the protein band density against time showed that the elution of protein from Prep-gel fitted a positive skewed distribution. The reason for this phenomenon was complicated. Uneven gel column, uneven temperature, etc. could cause non-Gaussian distribution of the elution. As a result, fractions where target protein started and finished collecting had to be abandoned because those fractions always contained foreign proteins which had closer size as LHCP; especially the few fractions where LHCP started to collet, as they usually had quite a lot of LHCP as well. Prep-gel yielded between 15-30%, which was not very high but good enough for further experiments. Purified LHCP must be precipitated. Protein, which was taken from the elution and was directly applied for labelling right after getting rid of glycine and tris, had rather poor labelling yield.

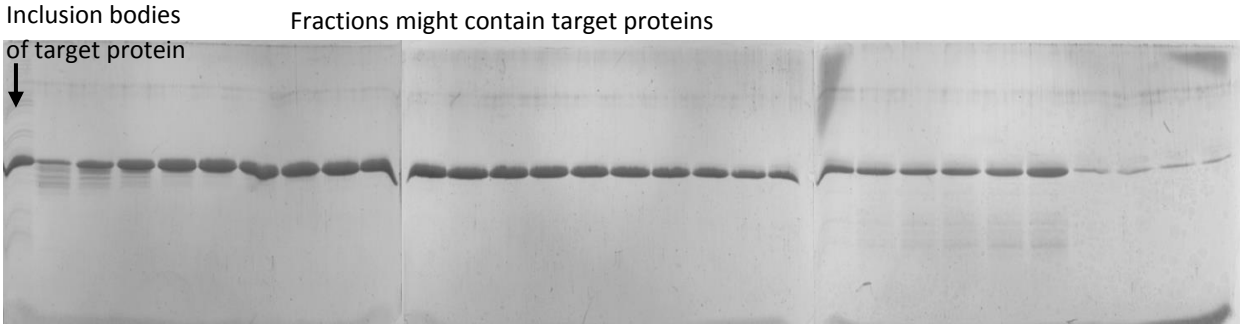

Fig.3.7. Aliquots of collected fractions from preparative gel electrophoresis were further analyzed by 15% denaturing SDS-PAGE to determine which fractions contain pure target protein.

CW-EPR proved that after preparative gel electrophoresis, most foreign proteins which could also be labelled were got rid of. Cys free mutant C79Sh and single Cys mutant S160Ch were chosen; both proteins having been purified from Prep-gel and not being purified were labelled by PROXYL. Labelled proteins then were dissolved in 1% LDS and prepared in determined protein concentrations; all samples

were loaded in 50 µl capillary with a liquid level of more than 2 cm high. All samples as well as pure PROXYL spin labels were measured by X-band (9.5 GHz) cw-EPR (1.5 gauss modulation and 16 microwave attenuation) at room temperature (Fig.3.8). Spin concentration of labelled protein was determined from the area of the peaks divided by the peak area from pure spin labels of known concentration. The spin concentrations calculated from the spectra were: C79Sh without Prep-gel purification had less than 20 µmol/l spin; after purification, spin concentration dropped down to less than 5 µmol/l; non-purified S160Ch had about 110 µmol/l spin and purified S160Ch had about 60 µmol/l spin. Converting to labelling yield, C79sh had about 20% foreign labelling before purification and less than 10% was left after Prep-gel. This small amount of spin was probably from free PROXYL labels, which were not cleaned by 70% ethanol in the washing steps. The real labelling yield of pure S160Ch was then corrected to 50-60%. Foreign proteins in non-purified S160Ch almost labelled equal amount of spin as the Cys residue in S160Ch. Purified S160Ch had similar dye labelling efficiency, about 60% dye labelling efficiency in both Rhodamine and DY-731. Double Cys mutants differed from each other. Most of them had in average about 50% labelling efficiency per each labelling site. However, some mutants, like A174C/V196C had not very good labelling, only 75% of total labelling. If both labelling sites were equally labelled, only 37.5% labelling yield per each site. If not equally labelled, protein which had both sites being labelled would take rather low proportion of total protein. It was unclear whether both Cys residues of double Cys mutant were properly labelled from the apoprotein samples; cw-EPR only told us how much spin in total. Nevertheless, we could conclude that preparative gel electrophoresis was so far the most effective method for LHCP purification; purified protein containing single Cys residue was able be to reach about 60% labelling yield.

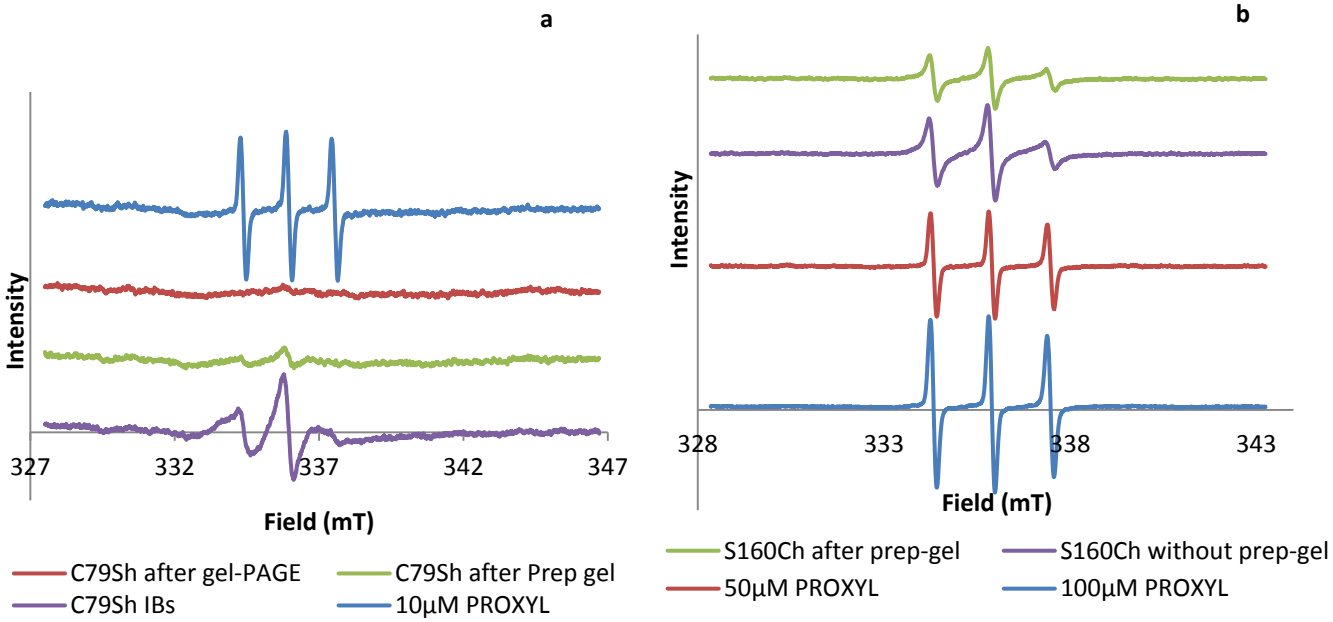

Fig 3.8. cw-EPR spectra of spin labelled LHCP with and without Prep-gel purification. All apoproteins were prepared in 1% LDS. a) C79Sh samples were prepared as 50µmol/l and compared with 10 µmol/l PROXYL-IAA; b) S160Ch samples were prepared as 100 µmol/l and compared with 50 and 100 µmol/l PROXYL-IAA. Pure spin label was dissolved in the same buffer which solubilized LHCP.

3.2. Comparison of LHC reconstitution methods for applying only Chl *a*

In *in vitro* work, LHCII can re-assemble using two methods: detergent-exchange method and detergent diluting method. In detergent-exchange method, LHCP was first denatured by SDS, total pigment mixture (TE) containg Chl *a*, Chl *b* and carotenoids was given. After incubation for reconstituting, OG was added and subsequently KCl was added to precipitate DS, the refolded LHCII were forced to move to OG micelles. This method could yield about 70% refolded protein. (Dietz, 2012). SDS-denatured detergent diluting method was used for kinetic study. Protein and pigment solution were kept in two individual syringes of stopped-flow device before mixing. It took about 15 min from one measurement start until the next one was ready. Each time, 1.5 ml of each solution was prepared and was able to have three measurements after equilibrating system. Therefore, it was very often that each solution stayed seperatedly for more than half an hour until the last portion mixed. To analyzed the reconsitution yield against time, mixing both solutions was performed manually. The first sample, which was operated immediately when pigment solution was ready, was regarded as "0 min" in Fig.3.9, indicating 0 min waited for the mixing. After 15 min incubation time, another mixing was performed and regarded as "15 min", meaning that each solution was kept separatedly before mixing. Every 1.5 ml of each solution was able to perform 6 times mixing. This method could reach more than 60% reconstitution yield, when both solutions were stayed separately for 45 min. After 1 hour, LHCII reconstitution yield slightly dropped but still was more than 50%. In general, the reconstitution yield gradually decreased against time. In the figure, an exception was: when both solutions has waited for 45 min before mixing, the sample gained the most reconstitution yield. We had to admit that the "green gel" was performed until the reconstituion from the last sample finished. This made all the samples could not be anaylzed by "green gel " immediately but waited for a certain time. It was unclear whether LHCII would decompose during the waiting time or not. These uncertainties made the "45 min result" might not be the maximal value in real. But we still felt confident to say that there were more than 50% reconsituted LHCII in the aqueous solution. The reconstitution yield was not as good as that from detergent-exchange method, but still feasible. In this case, we would speculate that there would be no less percent of LHCP associated with Chl *a* if we only omitted Chl *b* but kept the protein as well as Chl *a* and carotenoids at the same concentrations as they were in the reconstitution with TE.

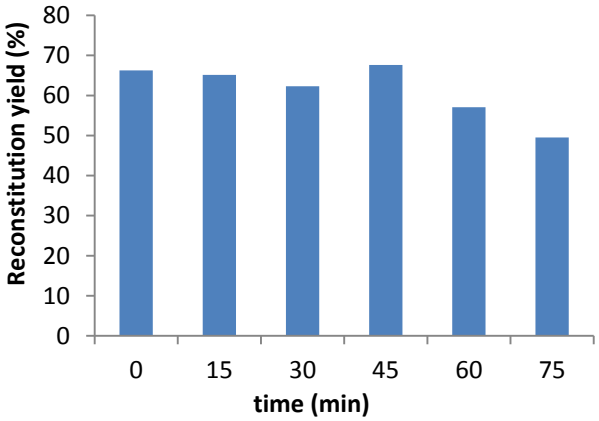

Fig.3.9. LHCII reconstitution yields against time following SDS-detergent diluting method mixed by hand. 1.5 ml protein and pigment solutions were prepared as stock solution, respectively. Measurements were initiated by manually mixing 250 µl of each solutions immediately after pigment solution was ready; mixing was repeated every 15 min. Reconstitution yields were analyzed by "green gel".

For intermediate complex, LHCP, Chl *a* and the complex reached an equilibrium due to the weak and reversible binding of Chl *a*.Therefore, in order to have more intermediate complex in the system, excess amount of Chl *a* over apoprotein were applied. Both methods were performed using Chl *a* and carotenoids instead of pigment mixure containing Chl *b* in the standard protocols. Chl *a* fluorescence was measured and compared with pure LHCII monomer with the same protein concentration (Fig.3.10). All measurements used non-labelled protein; therefore there was no FRET happened in the intermediate complex and due to the fact that excess amount of Chl *a* was used, the Chl *a* fluorescence intensity at 680 nm of intermedate sample should higher than that of pure LHCII monomer when they are at the same concentration and no pigments aggregate. In detergent-exchange reconstituted samples, one sample followed standard detergent-exchange protocol using pigment mixture containing only Chl *a* and carotenoids corresponding to an excess over protein of 4 (assuming 8 Chl *a* per LHCP) and 4 (assuming 4 xanthophylls per LHCP), respectively. Another sample was applied with the same amounts of LHCP and pigments but a lipid-detergent mixture containing 25% OG/ 0.8% PG/ 10% Tx instead of 10% OG in the protocol. Purified LHCII monomer was concentrated to about the same protein concentration as that after standard detergent-exchange method when no protein was assumed to be lost in the KDS precipitation step. This protein concentration was a little bit higher than the real protein concentration. Because 4-fold molar excess of Chl *a* was applied in the intermediate samples, if there were no big Chl aggregation and no big loss of pigments in the KDS precipitation step, the Chl *a* fluorescence emssion of the intermediate complex was thought to be higher than that of pure LHCII. However, the intermediate complex had much less Chl *a* emission than that of pure LHCII(Fig.3.10a). More lipids would help more Chl *a* stay in the aqueous solution, but the Chl *a* emission was still lower than the pure LHCII. This indicated that although excess amount of Chl *a* was applied, detergent-exchange method could not keep more than 8 Chl *a* molecules per LHCP in aqueous solution, and this might cause less intermediate complex in the solution.On the other hand, in the detergent diluting

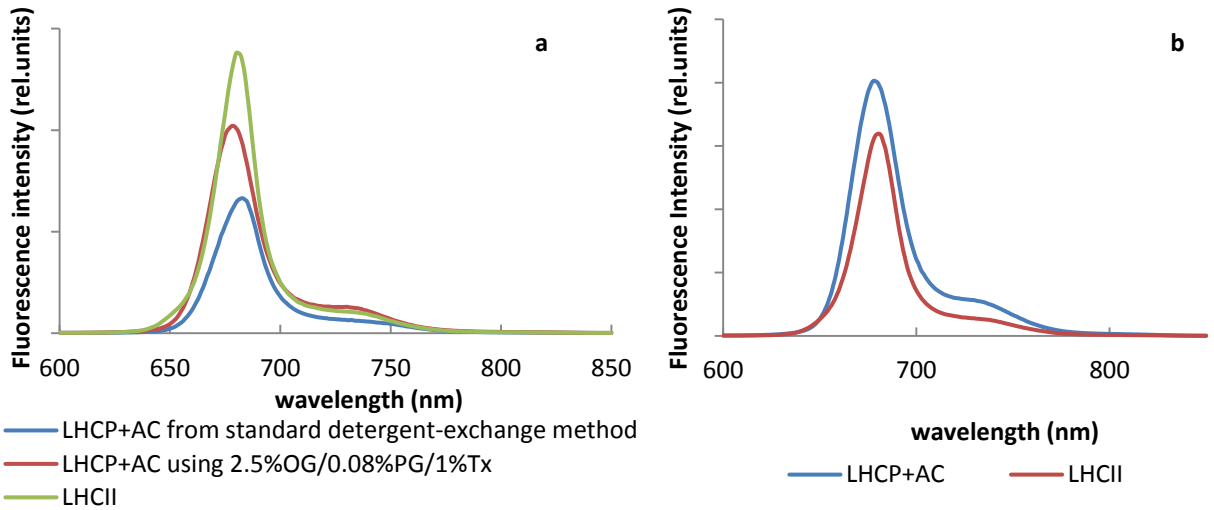

Fig.3.10. Fluorescence emission of Chl *a* intermediate complex prepared from *a)* detergent-exchange method and *b)* detergent diluting method in compare with LHCII fluorescence at the same protein concentration, respectively. All spectra were excited at 420 nm.

method (Fig.3.10b), LHCP was mixed with carotenoids and 3-fold molar excess of Chl *a*; although the emission at about 725 nm showed more aggregated Chl *a* in the intermediate sample than in pure LHCII monoer, higher emission at 680 nm still indicated excess amount of Chl *a* over protein in the system.

Another advantage of detergent diluting method is that this method is able to be applied for preparing EPR samples immediately after mixing protein and pigments. In Dockter's work (Dockter, 2009), time-resolved DEER measurements were done by manually mixing protein and pigment solutions containing high reactant concentrations; the protein solution contained 160 µmol/l spin-labeled LHCP. After the reaction time the sample could be mixed with 80% glycerol as a cryoprotectant then immediately loaded into an EPR tube and flash-frozen in liquid nitrogen. The final protein concentration was about 40-50 µmol/l. However, protein only reached about 10 µmol/l after detergent-exchange procedure. For DEER measurements, higher protein concentration was required for a good signal-to-noise ratio. Therefore, protein must be concentrated to much higher concertatration, usually 30-40 µmol/l, before adding glycerol. Using a centrifugal filter, we could not only get rid of excess KCl, but also concentrate protein. This method was based on centrifugation, molecules smaller than the molecular weight cut-off of centrifugal filter would pass through the membrane filter, and bigger molecules were stay above the membrane. And usually after centrifugation, detergent micelles containing protein and pigments were at the bottom of the filter unit close to the membrane; the local protein concetration was higher than the protein concentration close to the liquid level. The centrifugal force might cause protein re-assemble with pigments and pigment aggregation at the same time during centrifugation, because the higher local concentration at the bottom of the filter unit would increase the possiblity of protein-pigment and pigment-pigment "meeting" each other.

In the absence of Chl *b*, we could not determine whether Chl *a* molecule has bound or not, therefore an acceptor fluorescent dye was chosen and used as a monitor to observe Chl a bindings. The acceptor dye DY-731 had an absorption maximum at 736 nm and an emission maxima at 759 nm. According to the equation for FRET efficiency (Förster, 1948):

$$E = \frac{R_0^6}{r^6 + R_0^6} \tag{1}$$

Where *E* is the FRET efficiency, R_0 is the Förster critical distance and r is the donor and acceptor radius. When r equals the Förster distance, the transfer efficiency is 50%, which means at this separation radius, half of the donor excitation energy is transferred to the acceptor via resonance energy transfer, while the other half is dissipated through other available processes, including fluorescence emission. R_0 of Chl *a* to DY-731 was calculated with the following equation:

$$R_0 = 0.211\ [\kappa^2 * \eta^{-4} * \Phi F * J(\lambda)]^{1/6} \tag{2}$$

Here κ^2 is the orientation factor, η the refractive index of the solvent, ΦF the fluorescence quantum yield of the Chl *a* and $J(\lambda)$ the overlap integral between donor emission and acceptor absorption spectra. As a first approximation κ^2=2/3 (for randomly oriented dipole moments) and η=1.54 (refractive index for protein environment) were used. The spectra overlap was calculated with the following equation:

$$J(\lambda) = [\int F_D(\lambda)*\varepsilon*\lambda^4 d\lambda]/[\ F_D(\lambda)\ d\lambda] \quad (3)$$

where F_D is the fluorescence intensity of the donor, λ is the wavelength, and ε is the molar extinction coefficient of the acceptor (Werwie, 2012). The calculated Förster critical distances of Chl *a* to DY-731 is about 59.85 Å.

In the fully folded LHCII, all Chl molecules are expected to be within this distance and, therefore, in principle to be able to transfer excitation energy to the dye. Consistently, purified DY731-labelled LHCII exhibits an energy transfer efficiency of ~90% (Boggasch, 2006). Fig.3.11. showed Chl emission of dye-labelled LHCII trimer had nearly all quenched. The acceptor dye was attached site-specifically to the stromal loop domain in LHCII, early study (Horn, 2004) had shown that fluorescent dyes in this position did not have an effect on the folding kinetics compared to the non-labelled protein,

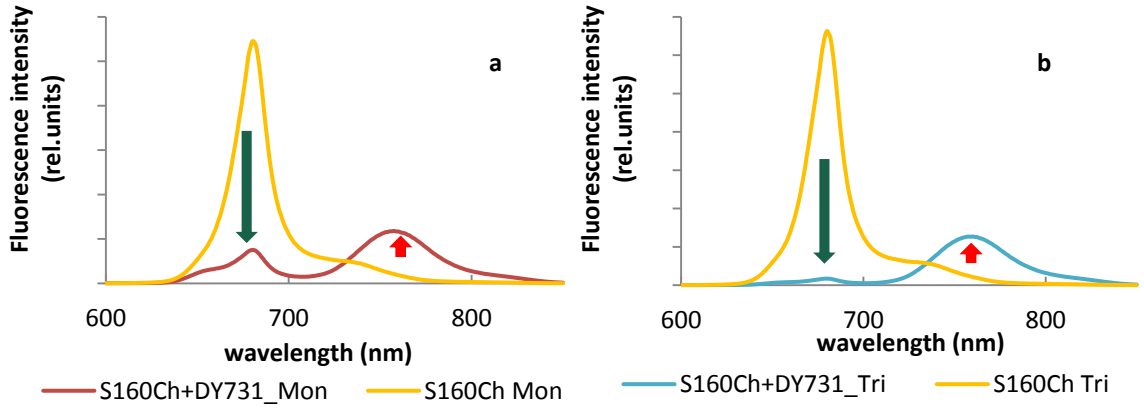

Fig.3.11. Steady-state fluorescence emission spectra of *a)* monemers and *b)* trimers of dye-labelled and non-labelled S160Ch. All spectra were excited at 420 nm, which was the wavelength where Chl *a* molecules were mainly excited and Chl *b* had very less absorption.

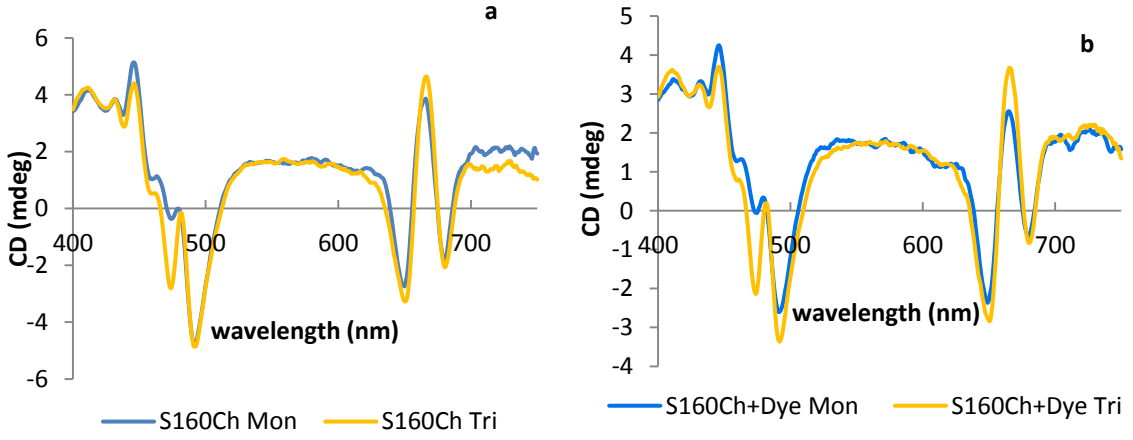

Fig.3.12. CD spectra of purified reconstituted *a)* non-labelled and *b)* labelled LHCII monomers and trimers.

demonstrating that the labels do not interfere with protein folding or complex assembly. CD spectra (Fig.3.12) also showed that the fluorescent dye had no effect on the structure of the complex. Therefore, all 8 Chl *a* molecules were supposed to transfer all their energy to the acceptor dye in pure labelled LHCII monomer.

DY-731 labelled LHCP as well as a labelled negative mutant S3CΔC49, which lacks of 49 C-terminal amino acids and can't fold, mixed with Chl *a* and followed detergent-exchange protocol. After removal of precipitated KDS, Chl *a* emission was measured before washing step. Samples were first centrifuged to half of the volume, washing buffer was added to reach the original volumn, repeated the step above 3 times. KCl should go through membrane and left protein and pigment in detergent micelles in the filter. In Fig.3.13, we noticed Chl *a* emission at 680 nm of each sample before washing step had lower intensity than Chl *a* emission of LHCII monomer. After washing step, the negative control protein had almost no change at the dye emission, LHCP mixed with Chl *a* had a little decrease of dye emission and LHCP mixed with TE had significant Chl *a* quenching. In the negative control measurements, no energy tranfer was found between Chl *a* and the acceptor dye, the small quenching of Chl *a* emission was assumed to be the aggregated Chl molecules and probably also a small amount of loss during the centrifugation. Fluorescence image (Fig.3.13e) of LHCP mixed with Chl *a* and carotenoids showed the protein concentration was almost the same before and after washing step. In the lane of LHCP mixed with TE before washing step, LHCP and LHCII monomer bands had almost the same density on coomassie stained "green gel", indicating about 50% reconstitution yield. While LHCP mixed with TE after washing step had green band at the position where the molar mass was higher than where LHCII monomer was (Fig.3.13d). The highest band looked like where LHCII trimer appeared and the density of this band was higher than that of LHCP band in the fluorescence image. This indicated the formation of LHCII oligomers and some re-assembly of LHCII, and also could explained the big quenching of Chl *a* fluorescence. Because the sample was first concentrated and then diluted to the original concentration. We would assume the formation of oligomer was happened at the concentrating step. According to the results from LHCP mixed with Chl *a* and carotenoids, we could also presume that it's very possible that Chl *a* would aggregate if we concentrate the sample to EPR sample concentration. Therefore detergent-exchange method was not suitable for studying intermediate complex. Detergent diluting method was chosen for preparing FRET and EPR samples.

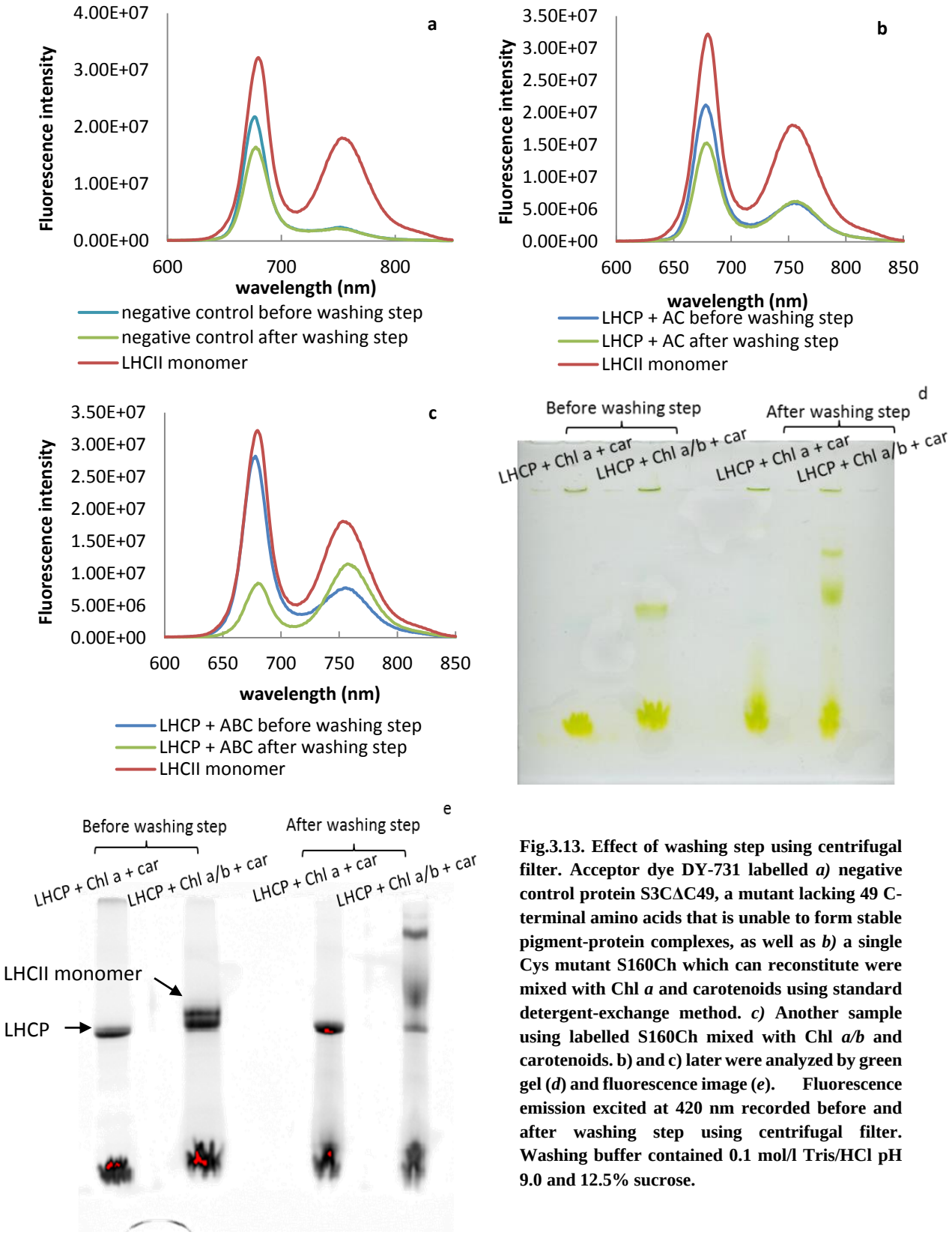

Fig.3.13. Effect of washing step using centrifugal filter. Acceptor dye DY-731 labelled *a)* negative control protein S3CΔC49, a mutant lacking 49 C-terminal amino acids that is unable to form stable pigment-protein complexes, as well as *b)* a single Cys mutant S160Ch which can reconstitute were mixed with Chl *a* and carotenoids using standard detergent-exchange method. *c)* Another sample using labelled S160Ch mixed with Chl *a/b* and carotenoids. b) and c) later were analyzed by green gel (*d*) and fluorescence image (*e*). Fluorescence emission excited at 420 nm recorded before and after washing step using centrifugal filter. Washing buffer contained 0.1 mol/l Tris/HCl pH 9.0 and 12.5% sucrose.

The apoprotein can also be reconstituted starting from a solution in guanidine hydrochloride (GuCl). Reconstitution was done following the method described in Yang, *et al.*(2003). LHCP is very insoluble in OG solution. 4 mg/ml LHCP was first denatured in 6 mol/l GuCl. After mixing LHCP GuCl solution and pigment solution without pigment in the ratio of 1:10, LHCP quickly precipitated.

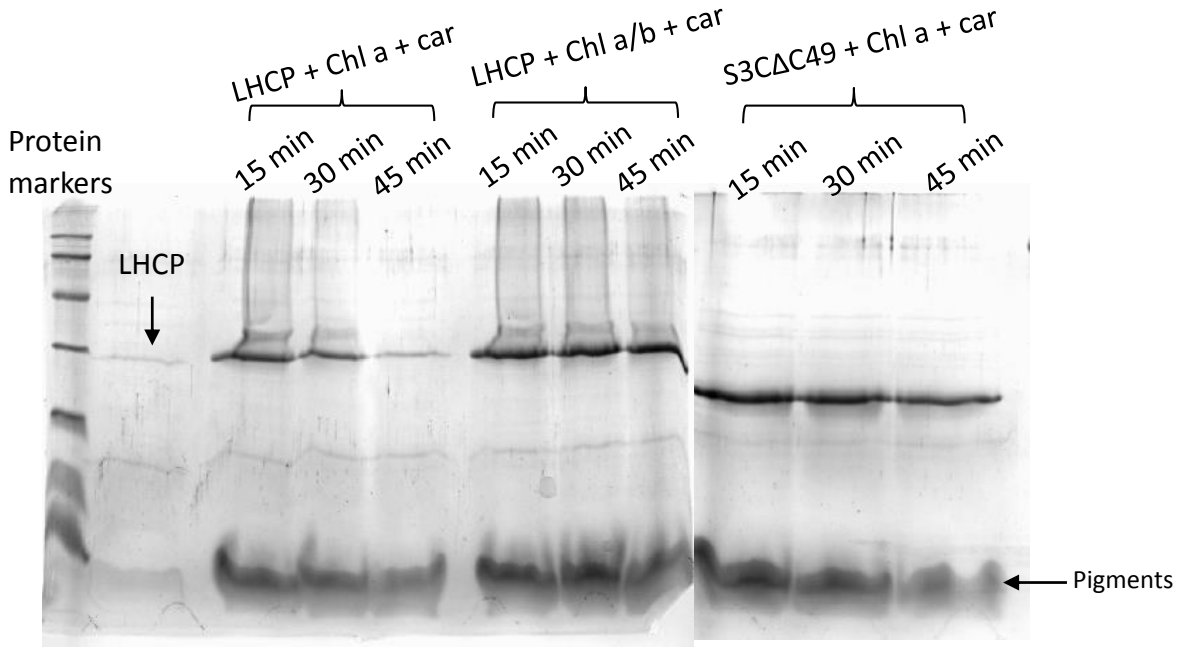

Fig.3.14. PAGE analysis of reconstituted from GuCl dissolved LHCP. LHCP as well as negative control protein S3CΔC49 was dissolved in 6 mol/l GuCl, respectively. Pigments were dissolved in OG/PG buffer. The reconstitution was initiated by manually mixing the pigment solution and GuCl-denatured protein solution at a ratio of 10:1. After 15 min incubation, samples were centrifuged. 32 µl supernatant was taken from the supernatant and loaded on 15% PAA gel; after another 15 min, centrifuged samples again and took 32 µl from the supernatant for gel. The step above was repeated again. LHCP mixed with only pigment buffer without pigment was loaded on the first lane next to protein marker.

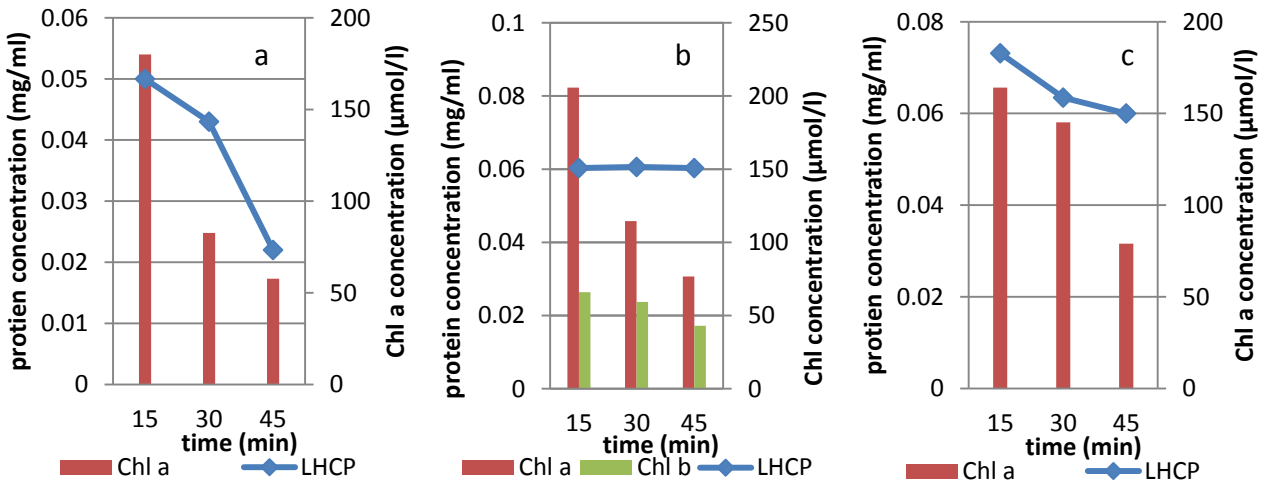

Fig.3.15. Chl and protein concentrations against time of GuCl reconstitution from *a)* LHCP mixed with Chl *a* and carotenoids, *b)* LHCP mixed with TE and *c)* negative control protein S3CΔC49 mixed with Chl *a* and carotenoids. Protein concentrations were determined by denaturing gel from Fig.3.14 and Chl concentrations in the supernatant were measured from absorption.

After centrifugation and measured absorption of the supernatant at 280 nm, LHCP concentration left only about 13.87 µg/ml and showed very weak band on denaturing gel (Fig.3.14). Pigments were able to increase the solubility of the protein in OG solution. Chl *a* in the pigment solution was about 1.5 molar excess over protein before mixing (assuming 8 Chl *a* molecules per LHCP). After mixing and 15

min incubation, the protein concentrations of LHCP mixed with Chl *a* and carotenoids, LHCP mixed with TE and S3CΔC49 mixed with Chl *a* and carotenoids were 0.05, 0.06 and 0.07 mg/ml, respectively. Chl *a* concentration was more than 8-fold molar excess over protein. Without Chl *b* stabilizing the proteins, both Chl *a* and LHCP concentrations decreased against time (Fig.3.15). In the presence of Chl *b*, although Chl *a* concentration quickly dropped, the protein concentration was rather stable. The negative control protein S3CΔC49 had the highest density of protein band. From the gel, we could see LHCP had not very good distribution in the lane during the gel running due to the GuCl in the solution and it disturbed quantifying band density, which reflected protein concentration. In general, GuCl reconstitution ended up at very low protein concentration, and it is not ideal for preparing EPR samples

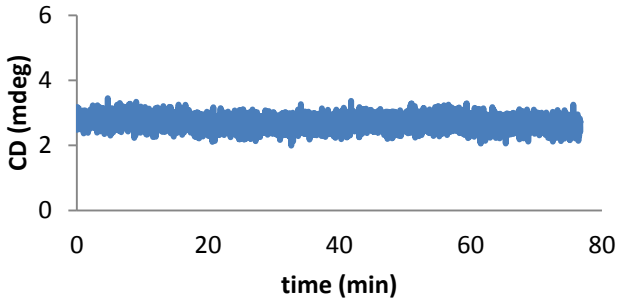

Fig.3.16. Time-resolved CD recorded at 700nm at room temperature for checking Chl *a* aggregation. Measurement initiated by manually mixing 6 mol/l GuCl and pigment solution; sample was immediately transferred to 1 mm CD cuvette.

A control measurment of investigating whether pigments aggregated in GuCl and

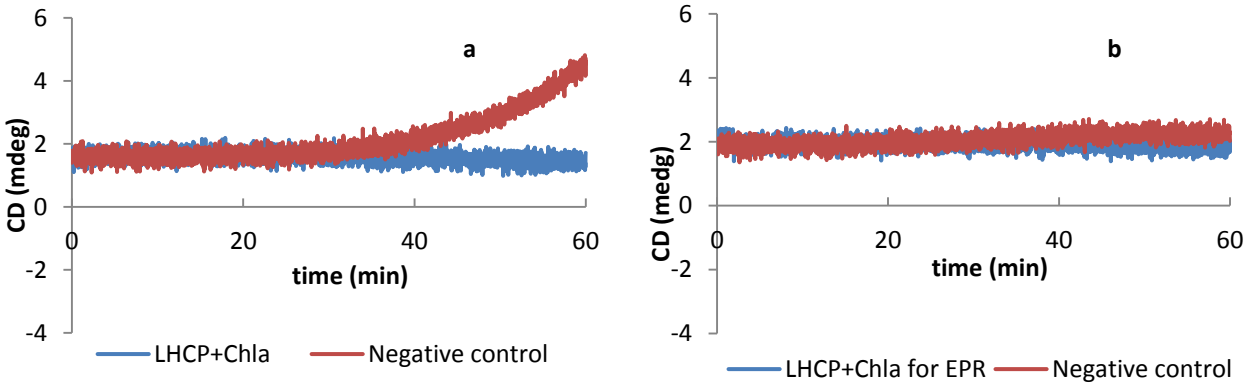

Fig.3.17. Chl *a* aggregation checked by time-resolved CD measurement recorded at 700nm at room temperature. LHCP and the negative control non-functional protein S3CΔC49 mixed with Chl *a* and carotenoids using *a)* standard detergent diluting method or *b)* rapid-mixing for EPR method.

OG mixtured was performed by time-resolved CD at 700 nm (Fig.3.16). If Chl aggregated, the CD signal at 700 nm would dramaticly increase. Time-resolved CD showed that Chl *a* had no significant aggregation in the first 75 min by mixing only 6 mol/l GuCl and pigment solution. The intensity at the end of the measurement was only slightly lower than that when measurement started. This indicated the decreased Chl *a* concetration was possibly due to the precipitated LHCP. Simlar measurements were performed in standard SDS-denatured detergent diluting method and the rapid-mixing method for preparing EPR samples. Fig.3.17 showed that in about 30 min after mixing protein and pigment solutions, no significant pigment aggregations were seen for both functional and negative control mutants in standard detergent diluitng method and Rapid-mixing EPR method. After 30 min, the negative control

measurements started having aggregated pigments, while pigments stay longer time in aqueous solution when mixed with functional protein; thereby all measurements using either of there two method should be done in 30 min after mixing.

3.3. Time-resolved fluorescence measurements

To optimize detergent diluting methods, we increased detergent concentration and checked time-resolved fluorescence to see whether Chl molecules could be able to stay in aqueous solution as long time as possible. We measured time-resolved fluorescence LHCII reconstitution in different detergent concentration and recorded both Chl *a* and *b* emission. Protein and pigment solutions were loaded in two syringes of stopped-flow device, measurements started 3 seconds before pressing mixing trigger. Each prepared samples were able to finish three continously measurents after calibrating the device; each measurement took about 700 seconds; measurement was started as soon as last one finished. Detergent concentration of 0.1%SDS, 1%OG, 0.04% PG was regarded at 1 time detergent. Chls were 3 fold molar excess over protein, assuming 14 Chl molecules per LHCII, Chl *a*: *b* ratio was 3:1; carotenoids were 1.7 fold molar excess, assuming 4 xanthophylls per LHCII. Measurements were excited at 470 nm, where Chl *b* absorbed most. As Fig 3.18. showed, when detergent concentration was increased to 1.3 fold, which was 0.13%SDS, 1.3%OG and 0.052% PG in the final concentration, the samples had highest fluorescence intensity, which meant that these samples had most Chls in the solution. We also calculated time constants of each kinetic trace (Table 3.2).

All three continuesly measurements showed repeatable kinetic data, when the detergent concentration was 1.3 fold. We also noticed that 1.3 x detergent concentration sample had the highest fluorescence intensity where fluorescece emission started to change, while 1 x detergent had the lowest. Between 1 and 1.3 x detergent, increased detergent concetration would also increase Chl fluorescence intensity. When detergent concentration was more than 1.3 fold, Chl *b* emissions of both 1.4 and 1.5 fold detergent were quite similar and both time constants τ_1 and τ_2 were very close, but Chl *a* emissions of these two were a little bit lower and τ_2 derived from the biexponential fit of Chl *a* siganls increased compared with that of 1.3 fold detergent concentration. When detergent concentrations were 1.2, 1.3 and 1.4 fold, time constants τ_1 and τ_2 were more stable than the other three. Amplitudes of each measurement varied but in average, amplitudes of fast component were ~61% of that of τ_1 for Chl *a* fluorescence and ~65% for Chl *b* fluorescence. Control measurements without adding proteins and with mutant S3CΔC49 which can't fold showed that in less than 1 s, both protein and pigment solutions were mixed after both of them were injected into the measuring cuvette (Fig.3.19).Both Chl *a* and Chl *b* emission had slightly decreased after 700s measurements. Chl *a* fluorescence intensity decreased a little bit more after the first measurement. But in general, there was no significant

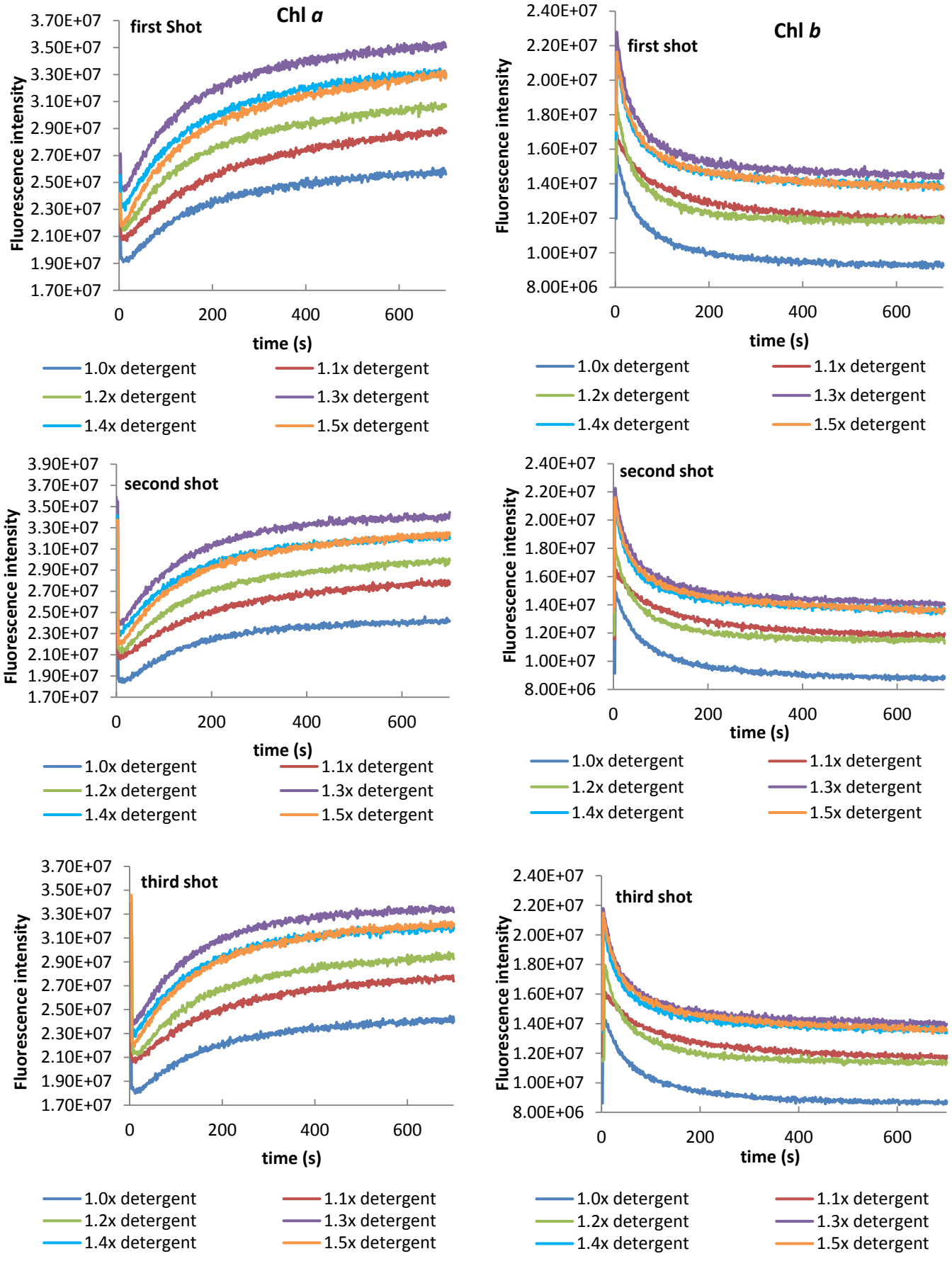

Fig.3.18. Time-resolved fluorescence measurements of LHCII assembly in three continuing rapid-mixing at different detergent concentrations recorded at both Chl *a* and Chl *b* emission simultaneously. Detergent concentration of 0.1%SDS, 1%OG, and 0.04% PG was regarded at 1xdetergent (Horn, 2004). Excitation wavelength 470 nm.

Table 3.2 Time constants from time-resolved fluorescence measurements of different detergent concentrations. Time constants $\tau_1$and τ_2 and amplitudes A_1 and A_2 are derived from a biexponential fit of the time-resolved signals under excitation at 470 nm and recorded at 660 nm for Chl *b* and 680 nm for Chl *a* .

Chl *a*						
1 shot	**1.0x**	**1.1x**	**1.2x**	**1.3x**	**1.4x**	**1.5x**
τ_1(s)	72	89	72	68	62	65
τ_2(s)	375	439	550	297	242	481
A_1/A_2	1.31	0.79	1.06	1.39	0.93	0.98
2 shot	**1.0x**	**1.1x**	**1.2x**	**1.3x**	**1.4x**	**1.5x**
τ_1(s)	90	99	71	55	79	68
τ_2(s)	1148	603	377	132	336	322
A_1/A_2	2.87	1.32	1.40	0.53	2.98	1.46
3 shot	**1.0x**	**1.1x**	**1.2x**	**1.3x**	**1.4x**	**1.5x**
τ_1(s)	85	91	72	67	77	65
τ_2(s)	564	357	465	169	223	212
A_1/A_2	1.84	1.33	1.43	1.56	2.44	1.21
average	**1.0x**	**1.1x**	**1.2x**	**1.3x**	**1.4x**	**1.5x**
τ_1(s)	82 ±10	93 ±6	72 ±1	63 ±8	72 ±10	66 ±2
τ_2(s)	696 ±452	348 ±255	464 ±87	199 ±98	267 ±69	338 ±126
A_1/A_2	2.01 ±0.8	1.15 ±0.36	1.30 ±0.24	1.16 ±0.57	2.12 ±1.19	1.22 ±0.24

Chl *b*						
1 shot	**1.0x**	**1.1x**	**1.2x**	**1.3x**	**1.4x**	**1.5x**
τ_1(s)	29	35	19	30	23	26
τ_2(s)	126	152	75	161	127	148
A_1/A_2	1.89	0.92	1.32	2.84	2.22	2.12
2 shot	**1.0x**	**1.1x**	**1.2x**	**1.3x**	**1.4x**	**1.5x**
τ_1(s)	31	37	24	29	26	31
τ_2(s)	138	172	99	172	156	240
A_1/A_2	1.74	0.97	1.86	2.67	2.45	2.26
3 shot	**1.0x**	**1.1x**	**1.2x**	**1.3x**	**1.4x**	**1.5x**
τ_1(s)	24	41	27	27	23	24
τ_2(s)	109	192	107	157	129	164
A_1/A_2	1.36	1.2	2.07	2.44	2.14	2.10
average	**1.0x**	**1.1x**	**1.2x**	**1.3x**	**1.4x**	**1.5x**
τ_1(s)	28 ±4	38 ±3	23 ±4	29 ±2	24 ±2	27 ±4
τ_2(s)	124 ±15	172 ±20	94 ±19	163 ±9	137 ±19	184 ±56
A_1/A_2	1-66 ±0.3	1.03 ±0.17	1.75 ±0.43	2.65 ±0.21	2.27 ±0.18	2.16 ±0.1

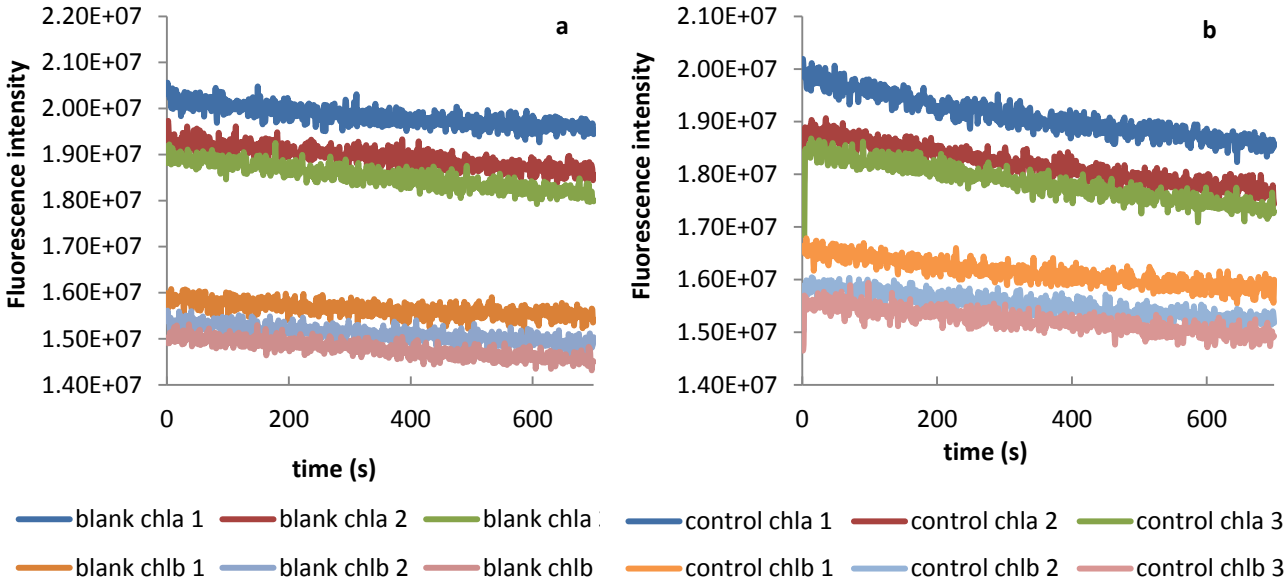

Fig.3.19. Control time-resolved fluorescence measurements of a) protein solution without protein mixed with total pigments and b) negative non-functional protein S3CΔC49 mixed with total pigments. Both measurements were performed the same as functional protein as 1x detergent of Fig.3.15. Number 1, 2 and 3 referred 1, 2 and 3 shot. Excitation wavelength 470 nm.

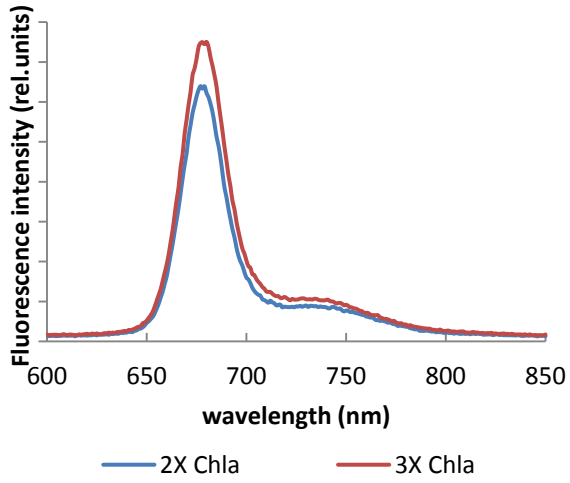

Fig.3.20. Steady state fluorescence of labelled LHCP mixed with different molar excess of Chl *a*.

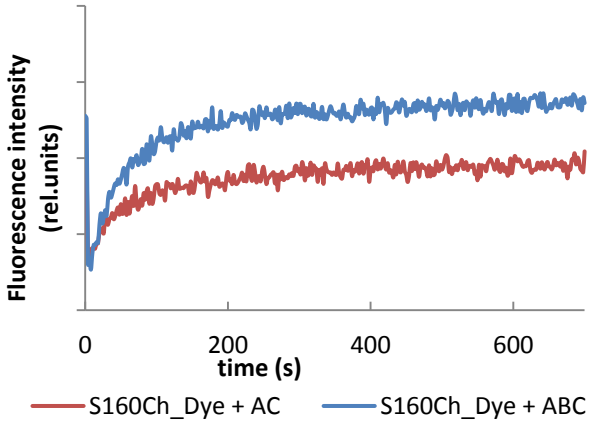

Fig.3.21. Time-resolved fluorescence of labelled LHCP mixed with Chl *a* + carotenoids and Chl *a/b* + carotenoids. Dye emissions were under excitation of 420 nm recorded at 760 nm for dye. Both samples contained equal amount of Chl *a*; Chl*a/b* mixture had a Chl *a:b* ratio=3)

quenching in both control measurements. This also showed in the measurements using funtional protein in Fig.3.18; in the measurements of time-resolved Chl *b* fluorescence, after 600s, Chl *b* emission had a very small decreased. This have been improved by adding more detergent; when detergent concentration increased at 1.2 fold. As lipids were removed by preparative HPLC column during the single pigment preparation, total pigments directly extracted from plant leaves had more lipids which assumably would keep pigments stay longer time in aqueous solution. Therefore we modified the old detergent diluting method and used a higher detergent concentration, which was 0.13%SDS, 1.3%OG and 0.052% PG (end concentration) for study intermediate complex.

In the total pigments extracted from pea leaves, Chl *a* took about 75.8% in the total Chls, which was a bit more than 3 times of Chl *b*. Time-resolved fluorescence measurements were taken under excitation at 420 nm, where Chl *a* molecules are excited. In Chl *a* reconstitution, Chl *a* was more than 2 fold molar excess over protein (8 Chl *a* molecules per protein), and carotenoids were 4 fold (4 xanthophylls per protein). Fig.3.20 showed that at 760 nm, the dye emission of the sample using 3 fold molar excess Chl *a* was only a little bit more than that of the sample using 2 fold molar excess Chl *a*. In this case, we would assume the percentages of protein being pigmented by Chl *a* in both samples were not very close. In reconstitution with TE containing 3 fold molar excess Chl *a*, the reconstitution yield was no less than 55% in the first 60 min when pigment solution was done. Therefore, we would assume that Chl *a* reconstitution with 3 fold molar excess Chl *a* would have no less than 55% protein being pigmented. The Chl *a* reconstitution with 2 fold molar excess Chl *a* would be presumed to have about 50% protein pigmented. For first investigation, reconstitution with 2 fold molar excess Chl *a* was adopted to have less Chl *a* aggregation. As a comparison, another sample contained Chl *b* was 0.95 fold (6 Chl *b*

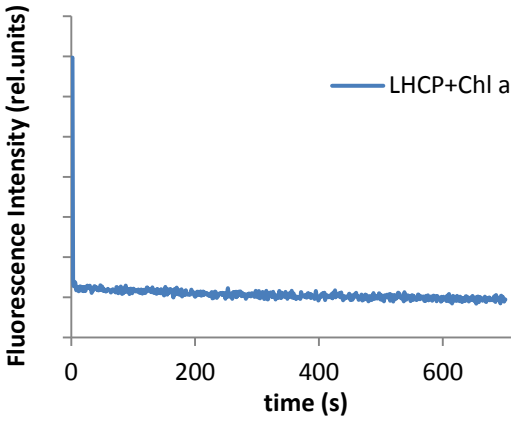

Fig.3.22. Time-resolved fluorescence of non-labelled LHCP mixed with Chl *a* and Carotenoids

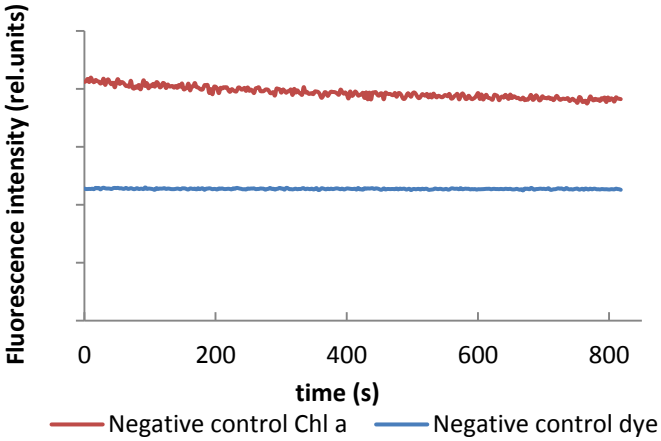

Fig. 3.23. Control time-resolved fluorescence measurements of labelled negative protein mixed with Chl *a* and carotenoids recorded at both Chl *a* and dye emission. Measurement was recorded under excitation of 420 nm.

molecules per protein) and equal amount of Chl *a* and carotenoids were used as that of reconstitution with only Chl *a* and carotenoids. Since both measurements were under the excitation wavelength which Chl *a* molecules absorb most, the energy transferred to the acceptor dye was regarded mostly from Chl *a* and minor from Chl *b*. If there were about the same percent of protein being pigmented in both cases and all 8 Chl *a* molecules were able to bind to the protein in the absence of Chl *b*, the sensitised dye in the Chl *a* only situtiation would have increased as much as the same of that in Chl *a/b* reconstitution, however, it only increased about half. (Fig.3.21). Control measurements of non-labelled apoprotein mixed only

Chl *a* (Fig.3.22) and labelled negative protein mixed with Chl *a* and carotenoids (Fig.3.23) showed the mixing of protein and pigments were very quick. The signal exhibited a very slow, almost linear

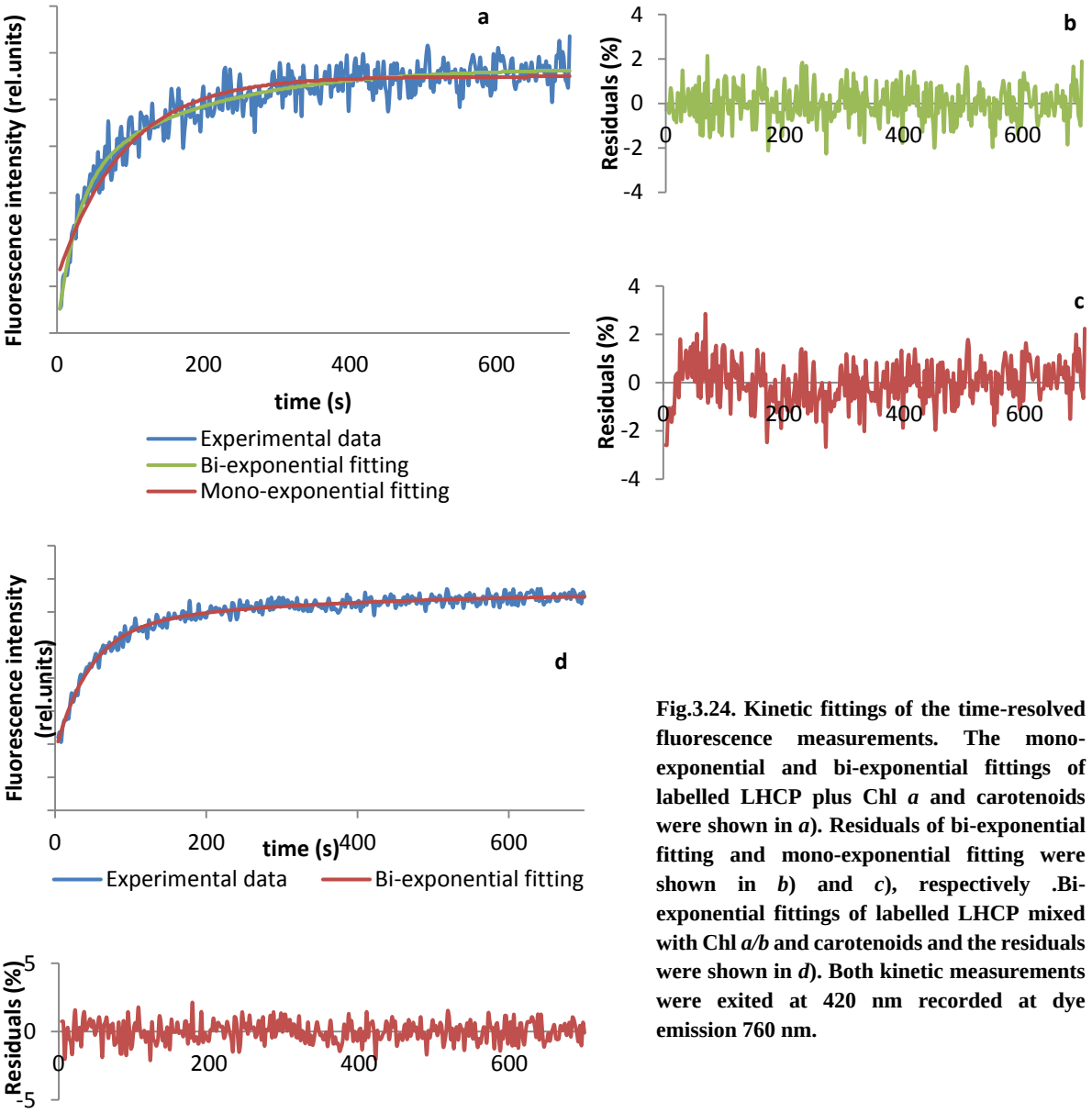

Fig.3.24. Kinetic fittings of the time-resolved fluorescence measurements. The mono-exponential and bi-exponential fittings of labelled LHCP plus Chl *a* and carotenoids were shown in *a*). Residuals of bi-exponential fitting and mono-exponential fitting were shown in *b*) and *c*), respectively .Bi-exponential fittings of labelled LHCP mixed with Chl *a/b* and carotenoids and the residuals were shown in *d*). Both kinetic measurements were exited at 420 nm recorded at dye emission 760 nm.

Table 3.3 Kinetic data extracted from time-resolvedfluorescence measurements. Time constants $\tau_1$and τ_2 and amplitudes A_1 and A_2 are derived from a biexponential fit of the time-resolved signals under excitation at 420 nm and recorded at 760 nm for acceptor dye.

Experiments	τ_1(s)	τ_2(s)	A_1/A_2
LHCP + AC	19	124	1.27
LHCP + ABC	30	199	3.37

decrease; there was no significant quenching in both measurements. Interestingly seeing when Chl *b* was omitted, the kinetic traces of Chl *a* reconsititution can also be fitted better by bi-exponential kinetics than mono-exponential kinetics (Fig.3.24a). The coefficients of determination

R^2 were 0.91 and 0.89 for bi- exponential and mono-exponential kinetics fittings, respectively. The mono-fitting had a time constant τ of 63 sec, however the first 30 sec was not fitted to the experimental data. Residuals of bi-exponential fitting (Fig.3.24b) had a better distribution than that of mono-exponential fitting (Fig.3.24c). Reconstitution with TE had quite goood bi-exponential fitting (Fig.3.24d), with a coefficient of determination R^2 0.97. The amplitude of the fast phase contributed about 56% of the total amplitude, indicating that not all Chl *a* molecules were bound to the protein at the same time; some of the binding sites were veryquickly filled in, only about 20 sec, w hile others took longer time, about 2 min. In Chl *a/b* reconstitution, on the other hand, the fast phase contributed more, about 77%. The time constants τ_1 and τ_2 in Chl *a* reconstitution were smaller than those in the Chl *a/b* reconstitution, especially τ_2, which was 75 sec slower in the Chl *a/b* reconstitution (Table 3.3). One possible explanation is that some Chl *a* bindings require interactions with Chl *b* molecules.

3.4. Quantification of Chl *a* bindings using FRET measurements

In order to figure out how much percent of protein were pigmented in both Chl *a* and Chl *a/b* reconstitutions, we reversed the direction of the energy transfer, used a fluorescent label serving as an energy donor to Chl *a*. Experiments were designed first to select a donor dye, which is able to transfer energy to Chl *a* molecules as long as one Chl *a* molecule bound to the protein. The fluorescent dye should have quite absorption between 550-590 nm, which is the "gap" of both Chl *a* and Chl *b*.

Three donor dyes were chosen and compared. All three fluorescent dyes have quite good absorption between 550-590 nm. The fluorescence spectrum of the each donor dye and absoption spectrum of Chl *a* were properly overlapped.

The labelling position of fluorescent dye was at the Cys residue at the stromal loop at position 160 which was in the hydrophlic domain and was quite flexible. The fluorophore bound at this position would have quite free rotational motion around single bond and the orientation between donor and acceptor would hardly stay at perpendicular.

Förster distances of three donor dyes between Chl *a* were showed in Table 3.4.

Table3.4 Förster distance R_0(Å) between fluoresecence dye and Chl

	Rhodamine Red C2	DY-615	DY-634
Chl *a*	64.42	46.53	64.70
Chl *b*	67.62	47.99	63.50

Among these three dyes, Rhodamine has the best fluorescence quantum yield (Φ_F). Therefore, although it has the least overlapping with the Chl absorption, it has the longest Förster critical distance. In addition, Rhodamine has quite good absorption at 550 nm, while the other two dyes absorb much less at this wavelength. Moreover, Rhodamine maximal emission at about 590 nm is very easy to be distinguished from Chl emission, and it already showed nearly 100% donor quenching between Rhodamine and LHCII (Gundlach, 2009). We assumed the energy transfer between Rhodamine and Chl *a* should be sufficient to observe how much percent of the proteins are pigmented when looking at the quenching of donor dye afterreconstitution; the energy of Rhodamine should be efficiently transferred to Chl as long as the pigments were bound.

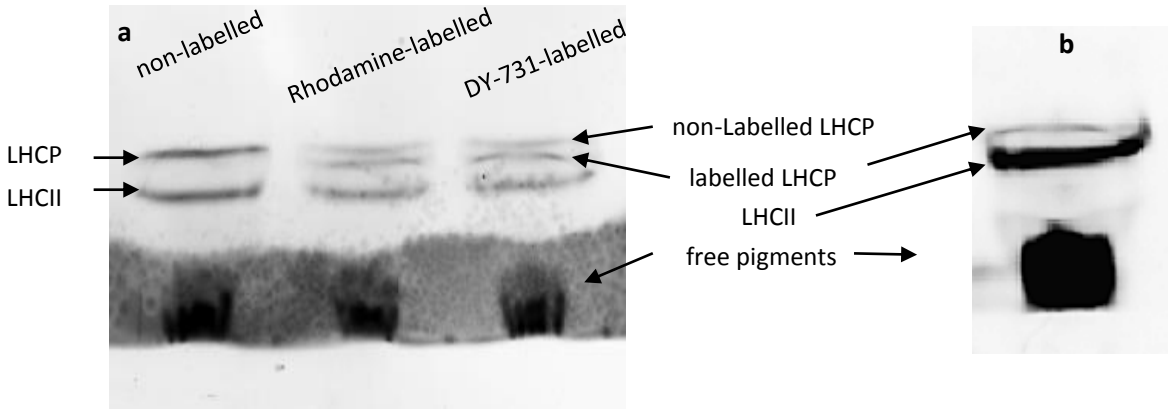

Fig.3.25. Partially denaturing gel electrophoresis. Non-labelled and dye labelled LHCP were mixed with total pigments (Chl*a:b* ratio=3) following detergent diluting method. *a)* Reconstitution yields were calculated by comparing band density after coomassie staining. *b)* Dye labelled LHCP was distinguished by fluorescence imaging using filter RG9 which only show fluorescence emission above 700 nm.

The Chl *a/b* reconstitution yields of non-labelled and dye labelled protein were measured from partially denaturing gel. Fig.3.25 showed when the LHCP concentration was 3.9 µmol/l, Chl*a:b* ratio=3, and 3-fold molar excess of Chl *a* (8 Chl *a* per protein), 1.3-fold molar excess of Chl *b* (6 Chl *b* per protein) and 4-fold molar excess of xanthophylls (4 xanthophylls per protein) were used, non-lableled protein, Rhodamine labelled protein and DY-731 labelled protein had reconstitution yield about 57%, 57% and 61%, respectively; both fluorescent dyes had labelling efficiency around 60%. All three conditions had about the same reconstitution yield.

In the FRET measurements of using donor dye, the excitation wavelength was 550 nm, near the absorption maximum of the dye. Unlabeled LHCII excited at this wavelength, emits some fluorescence (orange line in Fig.3.26a). A significant donor quenching was observed in both labelled monomer and trimer. The ratio of the sensitized acceptor spectrum area (A_S) to the quenched donor spectrum area (A_Q) for labelled trimer calculated from the spectra was 0.38. According to the equation:

$$A_S/A_Q = \varphi F(acceptor)/\varphi F(donor) \quad (4)$$

Where φF (Rhodamine Red) = 0.5 and φF (LHCII) = 0.2, A_S/A_Q should be 0.4. The calculation was very close to the expected value. The energy transfer efficiency between Rhodamine and Chl in LHCII trimer, calculated from donor quenching, was about 90% and for monomer, a little bit lower, about 83%. Although the FRET efficiency of Rhodamine Red to Chl was lower than the literature, it's sufficient enough to be the monitor for observing pigment bindings. In Fig.3.26b, we noticed that the labelled negative control protein mixed with pigments had much lower dye emission at 685 nm compared with labelled apoprotein. Negative control plus Chl *a* and carotenoids already quenched half of the energy and Chl *a/b* reconstitution had about 60% donor quenching. Both of them indicated quite obvious non-specific energy transfer. Despite not very high protein concentration, only 3.9 µmol/l in the final solution, the pigment concentration was rather high, more than 90 µmol/l Chl *a* and about 30 µmol/l Chl *b*. And because the energy transfer between Rhodamine to Chl *b* was more efficient than that to Chl *a*, it was no doubt that more non-specific energy transfer occurred in the presence of Chl *b*. Therefore the energy transfer appeared in labelled LHCP plus pigments would be the summation of the energy transfer due to pigment bindings plus non-specific energy transfer. In order to obtain the part produced by pigment binding, measurements using negative control protein, mixed with equal amount of pigments corresponding to labelled LHCP, were regarded as 0% pigmented protein instead of pure labelled apoprotein. Additional pigments were added to pure labelled monomer, the dye emission of monomer plus Chl *a* slightly increased and monomer with additional Chl *a/b* had about the same dye fluorescence. Additional pigments did not make the donor dye further quench. On one hand, the FRET efficiency between Rhodamine and LHCII monomer was quite good, most dye transferred energy to LHCII monomer. On the other hand, unbound pigments might not be like the pigments in trimer and have close distance to the donor dye. Therefore, we would directly compare LHCP after reconstitution with negative control and pure labelled monomer. For analyzing the spectra, all spectra were cut from 565 nm, because the excitation wavelength 550 nm was too close to where spectra started to record, a quite obvious signal jump was found in each spectrum. Despite that Chl had very poor absorption at 550 nm; the fluorescence emission at 590 nm was not zero. Spectra of non-labelled protein performed with the same measurements as labelled protein were used for subtracting Chl emission from the measured spectra, leaving dye emission part for further analysis. The reason for this was that in all the measurements, excess amount of Chls were applied, as time-resolved fluorescence measurement shown in chapter 3.3, Chl emission as well as concentration constantly slowly decreased in aqueous solution, while the change of the dye emission was only dependent on pigment-protein interaction after subtracting non-specific energy transfer if no significant protein aggregation occurred.

Spectra in Fig.3.26d and 3.26e could be regarded as superposition of Rhodamine and Chl emissions, and vice versa. Emission spectra could be dissected into these two components. Deconvolutions of spectra were shown in appendix and here we focused on the dye emission part of each spectrum.

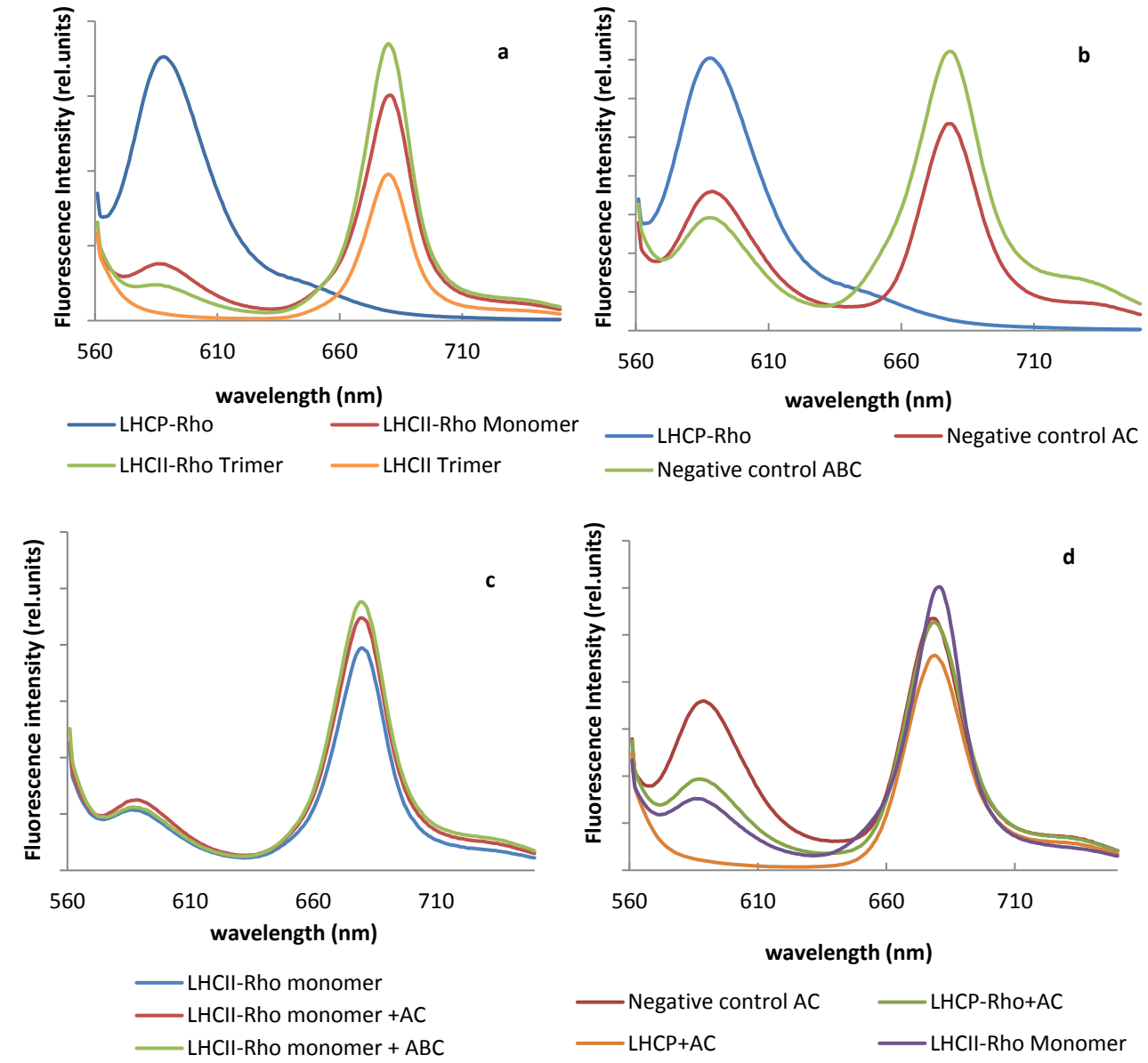

Fig.3.26. Energy transfer to Chl from Rhodamine. Steady-state spectra of fluorescence emission after excitation at 550 nm. *a*) Labelled apoprotein (blue), labelled LHCII monomer (red), labelled LHCII trimer (green) and non-labelled LHCII trimer (orange). *b*) Labelled apoprotein (blue), labelled negative control mutant mixed with Chl *a* and carotenoids (red), labelled negative control mutant mixed with Chl *a/b* and carotenoids (green). c) Labelled LHCII monomer (blue), labelled LHCII monomer with additional Chl *a* and carotenoids (red) and labelled LHCII monomer with additional Chl *a/b* and carotenoids (green). *d)* Chl *a* and carotenoids mixed with labelled negative control mutant (red), labelled LHCP (green), non-labelled LHCP (orange). Labelled LHCII monomer (purple). *e*) Chl *a/b* and carotenoids mixed with labelled negative control mutant (red), labelled LHCP (green), non-labelled LHCP (orange). Labelled LHCII monomer (purple).

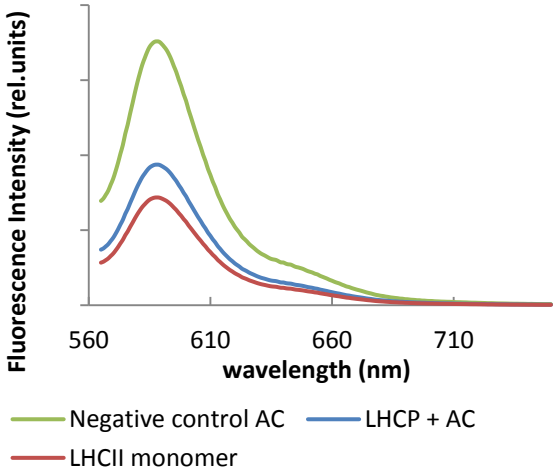

Fig.3.27. Dye emission spectra of Chl *a* reconstituion after subtracting Chl contribution from the emssion spectra of Fig.3.25d.

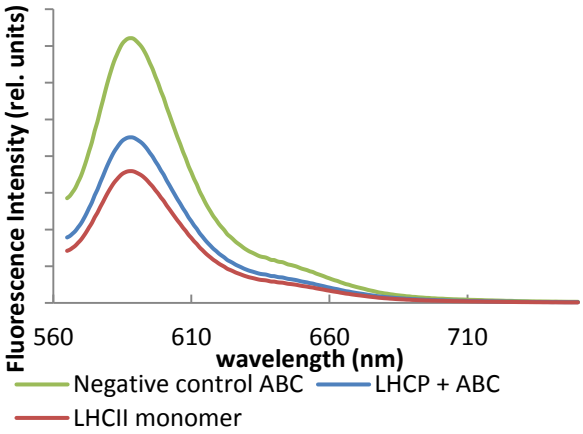

Fig.3.28. Dye emission spectra of Chl *a/b* reconstituion after subtracting Chl contribution from the emssion a of Fig.3.25e.

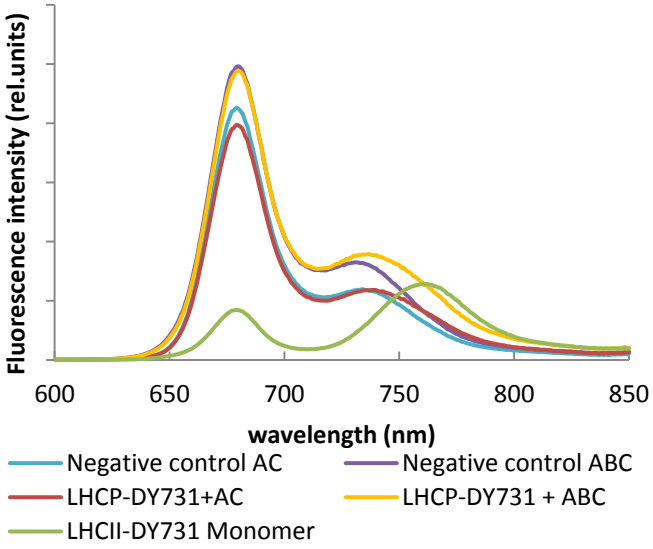

Fig.3.29. Energy transfer from Chl from acceptor dye DY-731. Steady-state spectra of fluorescence emission after excitation at 420 nm. Chl *a* and carotenoids mixed with Labelled negative control mutant (blue) with labelled LHCP (red); Chl *a/b* and carotenoids mixed with Labelled negative control mutant (purple), with labelled LHCP (orange), Labelled LHCII monomer (green).

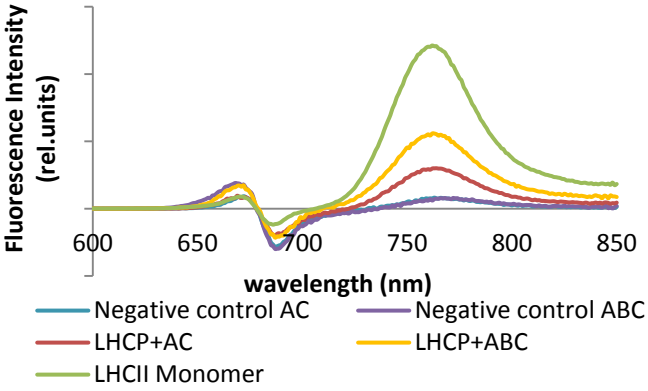

Fig.3.30. Dye emission spectra after subtracting Chl contribution from the emssion spectra of Fig.3.29.

Fig.3.27 showed the deconvoluted dye emissions of spectra in Fig.3.26d. The percentage of pigmented protein was calculated as:

$$\text{Pigmented protein (\%)} = \frac{A_{Neg}-A_{Re}}{A_{Neg}-A_{Mono}} * 100\% \quad (5)$$

Where A_{Neg} is the area of dye emission in the negative control, A_{Re} is the area of dye emission of LHC after reconstitutiohn and A_{mono} is the area of dye emission of pure labelledLHCII monomer.

In Chl *a*-reconstitution, Rhodamine dye quenched about 79% fluorescence in compare with negative control protein and monomer. In Chl *a/b* reconstitution, the donor dye had about 75% quenching. Both of them had about the same percentage of protein being pigmented.

In Chapter 3.3, it has been shown that acceptor dye in time-resolved fluorescence measurement of Chl *a*-reconstitution only received half of the energy transfer as that in Chl *a/b* reconstitution. Further quantification was done by steady state fluorescence. DY-731 only absorbed very little light at 420 nm. There was also some non-specific energy transfer. The increased dye emission in negative control measurement only consisted about 3.5 % of the increase in pure LHCII monomer (spectra not shown). It's not significant, but labelled negative control mutant was still used instead of pure labelled LHCP for excluding non-specific energy transfer. The overlapped dye emission and Chl emission at far red region disturbed dye emission analysis. After subtracting Chl emission from the spectra, two negative measurements had almost the same dye emission at 760 nm (Fig.3.30). Deconvolutions of spectra were shown in appendix. Comparing with the increased dye emission of pure LHCII monomer, dye emissions from Chl *a* and Chl *a/b* reconstitution only increased about 19% and 43%, respectively. "Green gel" showed that Chl *a/b* reconstitution had more than 50% reconstitution yield. In the deconvoluted spectra, emission curves from 645 to 710 nm, where Chl fluorescence emitted, were distorted after subtracting Chl emission. The fluorescence maximum peak of Chl *a* always had about 2-3 nm shift; Chl emission at far red range, where it had some overlap with dye emission, also differed a little bit among samples. These would cause some errors in analyzing spectra. In general, results from acceptor dye were still reasonable. Energy transfer in Chl *a* reconstitution was about 43% of it in Chl *a/b* reconstitution. As in Chl *a/b* reconstitution, energy transfer was mainly from Chl *a* but also a small amount from Chl *b*, due to the fact that Chl *b* also had some absorption at 420 nm as well. Therefore, the energy transfer from Chl *a* to DY-731 in Chl *a* reconstitution was presumed to be about half of it in Chl *a/b* reconstitution. Because results from donor dye indicated that the percentage of pigmented protein in both Chl *a* and Chl *a/b* reconstitutions were about the same, we deduced that the number of Chl *a* molecules bound to the protein in Chl *a* intermediate would be about the half of the number in Chl *a/b* reconstitution. The reconstituted LHCII monomer contains 8 Chl *a* molecules, therefore the number of bound Chl *a* molecules in the Chl *a* intermediate was assumed to be about 4. If compared the energy transfer in Chl *a* reconstitution directly with it in pure LHCII monomer, the number of Chl *a* molecules could be calculated from the equation:

$$\frac{\text{Pigmented protein yield} * \text{Chl } a \text{ Number}}{100\% * 8} = \text{x\% energy tranfer}$$

Here the pigmented protein was 79% and the energy transfer was 19%, therefore the number of Chl *a* was calculated as about 2. Which number was correct required further disscussion, and the inferences above were both based on the hypothesis that the protein molecules were monomolecularly dispersed in the solution.

To investigate whether Chl *b* ration had any influence on the percentage of pigmented protein, the same measurements were done by changing the Chl *b* ratio in the pigment mixture using only Chl *a*, Chl *a:b*= 3:2 and Chl *a:b*= 1:1. Chl *a* and xanthophyll concentrations were kept the same as former measurements

of Chl *a:b*= 3:1. Fig.3.31a showed when carotenoids were also omitted in Chl *a* reconstitution, labelled LHCP had a significant quenching compared with the labelled negative protein. Addition of extra Chl *a* caused dye emission slightly increased compared with pure monomer. The reason for this was unclear. When using acceptor dye, after subtracting Chl emission from the spectra, a far red peak shown at 730

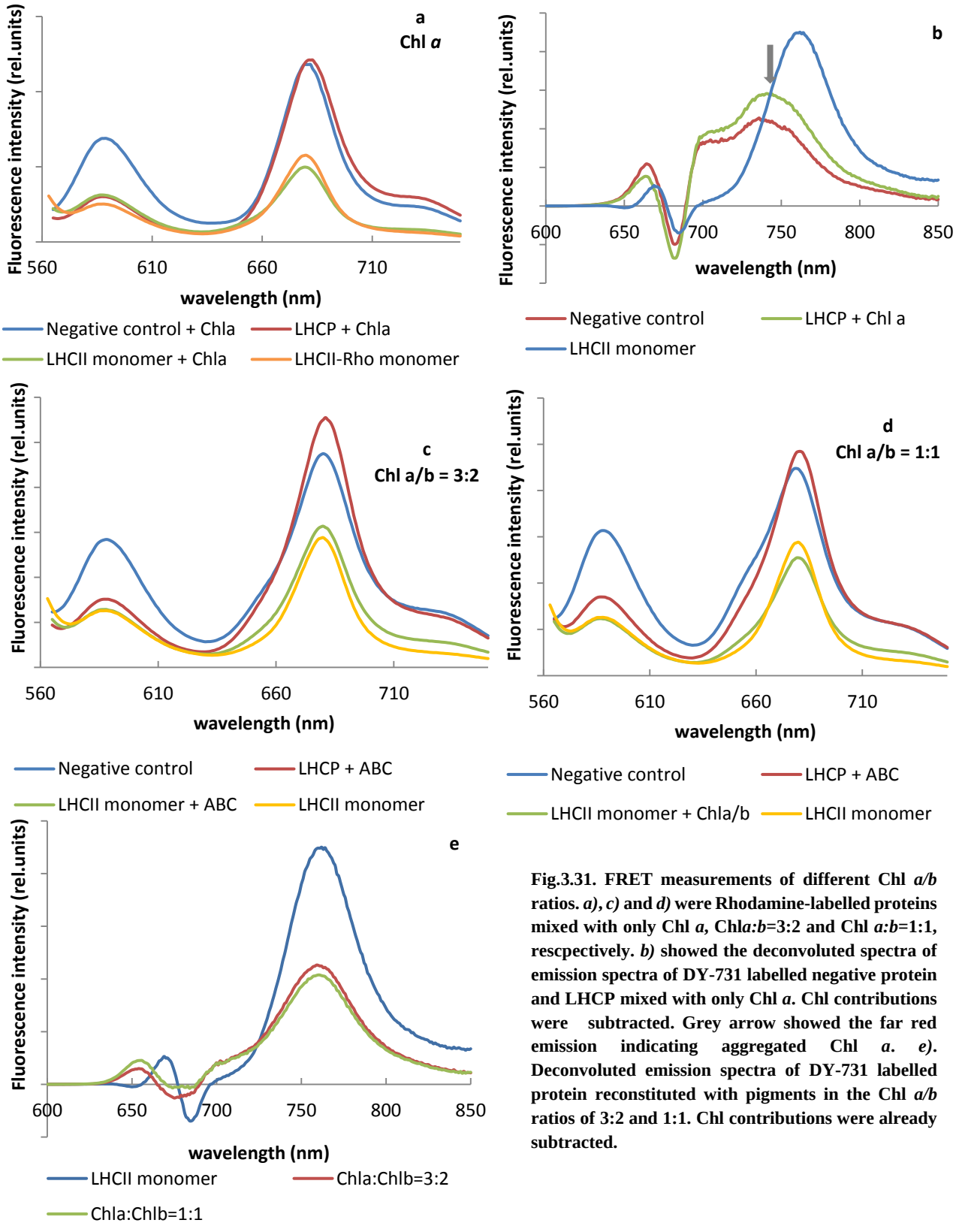

Fig.3.31. FRET measurements of different Chl *a/b* ratios. *a), c)* and *d)* were Rhodamine-labelled proteins mixed with only Chl *a*, Chl*a:b*=3:2 and Chl *a:b*=1:1, rescpectively. *b)* showed the deconvoluted spectra of emission spectra of DY-731 labelled negative protein and LHCP mixed with only Chl *a*. Chl contributions were subtracted. Grey arrow showed the far red emission indicating aggregated Chl *a*. *e)*. Deconvoluted emission spectra of DY-731 labelled protein reconstituted with pigments in the Chl *a/b* ratios of 3:2 and 1:1. Chl contributions were already subtracted.

nm (Fig.3.31b). It has been reported that the fluorescence of Chl had the maxima of aggregate and monomer emission bands, 720 and 685 nm, respectively in ethanol at 77K (Brody, 1961). This peak was not obvious in the measurements containing carotenoids. Chibisov et al. (Chibisov, 2003) also pointed out that Chl *a* in aqueous solution (2-6% acetone) is present as mono- and dihydrated aggregated forms which are characterized by specific ground state absorption spectra. The amount of dihydrated form is larger in the presence of macromolecules, such as bovine serum albumin (BSA), lysozime and polyvinyl alcohol (PVA). Carotenoids in the pigment mixture would help to slow the formation of dihydrated aggregated Chl *a*. This aggregation made it hard for us to tell how much dye fluorescence increased at 760 nm as well as how much protein were able to bind to the protein.. In reconstitutions of Chl *a:b* = 3:2 and Chl *a:b* = 1:1, donor dye had 85% and 75% quenching , respectively (Fig.3.31c and Fig.3.31d); the sensitized dye increased about the same, about 50% (Fig.3.31e), indicating that the reconstitution yields of these two were about the same. The green gel (Fig.3.32), although it was difficult to quantify band density, the darker LHCII monomer band suggested better reconstitution yield than reconstitution

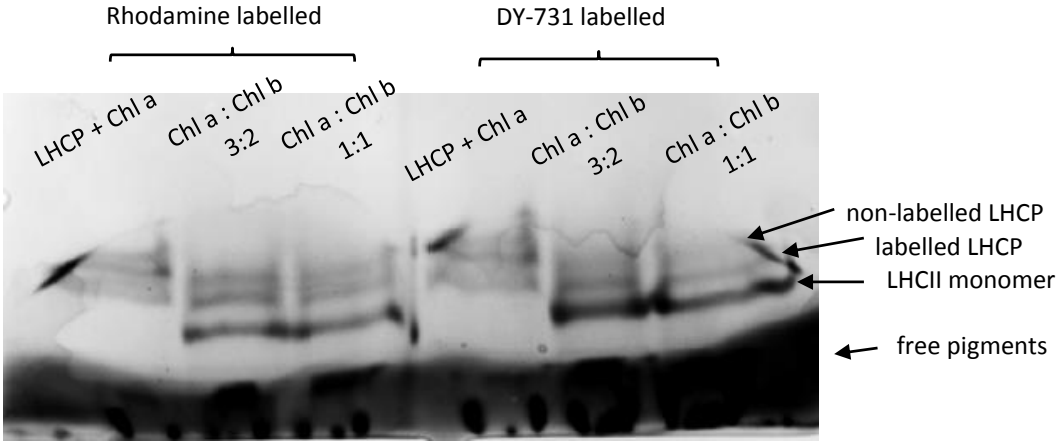

Fig.3.32. Partically denaturing gel electrophoresis of Rodamine-labelled and DY731- labelled LHCP mixed with with only Chl *a*, Chl*a:b*=3:2 and Chl*a:b*=1:1

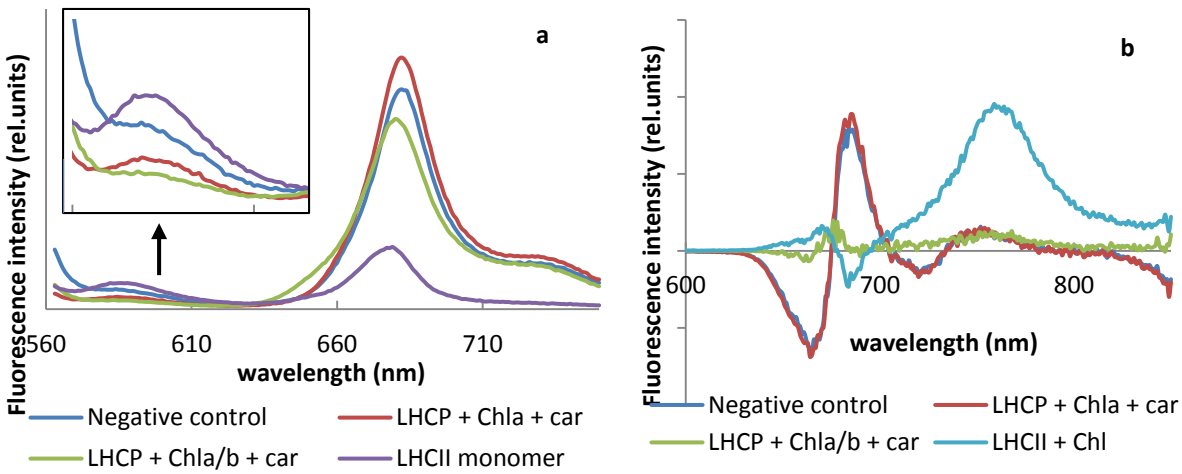

Fig.3.33. FRET measurements by GuCl reconstitution method of *a)* emission spectra of Rhodamine-labelled and *b)* spectra of DY731-labelled after extracting Chl contribution. The inset of Fig.3.32a showed the dye emission part of the spectra.

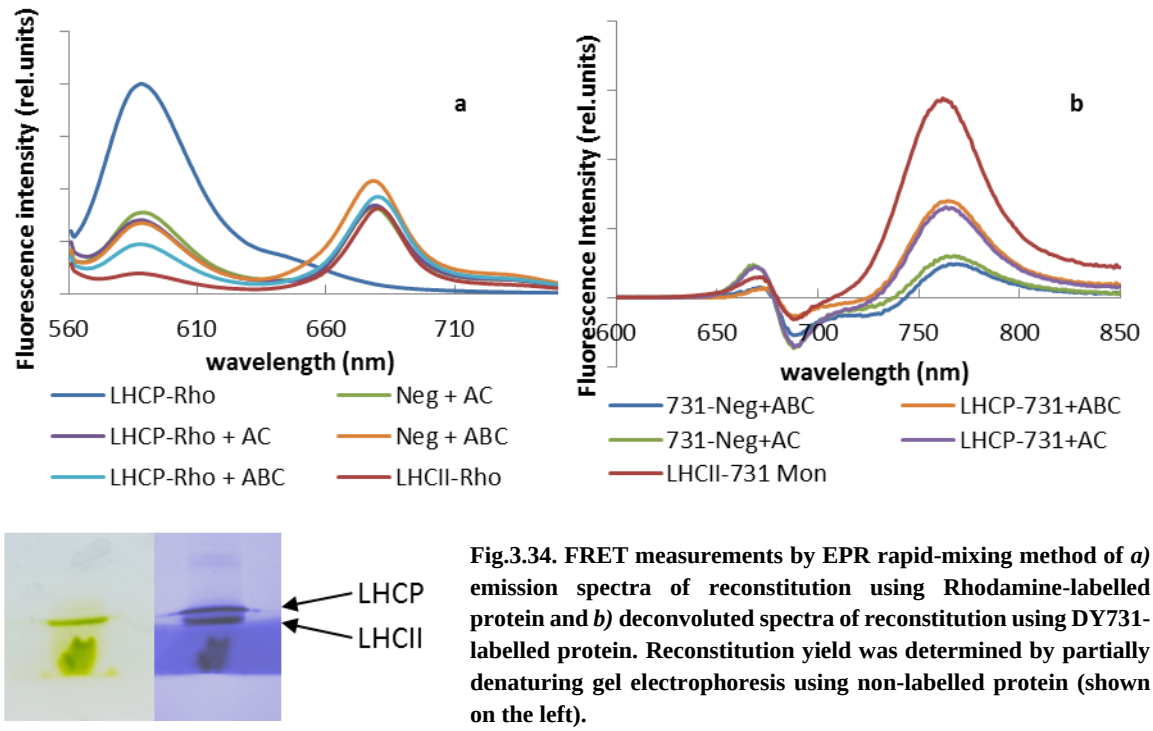

Fig.3.34. FRET measurements by EPR rapid-mixing method of *a)* emission spectra of reconstitution using Rhodamine-labelled protein and *b)* deconvoluted spectra of reconstitution using DY731-labelled protein. Reconstitution yield was determined by partially denaturing gel electrophoresis using non-labelled protein (shown on the left).

of Chl *a:b* = 3:1 (Fig.3.25). Reconstitutions of different Chl *a/b* ratio had about the same percentage of pigmented protein, if we used the same amount of Chl *a*. Increased amount of Chl *b* would also improve reconstitution yield. Here we could conclude, using SDS-detergent diluting method, when Chl *a* is 3 molar excess over LHCP, Chl *a* reconstitution and different Chl *a/b* reconstitution with different Chl *b* ratio had about the same percentage of pigmented protein. About half of Chl *a* molecules were able to bind to the protein in the absence of Chl *b*.

In GuCl reconstitution, pigments binding helped to increase the protein solubility in OG micelles. We were also interested in how much percent of protein being pigmented and how many Chl *a* molecules bound. Due to the fact that Chl *a* concentration was more than 8-fold molar excess over protein, which was more than 64 Chl *a* molecules per protein. LHCP was fully surrounded by pigments. The donor dye had more quenching in the negative control than the monomer (Fig.3.33a). Pure monomer plus additional pigments was used as 100% energy transfer in the acceptor dye measurements. Although GuCl reconstitution had about 40% reconstitution yield (green gel not shown), the sensitized dye had nearly no increase (Fig.3.33b). The shift of Chl *a* maximal emission also made it difficult to deconvolute spectra. Therefore FRET measurements are not an ideal option for analyzing both reconstitution yield and the numbers of pigment binding in this case.

FRET measurements also had poor results in the reconstitution using EPR rapid mixing method. In the measurements using donor dye (Fig.3.34a), negative control protein (green line) and LHCP (purple line, overlapped with orange line) had almost as much as the same donor quenching .The LHCII monomer also show a different emission spectrum as what we have seen before, similar as the trimer spectrum in former SDS-detergent diluting measurements. In the measurements using acceptor dye, negative protein

showed more non-specific energy transfer (Fig.3.34b) and Chl *a* reconstitution had nearly the same amount of energy transfer as it in Chl *a/b* reconstitution. Reconstitution yield of this method was about 60%. The increased non-specific energy transfer was because in the EPR samples, protein ended up at a concentration 45 μmol/l, which was more than 11 times as it in standard SDS-detergent diluting reconstitution. Although Chl *a* to protein ratio was decreased to 2.3 fold molar excess, the final Chl *a* concentration was over 0.8 mmol/l. Too high protein and pigment concentrations made the molecules very close to each. Consequently energy transfer between donor and acceptor was more efficient. The emission spectrum of LHCII monomer in Fig.3.34a also indicated energy transfer from non-labelled LHCII to labelled LHCII. Therefore, FRET measurements are also not able to determine the percentage of protein being pigmented as well as the number of Chl *a* bindings when the protein concentration is too high.

3.5. UV-CD measurements

Secondary structure can be determined by CD spectroscopy in the "far-UV" spectral region (190-250 nm). *α*-helix, *β*-sheet and random coil structures each give rise to a characteristic CD spectrum. The approximate fraction of each secondary structure type that is present in any protein can thus be determined by analyzing its far-UV CD spectrum as a sum of fractional multiples of such reference spectra for each structural type via professional software. Previous study has detected 27% *α*-helix in SDS-solubilized LHCP, no virtually *α*-helix presented in GuCl solubilized and 41% *α*-helix in refolded LHCII.

The CD spectrum of LHCP dissolved in GuCl could only be measured down to 207 nm due to high UV absorption. Fig.3.35 showed that the negative CD signal at 220 nm of LHCP indicated virtually no α-helix present,which is the same as previous study; when Chl *a* was added, protein started show about 10% α-helical structures; and more α-helices coming when further Chl *b* was added; about 44% *a*-helices being detected. However, very strong noises in the spectra have been noticed. These noises also resulted in higher errors in estimation of secondary structure. Former study showed that in GuCl reconstitution, both Chl *a* and protein

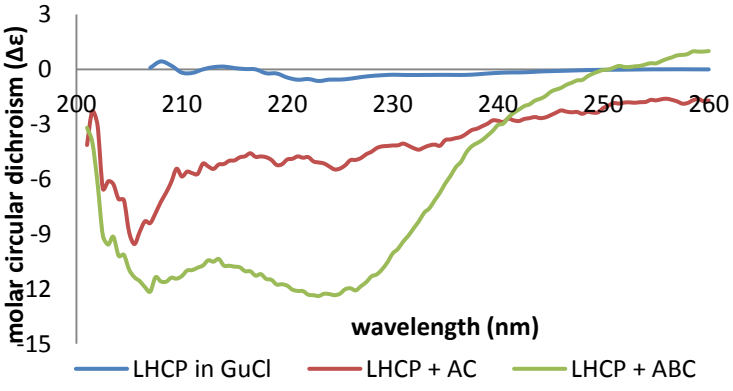

Fig.3.35. Far-UV CD spectra of LHCP, Chl *a* intermediate complex and reconstitution from detergent diluting method in GuCl. LHCP was dissolved in 6 mol/L GuCl; complexes were in GuCl and OG mixture. Spectra were recorded after centrifugation,protein concentration was determined from denaturing gel.

precipitated very quickly against time. Although samples were centrifuged and supernatant was taken for measurements, small amount of precipitated protein and pigments were still found after measurement finished. Therefore the increased *a*-helices was considered coming from both Chl *a* intermediate and aggregated protein. It was difficult to determine how much each of them contributed in the helix amount.

In the measurements from SDS-dissolved protein, purified LHCP was used and about 26% α-helices was detected in 0.13% SDS, 1.3% OG and 0.052% PG mixture, 28% in Chl *a* reconstitution and 38% in Chl *a/b* reconstitution (Fig.3.36). Purified LHCP was found about 21% α-helices in 0.26% LDS, about 5% more α-helices were resolved when OG was added (Fig.3.37). FRET measurements showed that in both Chl *a* and Chl *a/b* reconstitutions, about 75-80% of protein were pigmented. Because CD spectra measure a sum of of secondary structures, if we assumed 79 % of protein being pigmented in Chl *a*

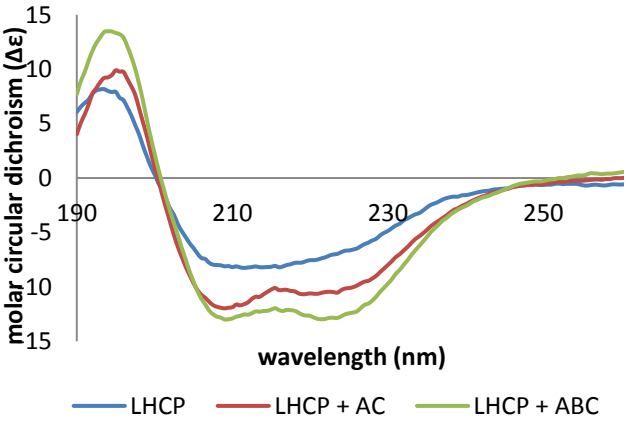

Fig.3.36. Far-UV CD spectra of LHCP, Chl *a* intermediate complex and reconstitution form SDS detergent diluting methods

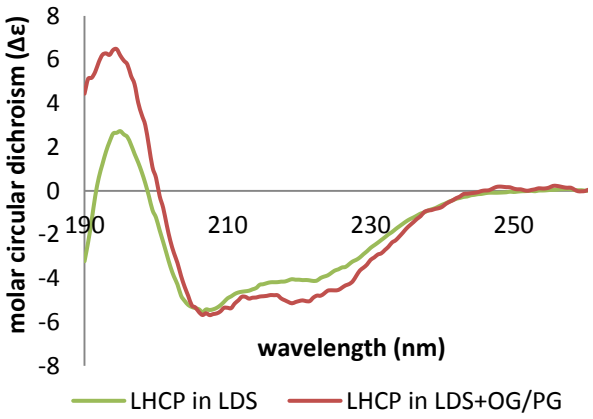

Fig.3.37. Far-UV CD spectra of LHCP dissolved in 0.26% LDS and 0.13%LDS/1.3%OG mixture

reconstitution, and in Chl *a/b* reconstitution, 80% protein would contribute as much of as it in folded LHCII, which contains 41% α-helices (Horn et al, 2002), while the rest 25% would contribute as apoprotein, containing 26% α-helices. The summed α-helix was calculated as

$$41\%*75\% + 26\%*25\% \approx 37\%$$

This result was very close the results estimated from the spectrum. On the analogy of this, 79% was consisted of Chl *a* intermediate presenting its α-helical amount, and 21% were apoprotein and in total they presented about 28% of α-helices. Therefore we deduced that Chl *a* intermediate had about 29% α-helices. Compared with apoprotein in LDS, α-helices increased about 8%, and because the addition of OG/PG has already resulted in about 5% more α-helices in the solution, only 3% increased α-helices was due to Chl *a* binding. Compared with refolded LHCII, Chl *a*- intermediate complex would have structure closer to apoprotein, the complex was regarded rather "relax". The rest helix forming to reconstitute LHCII required addition of Chl *b*.

3.6. DEER measurements

Single Cys mutant S160Ch was chosen for checking whether there are any protein aggregations in Chl *a* reconstitution and also used for background correction for double Cys mutants. Both LHCP and the intermediate had relative low modulation depth in the time measurements and had quite broad distance distribution (Fig.3.38a). Because each protein carried only one spin label, the distance distribution presented the distance between protein and its neighbors. Long distance contribution was usually integrated as a peak between 4-6 nm. In LDS sample, the spectrum was predominated by the peak at 5 nm, another peak was obviously much lower. This means in this sample most protein had a distance larger than 5 nm to the neighbor, protein molecules are monomolecularly dispersed. In the intermediate sample, the main peak was the peak around 4.7 nm. Although the peak at shorter distance had more contribution than it in LDS sample, most protein molecules kept a long distance to their neighbors. Therefore we still regarded most protein molecules were monomolecularly distributed. Due to the fact that the protein concentration in DEER samples was about 7 times as much of it in standard detergent diluting experiments, protein in those samples would be considered monomolecularly dispersed as well.

Double Cys mutant 3/160 has both Cys at N-terminus and stromal loop. Differences between fully folded and unfolded protein were significant (Fig.3.38b). The purified monomer was dominated by the shorter distance peak at about 3 nm, and due to the flexibility of the N-terminus where Cys was labelled at position 3, the short distances presented a broad distribution. On the other hand, the unfolded LHCP show distance distributions dominated by the longer distances. Both LHCP and Chl *a* complex showed similar distance distributions.

Another stromal double Cys mutant 52/160 (Fig.3.38c) showed similar results as 3/160 that LHCP and Chl *a* complex had almost the same distance distributions, apart from a very minor increase of the modulation depth. Although we do not have the distance distribution of 52/160 from pure folded LHCII, considering the restriction to position 52, this mutant was presumably dominated by a shorter distance peak which should be narrower than that of mutant 3/160.

Mutant 106/160 which had spin pair located on either end of the second transmembrane helix showed no distinguishable differences between unfolded LHCP and Chl *a* complex (Fig.3.38d).

A controversial result was from the mutant 90/196 (Fig.3.27e). Sample 1 and 2 were two batches of samples. In the first batch, sample 1, the apoprotein (orange line) showed a pretty broad distance distribution, after reconstituted with Chl *a*, the broad distribution at short distance region had a slight organization towards to the distance peak at about 3.7 nm, which was the distance peak of folded LHCII. The sample 2, on the other hand instead of repeating sample 1's results, had a distance distribution of LHCP initially predominated by short distance. After adding pigments, distance distribution moved towards to longer distance. We have also notice the distance distribution of Chl *a* intermediate in both

samples had no significant difference. LHCP presented different results in these two samples. LHCP performed in former measurement (Fehr, 2014) had similar distance distribution as the one in the first sample. The difference might attribute to sample preparation. But which caused the difference was still unclear.

Distance distributions of Chl *a* intermediate from the mutants 52/160 at stromal loop and 90/196 at luminal loop were quite similar. So far all the samples of Chl *a* intermediate showed that distance distributions were dominated by the longer distances and strongly attenuated shorter distance content. The difference between apoprotein solubilized in LDS and Chl *a* intermediate was not very obvious, indicating no significant changes in the structure.

Although we could not get to know how much of the protein is pigmented in EPR samples from FRET measurements due to too high protein and pigment concentrations, since Chl *a* was 2.3 fold molar excess over protein and the reconstitution yield in Chl *a/b* reconstitution was about 60%, we assumed that the percentage of pigmented protein would take the major portion in the mixture. Therefore the structure of intermediate complex so far is speculated virtually similar to unfolded apoprotein.

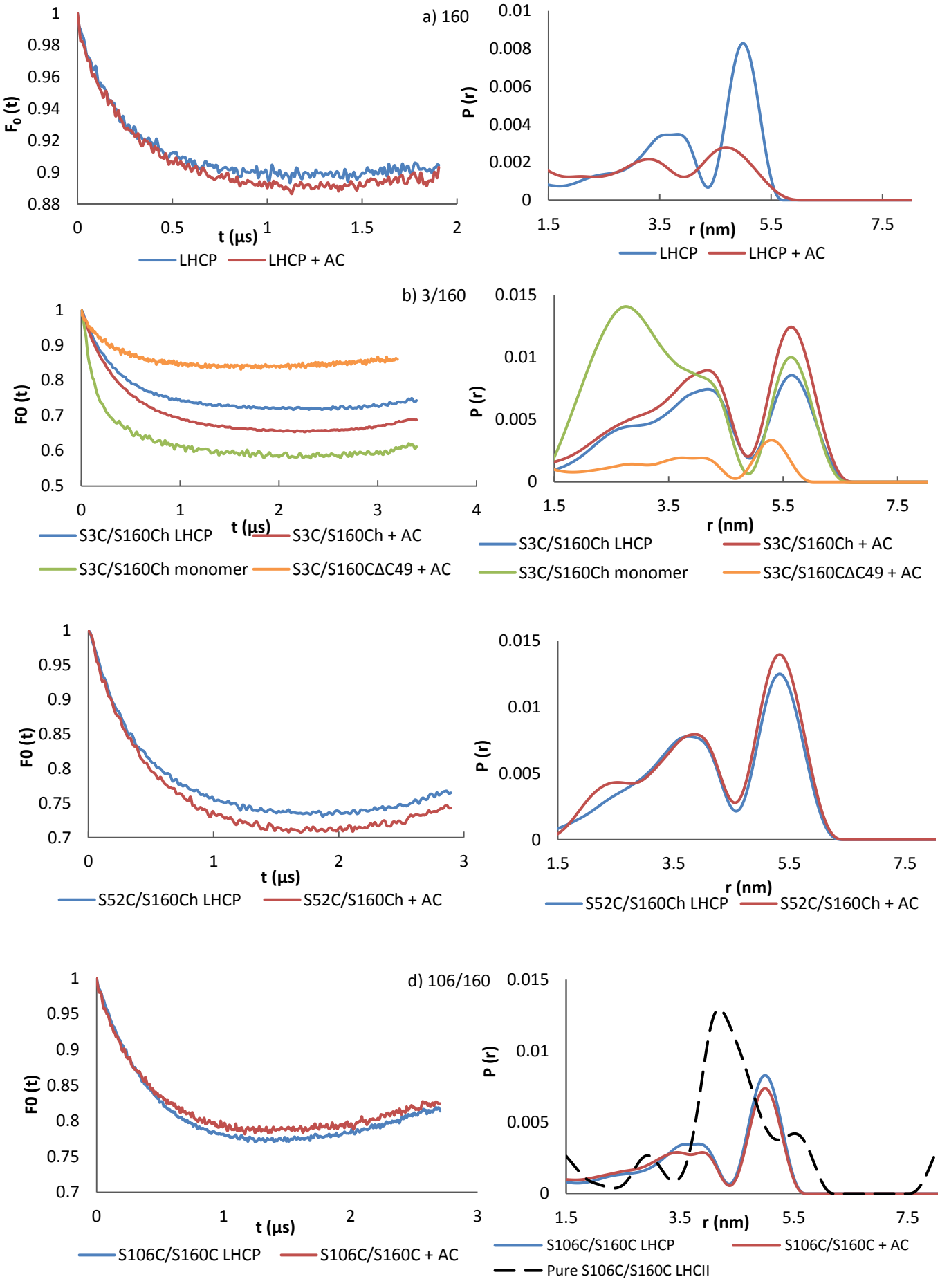
a) 160
F0 (t)
t (µs)
P (r)
r (nm)
LHCP
LHCP + AC
b) 3/160
FO (t)
S3C/S160Ch LHCP
S3C/S160Ch + AC
S3C/S160Ch monomer
S3C/S160CΔC49 + AC
S52C/S160Ch LHCP
S52C/S160Ch + AC
d) 106/160
S106C/S160C LHCP
S106C/S160C + AC
Pure S106C/S160C LHCII

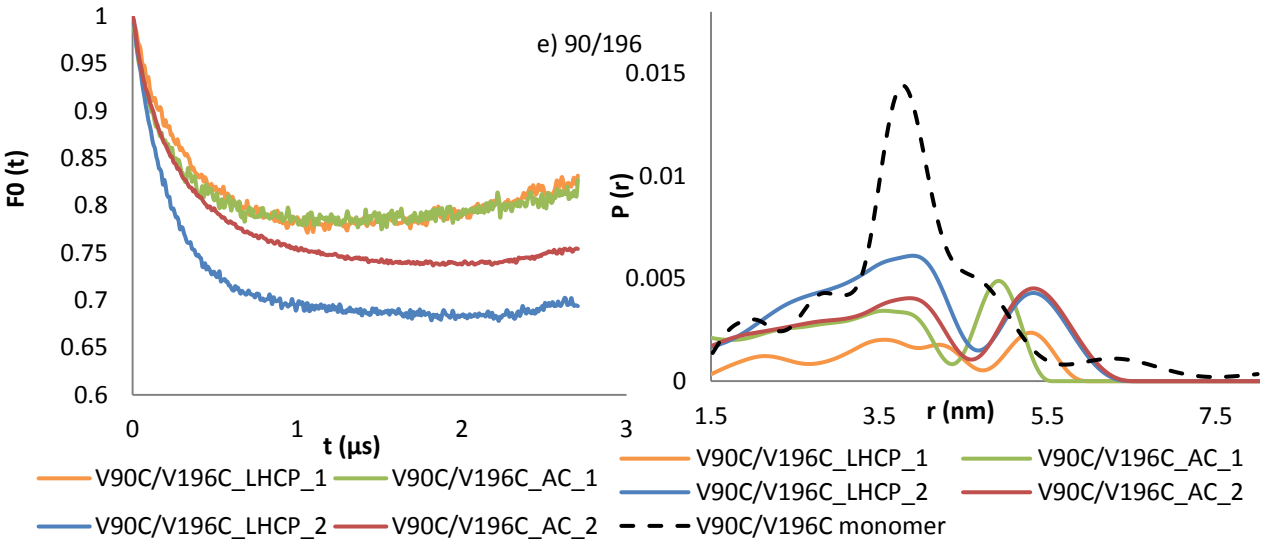

Fig.3.38 DEER-EPR results of different mutants measured in Q-Band. The black dash lane (- -) was the purified LHCII done by Dr. Niklas Fehr. All measurement settings of 4-Puls DEER-Experiments were in the table below:

	Sample	D2	Cut Off	Background Correction	Mean Distance
a) 160	LHCP	2200 ns	1904 ns	650 ns	3.76 nm
	Chl *a* complex	2200 ns	1912 ns	656 ns	3.81 nm
b) 3/160	LHCP	3500 ns	3392 ns	1000 ns	4.40 nm
	Chl *a* complex	3500 ns	3392 ns	1000 ns	4.51 nm
	monomer	3500 ns	3392 ns	1000 ns	3.78 nm
	Negative control	3200 ns	3200 ns	496 ns	3.92 nm
c) 52/160	LHCP	3000 ns	2896 ns	800 ns	4.45 nm
	Chl *a* complex	3000 ns	2896 ns	800 ns	4.49 nm
d) 106/160	LHCP	3000 ns	2704 ns	416 ns	4.13 nm
	Chl *a* complex	3000 ns	2704 ns	416 ns	4.01 nm
e) 90/196	LHCP_1	3000 ns	2704 ns	288 ns	3.78 nm
	Chl *a* complex_1	3000 ns	2704 ns	288 ns	3.44 nm
	LHCP_2	2800 ns	2704 ns	1000 ns	3.87 nm
	Chl *a* complex_2	2800 ns	2704 ns	1000 ns	3.93 nm

4. Discussion

4.1. Protein purification

Protein purification has played a very important role in this work and big efforts have been taken on finding a proper method for it Protein purity is essential for the reliability of the results measured by fluorescence, CD and EPR. As it shown at the beginning of Chapter 3, during the preparation of recombinant protein from overexpression in *E.coli*, most of the protein from bacteria were got rid of in the washing step and LHCP was able to yield more than 90%. In most of LHCII refolding study, reconstituted LHCII was able to be purified via Ni^{2+}-chelating Sepharose column and further by ultracentrifugation. The green bands obtained from sucrose gradient usually contained quite pure LHCII complex. However, in the study of this Chl *a* intermediate, Chl *a* binding was very weak and reversible, there was no further purification step after mixing LHCP and Chl *a*. Moreover, it had been noticed that there were about 30-50% apparent labeling from the foreign protein contaminants in the control measurement using Cys free mutant after labeling procedure, and these foreign proteins distributed among almost the whole lane of the denaturing gel (Fig.3.3), indicating these contaminants contained had pretty broad size distribution. Therefore it is very important to have pure LHCP before adding pigments.

In most *in vitro* work, proteins are usually purified on the basis of such characteristics as solubility, size, charge, and specific binding affinity. Affinity tags are highly efficient tools for protein detection, characterization, and purification. Immobilized Metal-Affinity Chromatography (IMAC), which is based on the interactions between a transition metal ion immobilized on a matrix and specific amino acid side chains, has been widely used for protein purification as well as other application, such as protein refolding, evaluation of protein folding status and so on (Ueda et. al, 2003). Affinity tags can be fused to the protein of interest via genetic approach (Hochuli et. al. 1988). The his_6 tag has been used for many years to

immobilize tagged LHCII monomers onto the Ni-column to form trimers. Ni^{2+} exhibits high affinity for adjacent histidine residues; non-specific binding of host proteins can be removed by a low concentration of imidazole. However, the presence of inherent cysteine- or histidine-rich regions in host proteins may result in binding with Ni^{2+}, leading to yield contamination or decreased purification efficiency (Young et.al. 2012). In this work, the purification of LHCP using Ni-column was not obvious, foreign proteins eluted together with LHCP. As proteins were denatured by 8M urea, both intermolecular and intramolecular hydrogen bonds should be destroyed. Addition of ß-ME should already destroyed disulfide bonds formed either between LHCP and other LHCP, or between LHCP and foreign protein containing cysteine. But low concentration imidazole did not elute foreign proteins. This indicated that the reason why foreign proteins were not able to be purified by Ni-column was because of either the interaction between LHCP and contaminating protein was so strong that imidazole was not able to separate them or the contaminants were not non-specifically bound to Ni-column. Bolanos-Garcia (Bolanos-Garcia and Davies, 2006) has found out that in *E. coli*, the proteins observed to co-purify with His-tagged target proteins could be divided into four groups: (i) proteins with natural metal-binding motifs, (ii) proteins with histidine clusters on their surfaces, (iii) proteins that bind to heterologously expressed His-tagged proteins, for example by a chaperone mechanism, and (iv) proteins with affinity to agarose-based supports. If the contaminating proteins have one of those characteristics (i) to (iv), .It is not easy to determine which one of above is the reason to explain why the contaminating proteins was co-purified with LHCP, the cultivation conditions and the bacterial strain have an influence on their abundance and, a consequence, their appearance as a contaminating species in the target protein preparation (Block et. al. 2009).

SDS-Polyacrylamide gel electrophoresis separates proteins primarily by mass. Preparative gel electrophoresis allows us to have protein purification, recover protein from gel matrices and collect purified protein in one step. This method has already presented high resolution; proteins with a difference as low as 2 kDa in their molecular weight can be separated by this method (Schmidt et. al., 1997). The advantages of this method are first all LHC mutants can be applied by this method; second, as mentioned above, it has protein purification, recovery and collecting

in one step; third, the purification is very efficient. In our samples, nearly no foreign proteins were found after purification. Fourth, purified protein can be either directly used for many measurements or precipitated for other use. The disadvantages of this technique are this method requires two days to cast the preparative gel column and each time only one mutant can be applied. Second, the yield of purified protein is low, only up to 30%. The reason for this could be various. One of them probably is in order to have the best purification and to load as much sample as we could, the longest gel tube length was applied in this work, and this also limited the sample volume for loading on the gel tube. Therefore protein was dissolved in a quite high concentration in LDS. As a consequence, the apoproteins required longer time being denatured in boiling water; after centrifugation, a few undissolved proteins were found at the bottom of the eppendorf tube. Also, if the proteins were not fully denatured, they may form oligomers or accumulate together, and they may not enter to the gel matrix if the size of the aggregates is too big. Air bubbles inside the gel matrix and inadequate cooling influence the quality of purification as well. It has been found after several uses of the dialysis membrane provided together with the device, the collected proteins contained very few amount of other proteins and were not as pure as those when the dialysis membrane freshly used. If the purified proteins need to be label with fluorescent dyes or spin labels, the eluted proteins need to be precipitate. Purified proteins are dissolved in Lammli buffer, which contain a lot of tris, glycine. The buffer was supposed to be replaced by other buffer via centrifugal filter. However, very poor labelling efficiency was found when the eluted solution, which was washed by neutral phosphate buffer for several times, was directly used for labelling experiments. Proteins after precipitation showed normal labelling yield, which was about 60%. Despite of quite a loss of the materials during the whole procedure, the final results from this method was still satisfying.

4.2. Comparison of different *in vitro* reconstitution methods for studying Chl *a* intermediate

For Chl *a* intermediate study, due to the fact that Chl *a* intermediate is not able to separate from unfolded LHCP, any information about this intermediate can only be deduced from the mixture

of LHCP and this intermediate in compare with LHCP and refolded LHCII. Quantification of the numbers of Chl *a* binding by FRET measurements requires that protein and Chl concentrations in all measured samples should be kept about the same after reconstitution being initiated.

Three major reconstitution methods have been compared and which can be used for what kind of measurements has been determined. The major reconstitution methods *in vitro* in general are divided into two types: detergent-exchange method and detergent diluting method. The detergent-exchange method was mostly used for producing refolded LHCII trimers. Removal of dodecyl sulfate allowed monomeric complexes to further trimerize in lipid vesicles (Hobe et.al. 1994) or on Ni^{2+}-Sepharose column (Yang et.al. 2003). Reconstituted LHCII monomers and trimers were further purified by sucrose gradients via ultracentrifugation. In this step, free pigments, aggregated pigments and proteins as well as foreign proteins were separated from refold complexes. This method usually can yield up to 70% refold protein; and the final products are directly stored in dodecyl maltoside (LM) in which refold LHCII is stable. During the removal of dodecyl sulfate, proteins are gently forced to move into OG micelles. Refolded LHCII monomers are stable in OG micelles; however, the solubility of the apoprotein is rather poor. Some unfolded proteins will co-precipitate with potassium dodecyl sulfate (KDS), leading to a decrease of protein concentration. The protein concentration after KDS precipitation is hard to determine, for in every measurement, reconstitution and precipitation differ. The pellet of the precipitated KDS is always found green, indicating co-precipitation of aggregated Chls. For pure monomer and trimer preparation, KCl is got rid of by either ultracentrifugation or Ni-column. In the measurements for Chl *a* intermediate study, sample preparation stopped at the second centrifugation for removing KDS. The remained KCl in the supernatant kept dodecyl sulfate slowly being precipitated. KCl was removed by centrifugal filter, but Chl *a* fluorescence intensity also decreased after this washing step as well; green aggregates could be found on the membrane filter, indicating the loss of pigments. We could always found that above the filter, the lower solution was greener than the upper part right after centrifugation. Pigments tended to move to the filter due to the centrifugal force; this also increased the possibility of forming pigment aggregates. If the protein concentration needed to

be determined, denaturing gel was required, which would take another a few hours until the protein concentration could be determined by the visualized band. When the gel was running, unbound molecules would slowly aggregate and some Chl *a* molecules dissociate from the protein. Therefore, the ever changeful protein and pigment concentration made detergent-exchange method not an ideal method for studying Chl *a* intermediate.

The SDS-denatured detergent diluting method was first invented for kinetic study of LHCII assembly, which was initiated by mixing equal volumes of protein and pigment solutions in a stopped flow device. Measurements were accomplished by monitoring the changes of both Chl *a* and Chl *b* fluorescence based on the energy transfer from Chl *b* to Chl *a*. In these measurements, both protein and pigments concentration were kept almost constantly after mixing protein and pigments. Therefore, this method fitted the requirements of studying Chl *a* intermediate. When time-resolved fluorescence measurements were repeated, the repetitiveness of three measurements from the same sample was found not satisfied. In the control measurements, Chl fluorescence intensity of the second measurement was obviously lower than the first one, indicating formation of some Chl aggregations. Situation was improved when a little bit more detergent and lipids were added. Three measurements presented quite good reproducibility. The adjustment of detergent concentration was also important for studying Chl *a* intermediate. Total extract, which was extracted from plant leaves, usually consists of Chl *a*, Chl *b*, carotenoids and some native lipids. These lipids slowed down Chl aggregations in the aqueous solution. However, they were removed during the single pigment preparation by preparative HPLC column. Therefore, this increased detergent concentration kept pigments staying longer time in aqueous solution.

In previous research, modified SDS-denatured detergent diluting method was applied for time-resolved CD measurements and kinetic EPR measurements for monitoring the changes of protein structure (Horn, et al. 2002; Dockter, et. al. 2009). Results from measurements provided us opportunities to obtain structural information about this intermediate.

Another modified detergent diluting method use GuCl instead of SDS to solubilize apoproteins (Yang, et. al. 2003). In SDS, LHCP presents approximately half of its α-helical folding of the native structure, while in GuCl the protein contains no detectable helical structure. It is reported

that the reconstitution products of GnCl-denatured protein exhibit very similar biochemical and spectroscopic properties as those of SDS-denatured protein; and the kinetics of LHCII assembly are virtually the same in both reconstitution procedures. Refolded LHCII from GuCl-reconstitution can be further purified via Ni-column and sucrose gradient. Manually mixed GuCl-denatured protein solution and pigment solution follow the method of GuCl reconstitution for time-resolved fluorescence measurements. About 85% protein were found precipitate after mixing and 5 min incubation In both Chl *a* and Chl *a/b* reconstitutions, Chl *a* concentration kept decreasing against time. LHCP without pigments had very poor solubility in OG solution after GuCl-reconstitution procedure, only 13.87 µg/ml (~0.54 µmol/l). Although both GuCl-reconstitution and detergent-exchange method had reconsituted protein kept in OG micelles, the progress, which forced the protein to be transferred into OG micelles, was different. In detergent-exchange method, LHCP was known to have about half of the α-helical structure in SDS; later, reconstituted proteins were first stored mixed micelles consisting of both SDS and OG. Hydrophobic α-helices were associated with the aliphatic "tail" of both detergent. OG molecules took the place of removed SDS via KDS precipitation at chilling temperature. Therefore, protein molecules were gently moved into OG micelles. KDS could also cause protein co-precipitatation when insoluble KDS formed. However, most of proteins were stayed in OG micelles, only small amount of protein co-precipitated. In GuCl-reconsitution, on the other hand, protein molecules were fully denatured in 6 mol/l GuCl; GuCl was immediately diluted after mixing with pigment solution and such low concentration disabled most of proteins from being solubilized in aqueous solution. In the reconstitution, protein molecules were pushed into OG micelles containing pigments. Because a complete reconsitution *in vitro* took about a few min, only the hydrophobic regions of proteins were to be surrounded by OG molecules and the hydrophilic portions would exposed to the aqueous medium; most of the protein failed to be reconsituted before being protected by OG micelles. Some of them were surrounded by lots of pigments and succeeded in forming stable complexes, after vortex. In Chl *a* reconsitution, protein could not form a stable structure; Chl *a* molecules easily dissociated from the protein. Therefore, water molecules could enter and both proteins and Chl *a* precipitated. An interesting result was from the control protein unable to reconstitute into LHCII, it showed a little bit higher concentration than the protein which could fold in Chl *a*

reconsitution. It was unclear why this negative protein precipitated less in the first 45 min after mixing. One possible explanation would be that after deletion, the C-terminal of this control protein was hydrophobic and could interact with OG molecules. These OG molecules somehow made the control protein meet each other difficult from C-terminus. While the LHCP had both terminuses expose outside OG micelles and had higher possibility to find each other. Owing to the constantly precipitated LHCP in Chl *a* reconstitution, GuCl-reconsitution is also not an ideal method for FRET measurements. The attempt shown in Fig.3.32. indicated the non-specific energy transfer was more than energy transfer due to pigment bindings; the covalently bound fluorescent donor dye was completely quenched by the "Chl environment", which provided a hydrophobilic enviroment for LHCP and enabled the protein to be solubilized in aqueous solution. But this method is possibly applied for UV-CD measurements, which will be further discussed in next session.

4.3. Chl *a* intermediate structural analysis by UV-CD and DEER measurements.

Single Cys mutant S160Ch measured for background correction could directly showed whether any protein aggregations formed in both Chl *a* reconstitution and LDS solublization. As what we expected, the distance distributions of both apoprotein and the intermediate were predominated by longer distance, suggesting protein molecules monomolecularly dispersed in aqueous solution. These results implied that in standard detergent diluting measurements, in which proteins were more diluted, no aggregated proteins should form. Therefore these results also supported the hypothesis of the quantification of Chl *a* bindings by FRET measurements in Chapter 3.4; the energy transfer of FRET measurements was intramolecular between fluorescent dye and pigment bindings. In standard detergent diluting reconstitutions, FRET measurements using donor dye quenched about 75-85% of that in pure LHCII. We assumed the energy transfer efficiency was about the same in Chl *a* reconstitution, Chl *a/b* reconstitution and pure LHCII monomer. Because the protein was at low concentration, only 3.9 µmol/l of end concentration and the non-specific energy transfer was excluded by the labelled negative mutant, and the energy transfer between donor dye to Chl molecules was efficient enough, we

assumed that the percentage of proteins that actually bound Chl *a* and carotenoids in the samples would be no less than 75-85%. In the samples for DEER measurments, since the reconstitution yield estimated from "green gel" was about 60%, we speculated that the percentage of pigmented protein would be no less than 60%.

4.3.1 Chl *a* intermediate presented a secondary structure closer to unfolded apoprotein

CD is an excellent method of determining the secondary structure of proteins. When the chromophores of the amides of the polypeptide backbone of proteins are aligned in arrays, their optical transitions are shifted or split into multiple transitions due to "exciton" interactions (Sreerama and Woody, 2004). The result is that different structural elements have characteristic CD spectra. For example, α-helical proteins have negative bands at 222 nm and 208 nm and a positive band at 193 nm. Proteins with well-defined antiparallel β-pleated sheets (β-helices) have negative bands at 218 nm and positive bands at 195 nm, while disordered proteins have very low ellipticity above 210 nm and negative bands near 195 nm (Greenfield, 2006). There are many different methods to analyze CD spectra to estimate secondary structure. Software and online-tools are provided for computation and analysis of protein CD spectra. All methods of analyzing CD spectra assume that the spectrum of a protein can be represented by a linear combination of the spectra of its secondary structural elements, plus a noise term. There are two general classes of methods to evaluate protein conformation. The first uses standards of polypeptides, with defined compositions in known conformations, which have been determined by X-ray scattering of films or by IR in solution (Reed, et. al, 1997). The second uses the spectra of proteins which have been characterized by X-ray crystallography as standards. Then they are compared to the spectra of unknown proteins.

CD spectra in this work were analyzed by software CDPro using SELCON3 algorithm. SELCON3 is based on the self-consistent method described by Sreerama and Woody (1993); the spectrum of the protein analyzed is included in the basis set, and an initial guess. Reference protein set contains 43 water-soluble proteins and 13 membrane proteins and spectra are analyzed in the wavelength range 190-240 nm.

LHCP in 2% LDS before reconstitution showed about 20.7% α-helices, while in the reconstitution solution, where the reconstitution initiated, about 5% more α-helices presented. Ionic detergent SDS binds both hydrophilic and hydrophobic regions of protein. SDS denatures protein by breaking the non-covalent bindings and protein loses part of its secondary structure. While nonionic detergent OG only associates with hydrophobic parts of the protein and enable protein molecules to keep their native and active forms. Therefore, a few secondary structures might be resolved after OG molecules entered and formed a mixed micelle. Chl *a* binding only introduced a slightly increased of α-helical amount; but in Chl *a/b* reconstitution, the changes of α-helix amount was significant; indicating the rest of the helical structure was resolved when Chl *b* molecules were bound. Similar results were found in GuCl reconstitution. The apoprotein denatured in 6 mol/l GuCl showed virtually no α-helix. But after Chl *a/b* reconstitution and getting rid of precipitated proteins and pigments, the complex in the supernatant showed almost the same amount of α-helices as the purified recombinant LHCII. In Chl *a* reconstitution, only about 10% α-helical structure was formed. However, we had to admit that due to the strong intrinsic UV absorption of guanidinium, protein dissolving in GuCl after reconstitution could only be measured down to 207 nm and 201 nm, respectively. The noisy signals also had strong effect on the reliability of fitting with a set of reference spectra. Moreover, LHCP slowly precipitated against time in the absence of Chl *b*. The spectrum of Chl *a* reconstitution presented the summation of Chl *a* intermediate and precipitated proteins which were formed as aggregates. Nevertheless the increase in compare with apoprotein and refolded LHCII was still small. We have noticed that the estimation of α-helical amount was lower than that was published in 2002, when different software was used. Greenfield (Greenfield, 2006) has compared different software and different algorithms pro and con. He pointed out that SELCON3 had very good estimates of the structure of globular proteins, in which the α-helix and β-sheet conformations were divided into regular and distorted fractions by considering a certain number of terminal residues in a given helical or strand segment. However, this algorithm gave poor estimates of turns and was unsuitable for the analysis of polypeptides and protein fragments. Sreerama and Woody (Sreerama and Woody, 2000) have also examined CONTIN, SELCON, and CDSSTR Methods packaged in CDPro software. Larger reference set was recommended for a reliable analysis. Although Matsuo (Matsuo, et. al, 2005) showed prediction of the secondary-structure

contents using the SELCON3 program was greatly improved, especially for α-helices, by extending the short-wavelength limit of CD spectra to 160 nm, measurements cannot be attained with a conventional CD spectrophotometer, which usually measures in the range 260 nm to 190 or 180 nm (Kelly et, al. 2005).

Nevertheless, since the FRET measurements we discussed at the beginning of Chapter 4.3 indicated that consider the yield of Chl *a*-reconstituted protein was no less than 75-85%, the estimation from UV-CD spectra hinted that Chl *a* intermediate only presented a few more α-helical structure formed than the apoprotein, indicating the structure of this intermediate would be close to the unfolded state.

4.3.2 DEER measurements revealed Chl *a* intermediate presented a similar structure as unfolded apoprotein

Four double Cys mutants were chosen and pairs of nitroxide labels were introduced site-specifically into unfolded LHCP. Labelling positions were determined due to their broad intramolecular distance distributions in apoprotein and remarkably shorter distances in the fully folded complexes. Double Cys mutants with labelling positions at either end of the second transmembrane helix (helix 3), mutant 106/160, near the luminal ends of the intertwined transmembrane helices 1 and 4, mutant 90/196, at N-terminus and stromal loop, mutant 3/160, and at the start of helix 1 and stromal loop, mutant 52/160 were chosen. Mutant 106/160 and 90/160 had similar distance distributions in both LDS and GuCl denatured apoprotein (Fehr, 2014). Mutant 52/160, which was almost symmetric to 90/196 but at stroma, was presumed to have broad distance distribution in both LDS and GuCl denatured apoprotein as well. Mutant 3/160 was speculated to be similar as 52/160, but broader distance distribution due to the flexible N-terminus.

Five out of six Chl *b* molecules were bound to the second transmembrane helix H3 of LHCII (Fig.4.1). All Chl *b* molecules were bound via ligation of the center Mg^{2+} and hydrogen bond to the formyl group. Distance distribution of mutant 106/160, which spanned along H3, changed between 40 and 150 sec in the kinetic study, yielding an apparent time constant of 50-60 sec. It

was predicted that in the first 255 ms, mixing two LDS and OG micelles in the transmembrane helix 1 and 3 region would lead to the helical formation of these helices (Fehr, 2014). However, the distance distributions of Chl *a* intermediate showed no virtually difference in compare with LDS-denatured LHCP. Both LDS and GuCl denatured protein showed similar distance distribution, suggesting that the apoproteins in LDS were almost denatured. Therefore the helical structure formation of H3 due to mixed SDS/OG micelles was considered not obvious. The increased shorter distance would be assumed to be resulted from that some of Chl *b* molecules started their bindings at around 40 sec, which mostly stabilized the helical structure, as time-resolved fluorescence measurements under EPR reconstitution condition showed apparent time constants of about 26 s (τ_1) and 178 s (τ_2) (Dockter, et. al. 2009) . In the crystal structure, Chl 12 ligates its Mg^{2+} with the O of Glu 139 and forms hydrogen bond at its formyl group with the N of Gln 131. Chl 12 strongly interacts with Chl 5 and Chl 10 via their phytol chains, the C13-keto group forms hydrogen bond with His 68. Mutation of Gln 131 by replacing it to Glu or Ser showed pronounced destabilization of the complex and loss of both Chl *a* and Chl *b* molecules, which were presumed to be Chl 6 and Chl 10 (Yang et. al. 1999). Chl 10 is also reported forming hydrogen bond with its formyl group with the N of Gln 131. Chl 6, Chl 10, Chl 13 and Chl 14 form a tetramer at the lumenal side; Chl 6 is weakly associated with H1. Therefore, we speculated that the formation of cluster at the lumenal side and binding of Chl 12 would drive H1 and H3 moving towards to each other in the later step.

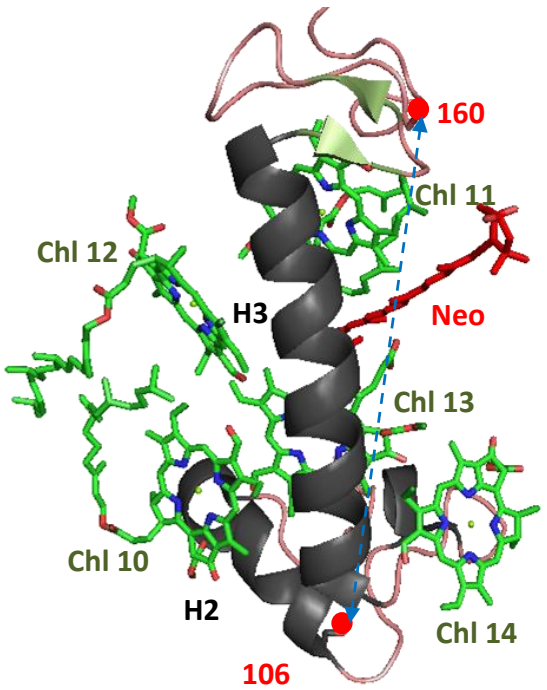

Fig.4.1. Side view of the second transmembrane helix (Helix 3) and its pigment bindings. The two labelling positions were marked in red.

For mutant 3/160, distance distributions of LDS denatured apoprotein and Chl *a* intermediate had no significant difference. 3/160 monomer showed expected shorter distance distribution. Two peaks centered

at 2.73 and 4.14 nm, which were close to the results labelled by tetramethylpiperidine-1-oxyl (TEMPO) (Jeschke, et. al, 2005). Negative control mutant 3/160ΔC49, which cannot fold, had about the same distance distribution as the functional mutant 3/160, when Chl *a* and carotenoids were added. Pure monomer indicated the labelling efficiency for double cysteine was fairly OK. Measurements using fluorescent dye have already proved the forming of Chl *a* intermediate. Mutant 52/160, which excluded the flexible N-terminus, also had similar distance distribution in both apoprotein and Chl *a* intermediate. Since this mutant had very broad distance distribution in the unfolded state and mutant 106/160 has already indicated no significant structure changes in H3, we assumed the structural changes of H1 and H2 were also minor.

Lumenal mutant 90/196 has been well studied for years. Fully folded protein showed a very narrow peak at 3.85 nm in the distance distribution. Kinetic study revealed that the formation of the super helical structure monitored by this mutant 90/196 fitted with a single exponential kinetic yielding an apparent time constant of about 300 sec (Dockter, et. al. 2009). Kinetic study by Stop-flow also proved the crossing of H1 and H4 forming intertwined structure was in the later step. Two measurements of 90/196 in Chl *a* reconstitution showed a little bit different results. In the first measurements, unfolded LHCP presented showed a quite broad distance distribution; this result was similar as the result of LDS denatured 90/196 in Dr. Fehr's doctoral work (Fehr, 2014). Chl *a* and carotenoids addition made the distance distribution a small organization towards to the distance peak at about 3.7 nm. In a repeating measurement, LHCP showed a much shorter distance distribution initially, and became broader after Chl *a* bindings. The Chl *a* intermediate in these two measurements showed similar distance distribution. It was unclear why LDS-solubilized LHCP behaved differently in these two measurements. One possible explanation could be when re-dissolved precipitated spin-labelled apoprotein in LDS in the second measurements, protein molecules were not evenly dispersed in solution. Precipitated proteins after ethanol washing step in the labelling

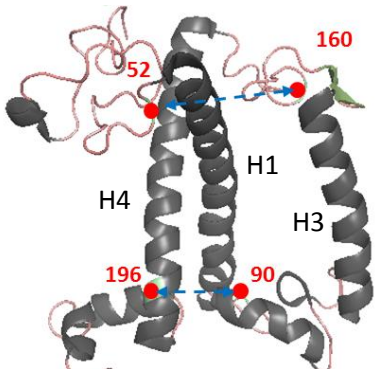

Fig.4.2. Side view of labelling position (marked in red) on the backbone of LHCII monomer based on the crystal structure (pdb ID: 2BHW).

procedure were often found not easy to be re-solubilized in 1% LDS at a high concentration. In the last few steps of spin labelling procedure, excess amount of spin labels were removed by 70% ethanol. The protein pellet was dried by ethanol volatilization. Small amount of water evaporated with ethanol. Ethanol may destroy the hydration shell of protein; some of the protein molecules would interact with each other during ethanol volatilization. Most interactions would be interrupted by vortex and ultrasonication during redissolving. Sometimes, the interactions were too strong, and they required long time in ultrasonic treatment. It was possible that these protein molecules still interacted with each other but did not form visible pellet. The interaction was broken by the diluting of pigment solution and vortexing, thereafter Chl *a* intermediate formed as monomericlly solubilized protein did.

Time-resolved DEER measurements in Dr. Fehr's doctoral work of mutants 59/90 and 174/196, which labelled spin labels along the H1 and H4 transmembrane helical domain respectively, showed some organizations in the shorter distance distribution in the first 255 ms, indicating a few more α-helices formed due to mixing OG into SDS and forming mixed micelles. Results from UV-CD showed about 7% increased α-helices in the Chl *a* intermediate compared with LDS solubilized apoprotein. However, measurements of Chl *a* intermediate of these two mutants have not been completed yet, it was hard to say, H1 and H4, which one had truly structural change. Distance changes in mutants 52/160 and 90/196 were not obvious; in Chl *a* intermediate, the whole protein chain was still quite "relax"; the whole structure in general was very close to unfolded state; Chl *a* molecules only bound to H1 and H4, but the juxtaposition of the intertwined helices of these two transmembrane helices has not formed in the absence of Chl *b*. The labelling positions of both 52/160 and 90/196 mutants spanned two transmembrane helices; spin labels were also very flexible. Therefore a small increased helical structure on just one α-helix was not very distinguishable in this case.

4.4. FRET measurements determined numbers of Chl *a* binding in Chl *a* intermediate

To better understand results from FRET measurements, models of how we designed the measurements were shown in Fig.4.3. In most FRET measurements, the observed object without FRET partner in the same measurement condition, such as labelled apoprotein, was used as "zero point" indicating no energy transfer. In our measurements, because the observed fluorescent dye had to give out/receive energy from not just one FRET partners in the reconstitution and both protein and pigments were enclosed in detergent micelles, pigments, which were in the same micelle where protein molecules were, would have non-specific energy transfer from/to the fluorescent dye, as what we have seen in Fig.3.25b, the labelled negative control protein did have donor quenching. And in measurements with higher protein concentration, for example the samples used for DEER measurements, the neighboring pigments almost quenched all the energy from Rhodamine. We could speculate the energy transfer in the functional protein would be a summation of bound Chls with dye and non-

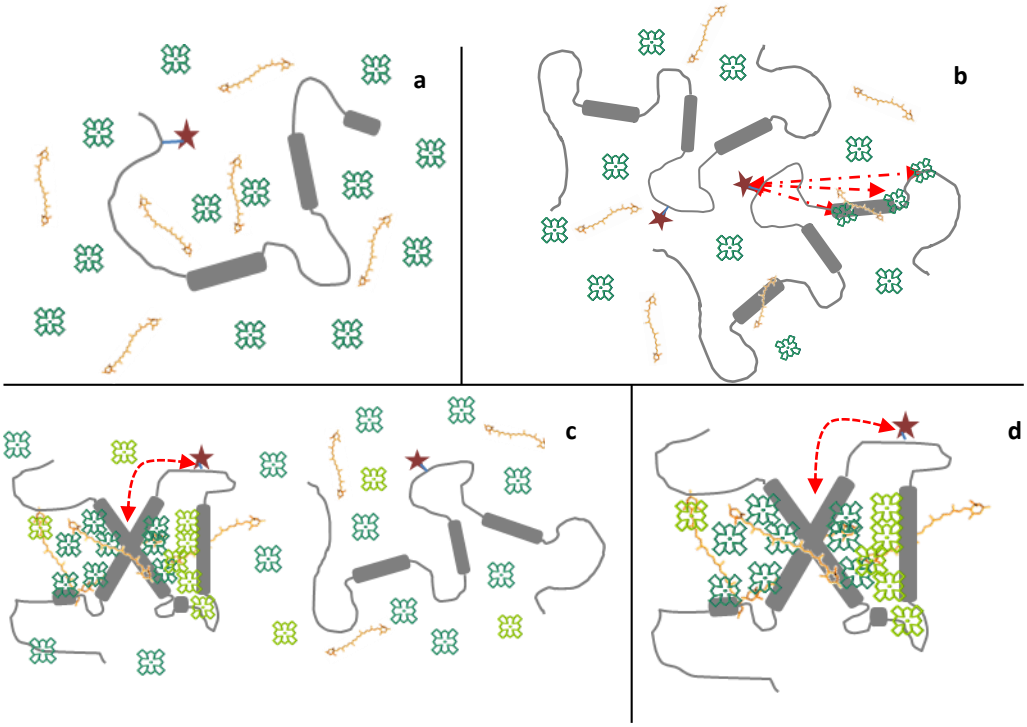

Fig.4.3. Models measured samples in FRET measurements. a) Fluorescent dye labelled on the negative mutant did not have energy transfer with pigments. b) Only Chl *a* molecules bound to protein backbone would have energy transfer with fluorescent dye. c) In Chl *a/b* reconstitution, only refolded LHCII would have energy transfer with dye. d) Purified LHCII monomer had the most energy transfer. Fluorescent dye was marked in dark red. Lines with arrow reflected FRET and its corresponding partners.

specific energy transfer. Those non-specific energy transfers could be decreased in diluted samples. However, in Chl *a* reconstitution, diluting would break the equilibrium and decrease the yield of pigmented protein. Therefore, the negative control protein was used instead of pure labelled functional protein to subtract the non-specific energy transfer from the measured energy transfer. From Fig.3.30, the non-specific energy transfer was less significant in the measurements using acceptor dye. The reason for that might be when using donor dye, Rhodamine Red C is a hydrophobic dye, although the labelling position is at stromal loop, which is the hydrophilic domain in the molecules, the dye molecule might also embraced by detergent which contains pigments. And if we excited at 550 nm where Rhodamine absorbs most, we would see the energy transfer from Rhodamine to its neighbor pigments within the micelle. Accordingly, additional pigments were added to the purified LHCII samples, so that both protein and Chl *a* concentration were identical in all samples. Here we need to point out that donor dye transfers energy to both Chl *a* and Chl *b*. It is difficult to distinguish how much each of them contributes, as the Förster critical distance between Rhodamine and Chl *a* is only about 3 Å less than it to Chl *b*. In both Chl *a* and Chl *a/b* reconstitutions, system consisted of pigmented proteins and non-pigmented proteins. As non-specific energy transfer was subtracted by negative control protein, here we assumed that only those pigments which were bound to the protein backbone would do energy transfer.

Another observation was when carotenoids were also omitted from the pigment mixture, donor dye energy all quenched and a distinct Chl *a* aggregation peak appeared after deconvoluting Chl *a* emission peak at 680 nm, which was the emission of Chl *a* monomer (Amster, 1969). It has been reported that in dilute ethanol solutions, Chl *a* is in monomeric form and has fluorescence emission; and solvated dimers formed by a π-π interaction between the Chl monomers in highly concentrated ethanol solutions, showing a emission band at about 724 nm at low-temperature (Brodye and Brody, 1967; Vladkova, 2000). Aggregation can be suppressed in the presence of macromolecules or peptides due to a coordination of macromolecule bound ligands to Chl *a* (Uehara et. al. 1988; Dudkowiak et. al. 1998). It was also showed that energy was transferred from the shorter to the longer wavelength forms, suggesting some Chl *a* aggregate forms were able to quench the energy from the monomeric form. In all reconstitution

measurements, pigments were first dissolved in small amount of ethanol and then transferred to aqueous solution. The emission spectra indicated that the protein molecules not only bound some Chl *a* molecules but also bound the aggregate forms of Chl *a*. These aggregations were not very obvious when xanthophylls existed. The possible reason might be on one hand xanthophyll molecule reduced Chl *a* molecular collisions; on the other hand xanthophyll molecules might enhance Chl *a* bindings as well. From LHCII crystal structure, some Chl *a* molecules are strongly interact with lutein molecules around intertwined helices. It is likely that some Chl *a* bindings require the association with xanthophyll. Thus, we speculate that in the presence of carotenoids, the apparent pigmented protein yield relies on protein and Chl *a* ratios. Under this presumption, we assumed in both Chl *a* and Chl *a/b* reconstitutions (Chl *a:b* =3:1), the percentages of proteins that actually bound Chl *a* and carotenoids were the same.

In the acceptor dye measurements, Fig 3.30 showed non-reconstituted proteins had nearly no energy transfer and Fig.3.11 showed pure LHCII exhibited an energy transfer efficiency of ~90%; around 50% energy transfer was seen in Chl *a/b* reconstitution in compare with purified labelled LHCII monomer, indicating about 50% reconstitution yield, which was in the agreement of the analysis by partially denaturing gel. In the Chl *a* intermediate sample, the acceptor dye only received about half of the energy of it from reconstituted LHCII. The acceptor dye did not give information of how much percent protein were pigmented in the Chl *a* reconstitution. Therefore, if we wanted to quantify the number of how many Chl *a* molecules were actually bound to the protein, we needed to first figure out how many protein were pigmented. To answer this question, we used donor dye and we assumed that the energy of the donor dye would quench as long as there was one Chl *a* molecule bound to the protein; the energy transfer efficiency was assumed to be 100%. And the number of bound Chl *a* molecules was assumed not to affect the energy transfer efficiency, consequently the quenching of donor dye in both Chl *a* and Chl *a/b* reconstitutions were considered to be the same. In real measurements, the apparent yields of reconstitutions in all different Chl *a/b* ratios were more or less the same; about 75-85% donor quenching was observed. Gundlach et.al.(Gundlach et. al. 2009) pointed out that Rhodamine and LHCII trimer had about 98% donor quenching; the energy transfer between Rhodamine and LHCII monomer would be ≥ 90%. According to the

estimation from UV-CD, the intermediate had only a small increase in α-helical amount in compare with apoprotein. Most α-helical structure of three transmembrane helices were considered having not formed but still in random coil form, therefore the real distances between bound Chl *a* molecules and the dye would be speculated to be a bit larger than those in refold LHCII monomer. The energy transfer from donor dye to Chl in Chl *a* intermediate might be less efficient than in refold complex, for in refold complex, Chl *b* molecules also acted as energy acceptors and had better energy transfer from donor dye. Although we could not tell what exactly the energy transfer efficiency in Chl *a* reconstitution, we still could say that the yields of protein truly bound Chl *a* in the intermediate samples would be at least no less than those in Chl *a/b* reconstitutions. Since about 75-85% donor quenching was observed in both Chl *a* and Chl *a/b* reconstitutions, a conservative estimate of the yield would be no less than 75%.

Now we went back to the acceptor dye. In chapter 3.4, we have already known that the sensitized dye fluorescence showed the increase in the intermediate sample was about 44% of that in Chl *a/b* reconstitution ($\frac{19\%}{43\%} \times 100\% \approx 44\%$, 19% and 43% were the increased dye emissions calculated from Fig.3.30.). In the refold LHCII monomer, the energy transfer of Chl *a* to acceptor dye was regarded as 100%, all bound Chl *a* molecules were considered to have the same in energy transfer, and the unbound Chl *a* molecules did not do any energy transfer, so the 43% increased dye emissions were considered all coming from refold LHCII, which has 8 Chl *a* molecules bound. If the percentages of pigmented protein were assumed to be the same, in each intermediate molecule, the energy transfer from Chl *a* to the acceptor dye reached only 43% of it in Chl *a/b* reconstitution. And this was 43% of 8 Chl *a*, which was 3.4. If the percentage of pigmented protein were not the same, the most extreme situation would be that the protein were 100% pigmented in Chl *a* intermediate, while only 75% protein were pigmented in Chl *a/b* reconstitution. In this case, the calculated bound Chl *a* molecules in Chl *a* intermediate was about 2.6. Since the number should be an integer, the number of bound Chl *a* molecules in Chl *a* intermediated would be speculated to be 2, 3 or 4. The same as it when using donor dye, the energy transfer from Chl *a* molecules to the acceptor dye in Chl *a* intermediate in real measurements would be less efficient than in refold complex. The number of bound Chl *a* molecules in Chl *a* intermediate would be more than 2.6. The energy transfer

efficiency of DY-731 in LHCII monomer was about 90%. Because the intermediate structure was close to the apoprotein; Chl *a* molecules were less restricted by the protein backbone, therefore it's very rare that all Chl *a* molecules keep stayed perpendicular to the dye molecules and no energy transfer at all. Also the resonance energy transfer between neighbored Chl *a* molecules should not be neglected. Therefore we still considered that Chl *a* molecules could transfer most of the energy to the acceptor dye. If we assumed that the energy transfer in Chl *a* reconstitution in average were 30% less efficient than that in Chl *a/b* reconstitution, the calculated number in the first and second extreme situation above would be 4.8 and 3.7, respectively. Thus the number of bound Chl *a* molecules in Chl *a* intermediated would be speculated to be 3, 4 or 5.

When directly compared Chl *a* intermediate sample with LHCII monomer, the calculated number of Chl *a* was 2. Considering the less energy transfer efficiency, larger distance between bound Chl *a* molecules and fluorescent dye, and unknown orientation of Chl *a* and dye in the Chl *a* intermediate, the calculation of Chl *a* numbers in intermediate was underestimated as well. Therefore the number of Chl *a* would be larger than 2. To determine which one was the right number, we needed to analyze from the refold complex structure.

4.5. Proposed a structure model of Chl *a* intermediate *in vitro*

Both Liu and Standfuss (Liu et. al, 2004; Standfuss et. al., 2005) have reported coordinations of chlorophylls and their interactions with local environments according to the crystal structure of LHCII trimer (Fig.4.4). Some Chl *a* molecules show strong interaction with neighboring Chl *b* molecule. We have known that only 3-5 Chl *a* molecules were able to bind to the protein in the absence of Chl *b*. Then Chl *a* binding would also be divided into two steps: the first step, assumed to be the fast step, around half of the Chl *a* molecules bound to the protein backbone very likely with lutein; the second step, the rest Chl *a* molecules either bound together with Chl *b* molecules or bound to stabilize the intertwined H1 and H4 when they were very close to each other.

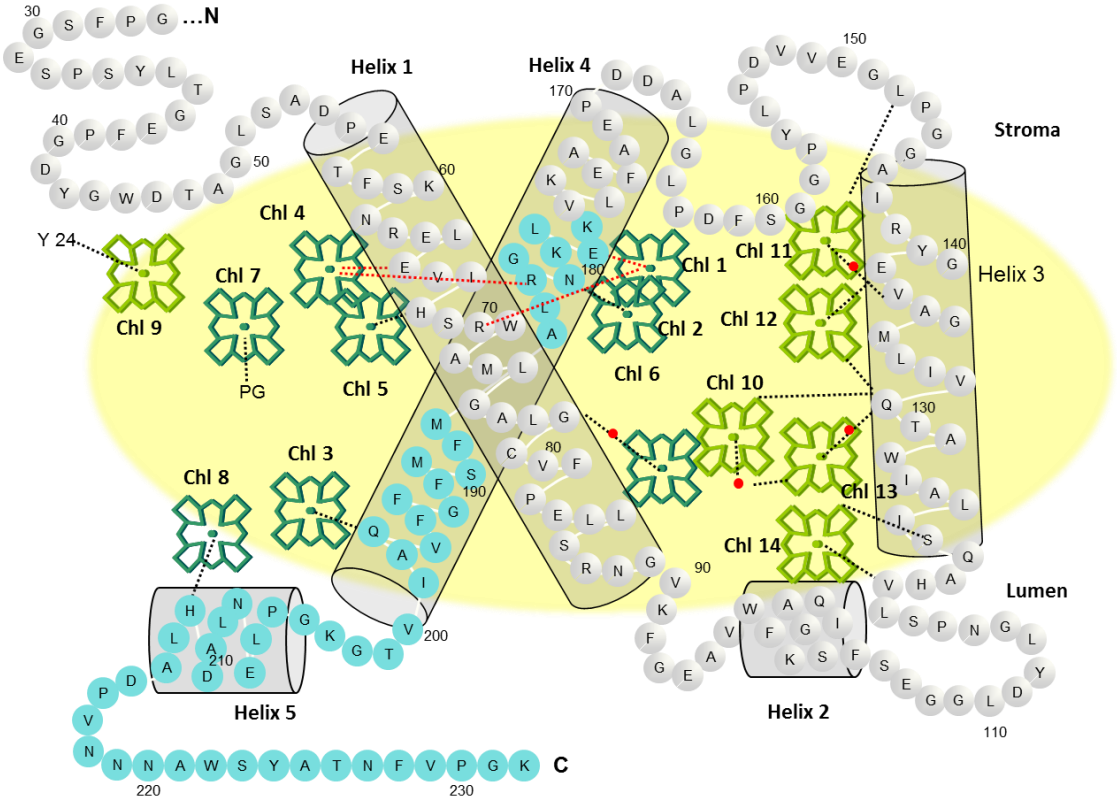

Fig.4.4. Coordinations of chlorophylls and their environments. Ligations to Mg2+ and hydrogen bonds to Chl *b* formyl group were black dot lines. Ion pair bridges were red dot lines. Red dots were water molecules involved in pigment ligations. Deleted amino acid residues in negative mutant were marked blue.

In LHCII monomer, Chl molecules mostly bind His, Glu, Gln, Arg, Asn and Val. Five Chl *b* molecules around H3 not only have ligation at the central magnesium but also form hydrogen bond on its formyl group. Gln 131 has showed exclusively binding Chl *b* molecules. This amino acid residue ligates Chl 13 in cooperation with water molecules and forms hydrogen bonds with Chl 10 and Chl 12. Chl 12 strongly interacts with Chl 5.

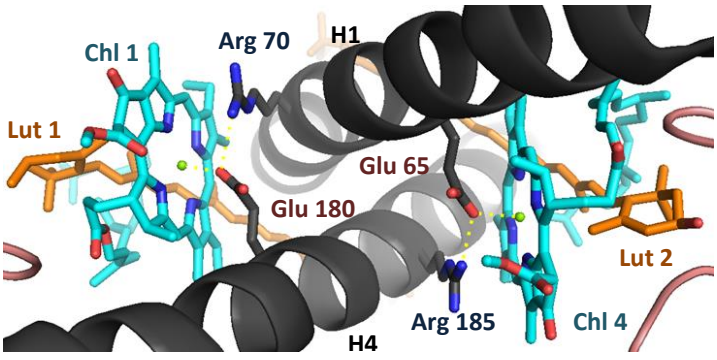

Fig.4.5. Top view of Chl 1 and Chl 4 bindings and their interaction with Lut. Revised from LHCII trimer crystal structure. (pdb ID: 2BHW)

The negative mutant S3CΔC49 has deletion of the last 53 amino acid residues, which includes all the binding sites on H4. This mutant shows no pigment binding affinity, however, it keeps most of the hydrophobic

domain containing most of the binding sites, especially all the binding sites on H1 and H3. According to the crystal structure, lutein 1 (Lut 1) spanned along H4, motif DPLG at the stromal loop shapes like a hook and bound Lut1 one head group and Gln 197 fixed the other. The phytol tail of Chl 1 tightly locked Lut1 closely to protein backbone (Fig.4.5). The deletion obviously disabled Lut 1 binding. Chl 1 and Chl 4 lost their binding affinities as well. These two Chl *a* molecules were bound by ion pair bridges Arg 70-Glu 180 and Glu 65-Arg 185, respectively. Losing either of the amino acid residues in ion pair resulted in no Chl *a* binding in the negative mutant. Because the intertwined structure formed in the later step, it was very unlikely that the ion bridge pair amino acid residues were close to each other in the unfolded state. According to the crystal structure, Chl 4 and Chl 5 had pretty strong interaction. Although the binding site of Chl 5 is His 68, the negative mutant S3CΔC49 indicated that this binding site seemed not to be taken in the Chl *a* intermediate. The exchange of His 68 caused the loss of 2 or 3 Chl molecules as well as the stability of the complex. The losses of Chl molecules were predicted to be Chl 4, Chl 5 and Chl 12 (Yang, et.al. 1999). Therefore, we assumed Chl 1, Chl 4 and Chl 5 were bound in the slower step.

Chl 6, which is close to the luminal loop, forms a tetramer with Chl 10, Chl 13 and Chl 14. The binding of Chl 6 on the protein backbone is different from the other Chl *a* molecules. The central magnesium is proposed to ligate with water molecule and Leu 113 forms a hydrogen bond to its C13'-keto group. This unique structure make Chl 6 strongly interact with other Chl *b* molecules in the cluster. Chl 6 and Chl 13 were reported with the smallest centre-to-centre distance (8.05Å) in LHCII (Liu, et. al, 2004). It has also revealed that this cluster had influence on Neo binding. In addition to Tyr122, the chlorine rings of Chl 6 and Chl 13 lined the Neo binding site and the epoxy group of Neo made a polar contact with the keto group of the Chl 13 phytol chain (Barros, 2009). According to the structure, Lut 2 buried its head at luminal side into the cluster, indicating interactions with those Chl molecules. Judging from these, we assumed this Chl *a* binding requires formation of the tetrameric cluster as well as interacting with Lut 2.

So far, we have noticed that it seemed that all the Chl *a* binding sites on H1 were unable to be filled in in the absence of Chl *b*. Structurally, H1 stands between H3 and H 4. Most Chl

molecules bound between H1 and H 4, which allowed energy transfer efficiently from Chl *b* to Chl *a* via Chl clusters. And the tetrameric Chl *a/b* cluster equilibrated the energy between clusters. In the end, Chl 1-Chl 2-Chl 7 cluster on the outer side of the LHCII trimer transferred energy to other subunits of PSII (Novoderezhkin, et. al, 2005).

Both UV-CD and DEER measurements indicated that Chl *a* intermediate seemed to present a loosening structure close to the unfolded apoprotein. Chl 3 and Chl 8, which located at almost the end of LHCII might be the first bound Chl *a* molecules. Taking a closer look, Chl 8 bound to His 212, which located at the last helical motif close to luminal end. This part of LHCII looked quite like an amphiphilic peptide with histidine. Dudkowiak (Dudkowiak, et. al., 1998) has found out Chl *a* molecule ligated to a histidine residue located in the hydrophobic region and Chl *a* was shielded by the peptide α-helix. Chl *a* aggregation was suppressed by the peptide as well. Remelli et al. (Remelli et al. 1999) found that substitution of ligand Gln197 or His212 with Leu or Val, respectively, led to sub-integral loss of Chl *a*. Based on this; we assume Chl 8 is also capable to bind to the protein without Chl *b*. Chl 8

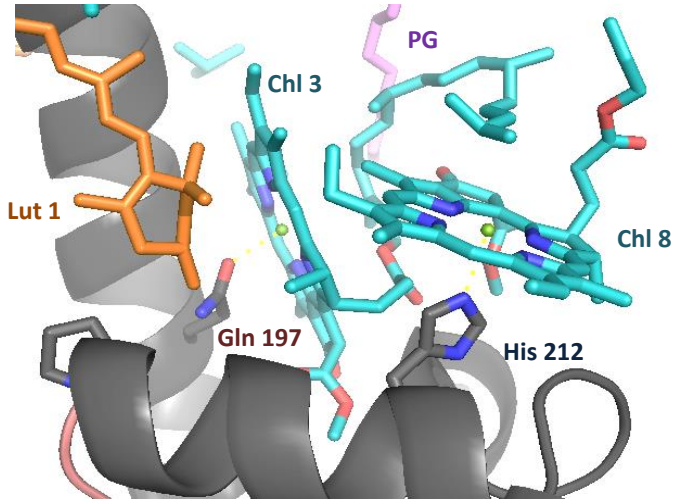

Fig.4.6. Side view of Chl 3 and Chl 8 bindings and their interaction with Lut 1. Revised from LHCII trimer crystal structure. (pdb ID: 2BHW)

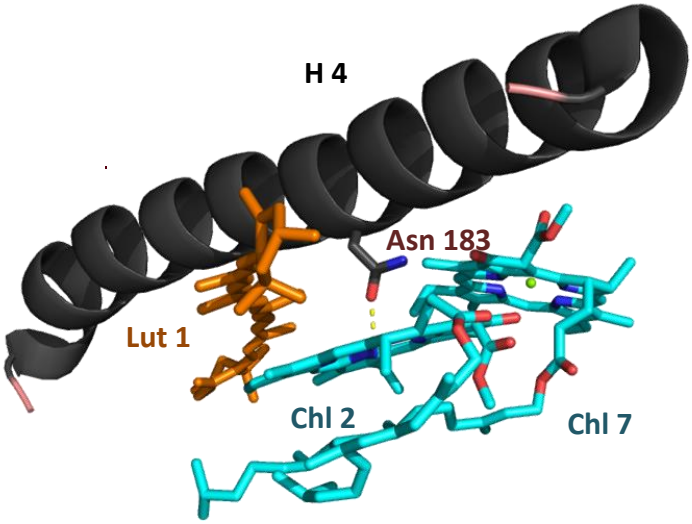

Fig.4.7. Side view of Chl 2 and Chl 7 bindings and their interaction with Lut 1. Revised from LHCII trimer crystal structure. (pdb ID: 2BHW)

also interacted with Chl 3, which ligated on Gln 197 (Fig.4.6). This amino acid also interacts with Lut 1 head group, while the other head group is "hooked" by DPLG motif in the stromal loop. Unlike Lut 2, Lut 1 was found to extract itself from behind the tightly bound chlorin ring of Chl 2 (Fig.4.7). However, the association between Lut 1 and Chl 2 is still significant. According to this, we assumed Chl 2 weakly bound to Asn 183 and Lut 1 hang along H4 together with Gln 197, which interacted with its lumenal end.

Replace Asn 183 by Leu caused a loss of both Chl 2 and Chl 7(Remelli et al. 1999). Chl 7 is the only Chl, which does not bind to protein backbone but to the oxygen of PG. This Chl is known to be the trimer-forming species. Therefore, it's hard to predict whether Chl 7 was able to bind in the intermediate. Violaxanthin (Vio) has the lowest binding affinity (Ruban et al, 1999; Hobe et al, 2000), only by hydrogen bonds of its OH groups to a glycerol OH of PG, and to the phytol carbonyl of Chl 10. In this case, we would not expect Vio bound in the intermediate.

Therefore, we speculated the number of bound Chl *a* molecules in Chl *a* intermediated would be 3 or 4; 3 Chl *a* molecules were very likely bound to the protein in the absence of Chl *b*. Chl 8 bound from the helical motif H5 by ligating with His 212, subsequently Chl 3 bound to Gln 197; Chl 7 might bind as well in the presence of PG, but it's hard to predict. A possible structure model for this unstable intermediate was proposed in Fig. 4.8. Chl 2 and Lut 1 binding seemed

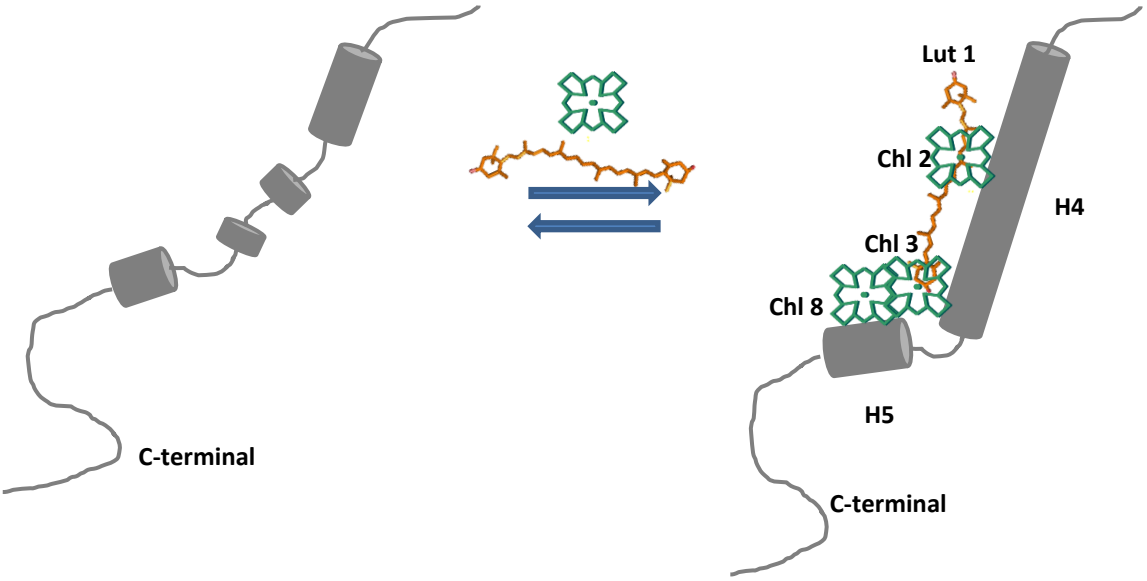

Fig.4.8. Speculated folding model for Chl *a* intermediate. Pigments bound to the transmembrane helix 4. Protein backbones: dark grey; Chl *a*: green. Lut: orange.

to be a little complicated. We did not know exactly Chl 2 and Lut1 which one would approach to the protein backbone first; the presence of Lut has showed decreasing Chl aggregation (Chapter 3.4 Fig.3.31). The bindings on H4 would introduce more helical structure in order to keep the interaction with Lut 1. This organization of transmembrane helix 4 might also explain the small increased α-helical structure which we saw in UV-CD and DEER.

This organization on transmembrane helix 4 might be essential too *in vivo*. It has been reported chloroplast signal recognition particle (cpSRP) cpSRP 43 binds to the L18 domain of LHCP, locating at the stromal loop during transport of LHCP into the thylakoid membrane(Tu et.al. 2000). Stengel (Stengel, etl al. 2008) pointed out that H 4 and L18 region of LHCP were recognized by cpSRP43, and the signal sequence–binding site of cpSRP54 M domain bound transmembrane helix 4 of LHCP forming transit complex (Cain, et. al. 2011). The reason for specific binding at H4 is so far not clear, however, we would speculate that this kind of structure would allow Chl *a* and Lut quickly bind to the protein forming intermediate, and subsequently the rest pigments bind and stabilize the complex. And it is conceivable to be much faster and more efficient.

In order to prove whether this model is true or not, further measurements could be performed. Exchange the single Cys mutant S160Ch at positions Asn 183, Gln 197 and His 212 into Leu, respectively; these mutants would be labelled with fluorescent dye and quantified Chl *a* numbers by FRET measurements as Chapter 3.4 showed. DEER measurements of Chl *a* intermediate using mutants 59/90 and 174/196 would further complement whether Chl *a* binding is focus on H4.

5. Summary

The major light harvesting complex II (LHCII) of higher plants is the most abundant membrane protein on earth. The known crystal structure and its reconstitution *in vitro* make it an ideal model for studying the folding pathway of this membrane protein and its structure changes. Former studies have shown that LHCII assembly occurs via an unstable intermediate state.

In this work, bacterially overexpressed apoprotein was first purified by gel electrophoresis to get rid of contaminant proteins. Different reconstitution methods were compared and LDS-detergent diluting method was chosen for preparing samples for, e.g., Förster resonance energy transfer (FRET), UV- Circular dichroism (CD) and double electron-electron resonance (DEER), which were used to analyze this intermediate. In UV-CD measurements, about 21% α-helices were detected in LDS solution; mixing LDS and OG micelles resulted in about 5% more α-helices; Chl *a* intermediate was estimated having about 28% α-helices, indicating that the intermediate complex has a structure closer to the apoprotein. DEER measurements of different doubly spin-labelled mutants showed similar distance distribution of both LDS-denatured apoprotein and Chl *a* intermediate, suggesting that the intermediate had not so significant structural changes comparing with apoprotein. Using donor and acceptor dye as monitors, respectively, the light-harvesting chlorophyll *a/b*-binding protein (LHCP) would gain about the same percentage of pigmented protein in both Chl *a* and Chl *a/b* reconstitution, when Chl *a* is 3 molar excess over LHCP. 3 or 4 Chl *a* molecules were able to bind to the protein in the absence of Chl *b*. A speculated intermediate model was proposed according to the LHCII crystal structure. The bound Chl *a* molecules in the intermediate were presumed to be Chl 2, Chl 3 and Chl 8. Lut 1 was assumed to be associated as well. Chl 1, Chl 4, Chl 5 and Chl 6 were considered to be added in the slower step. Chl 7 was unclear. Additional measurements were required to verify the speculations.

6. Zusammenfassung

Der Hauptlichtsammelkomplexes II (LHCII) höherer Pflanzen ist das häufigste Membranprotein auf der Erde.. Die bekannte Kristallstruktur und ihre Rekonstitution *in vitro* machen LHCII zum idealen Modell für die Untersuchung des Faltungsweg eines Membranproteins und seiner Strukturänderungen. Ehemalige Untersuchungen haben gezeigt, dass die Assemblierung des LHCII über einen instabilen Zwischenzustand erfolgt.

In dieser Arbeit wurden die bakteriell überexprimierten Apoproteine zunächst durch Gelelektrophorese gereinigt, um die verunreinigt Proteine abzutrennen. Verschiedene Rekonstitutionsmethoden wurden verglichen und die LDS/Detergen-Verdünnungsmethode wurden gewählt zur Probenherstellung für Techniken wie den Förster-Resonanzenergietransfer (FRET), den UV- Circulardichroismus (CD) und Double-Electron-Electron-Resonance (DEER), um so den oben genannten instabilen Zwischenzustand zu analysieren. In UV-CD-Messungen wurden ca. 21% der α-helikalen Sekundärstruktur in LDS-Lösung erkannt. Nur ca. 5% mehr α-helikalen Sekundärstruktur sind ausgebildet, nachdem die LDS und OG-Mizellen gemischt wurden. Das Chl *a*-Zwischenprodukt besitzt ca. 28% α-helikalen Sekundärstruktur, ähnlich wie das Apoprotein. Die Ergebnisse von verschiedenen doppelt spinmarkiert Mutanten zeigen, dass das Chl *a*-Zwischenprodukt keine erheblichen strukturellen Unterschiede zum Apoprotein aufwies. Mit Donor- und Akzeptor-Farbstoffen als Monitoren wurde gezeigt, dass das LHCII-Apoprotein ungefähr den gleichen Prozentsatz von pigmentierten Protein sowohl in der Rekonstitution mit Chl *a* wie der mit Chl *a/b* aufwies, wenn Chl *a* im dreifachen Überschuss über LHCP eingesetzt wurde. 3 oder 4 Chl *a*-Moleküle können an das Protein in Abwesenheit von Chl *b* gebunden werden. Ein spekulatives Modell für den Zwischenzustand wurde auf der Grundlage der LHCII-Kristallstruktur vorgeschlagen. Die gebundenen Chl *a*-Moleküle im

Zwischenzustand sind vermutlich Chl 2, 3 und Chl 8. Es wurde vermutet, dass Lut1 ebenfalls gebunden ist. Chl 1 Chl 4, Chl 5 und Chl 6 nach diesem Modell im zweiten Schritt gebunden. Chl 7 war noch unklar. Zusätzliche Messungen waren erforderlich, um die Spekulationen zu überprüfen.

7. Appendix

7.1 Abbreviations

ß-me	ß-mercaptoethanol
BSA	Bovine serum albumin
CD	Circular dichroism
Chl	Chlorophyll
da	dalton
ddNTP	Didesoxynucleotidtriphosphat
DEER	Double electron electron resonance
DGDG	Digalactosyldiacylglycerol
DMF	Dimethylformamid
DMSO	Dimethylsulfoxid
dNTP	Desoxynucleotidtriphosphat
DTT	Dithiothreitol
EDTA	Ethylendiamintetraacetat
EPR	Electron paramagnetic resonance
EtOH	Ethanol
FRET	Förster resonance energy transfer
his_{6}-tag	Hexa histidyl tag
IB	Inclusion bodies
IPTG	Isopropyl-β-D-thiogalactopyranosid

KCl	Potassium chloride
KDS	Potassium dodecylsulfate
KOH	Potassium hydroxide
LB	Luria Bertani
LDS	Lithium dodecylsulfate
LHCII	Light harvesting complex II
LHCP	light-harvesting chlorophyll *a/b*-binding protein
LDS	Lithiumdodecylsulfate
LM	n-Dodecyl-β-D-Maltosid
Lut	Lutein
µg	Microgram
mg	Milligram
$MgCl_2$	Magnesium chloride
N_2	Nitrogen
NaOH	Sodium hydroxide
Neo	Neoxanthin
ng	Nanogram
$NiCl_2$	Nickel chloride
NPQ	Non-photochemical quenching
OD	Optical density
OG	n-Octyl-β-D-glucopyranosid
PAA	Polyacrylamide
PAGE	Polyacrylamide gel electrophoresis
PCR	Polymerase chain reaction
PG	Phosphatidylglycerol

PROXYL-IAA	[3-(2-Iodacetamido)-2,2,5,5-tetramethyl-1- pyrrolidinyloxy], free radical
PSI	Photosystem I
PSII	Photosystem II
SDS	Sodiumdodecylsulfate
SH	Sulfhydryl
TCyEP	Tris-(2-cyanoethyl)phosphine
Tx	Triton X-100
U	Units
vio	Violaxanthin
w/v	weight /volume
w/w	weight/ weight

7.2 Amino acids three- and one-letter codes

Amino acid	three-letter code	one-letter code	Amino acid	three-letter code	one-letter code
Alanine	Ala	A	**Leucine**	Leu	L
Arginine	Arg	R	**Lysine**	Lys	K
Asparagine	Asn	N	**Methionine**	Met	M
Aspartic acid	Asp	D	**Phenylalanine**	Phe	F
Cysteine	Cys	C	**Proline**	Pro	P
Glutamine	Gln	Q	**Serine**	Ser	S
Glutamic acid	Glu	E	**Threonine**	Thr	T

Glycine	Gly	G	**Tryptophane**	Trp	W
Histidine	His	H	**Tyrosine**	Tyr	Y
Isoleucine	Ile	I	**Valine**	Val	V

7.3 Sequence

Clone C3.2h (Kosemund, 1999)

Line1: DNA base code

Line2: Amino acid one-letter code

Line3: Corresponding protein domains

1 ATG CGT AAA TCT GCT ACC ACC AAG AAA GTA GCG AGC TCT GGA AGC

1 Start R K S A T T K K V A S S G S

N-terminal

46 CCA TGG TAC GGA CCA GAC CGT GTT AAG TAC TTA GGC CCA TTC TCC

15 P W Y G P D R V K Y L G P F S

91 GGT GAG TCT CCA TCC TAC TTG ACT GGA GAG TTC CCC GGT GAC TAC

30 G E S P S Y L T G E F P G D Y

136 GGT TGG GAC ACT GCC GGA CTC TCT GCT GAC CCA GAG ACA TTC TCC

45 G W D T A G L S A D P E T F S

Helix 1

181 AAG AAC CGT GAG CTT GAA GTC ATC CAC TCC AGA TGG GCT ATG TTG

60 K N R E L E V I H S R W A M L

226 GGT GCT TTG GGA TGT GTC TTC CCA GAG CTT TTG TCT CGC AAC GGT

75 G A L G C V F P E L L S R N G

Lumenal loop

271 GTT AAA TTC GGC GAA GCT GTG TGG TTC AAG GCA GGA TCT CAA ATC

90 V K F G E A V W F K A G S Q I.

Helix 2

316 TTT AGT GAG GGT GGA CTT GAT TAC TTG GGC AAC CCA AGC TTG GTC

105 F S E G G L D Y L G N P S L V

361 CAT GCT CAA AGC ATC CTT GCC ATA TGG GCC ACT CAG GTT ATC TTG

120 H A Q S I L A I W A T Q V I L

Helix 3

406 ATG GGA GCT GTC GAA GGT TAC CGT ATT GCC GGT GGG CCT CTC GGT

135 M G A V E G Y R I A G G P L G

Stromal loop

451 GAG GTG GTT GAT CCA CTT TAC CCA GGT GGA AGC TTT GAT CCA TTG

150 E V V D P L Y P G G S F D P L

496 GGC TTA GCT GAT GAT CCA GAA GCA TTC GCA GAA TTG AAG GTG AAG

165 G L A D D P E A F A E L K V K

Helix 4

541 GAA CTC AAG AAC GGT AGA TTA GCC ATG TTC TCA ATG TTT GGA TTC

180 E L K N G R L A M F S M F G F

586 TTC GTT CAA GCT ATT GTA ACT GGA AAG GGT CCT TTG GAG AAC CTT

195 F V Q A I V T G K G P L E N L

Helix 5

631 GCT GAT CAT CTT GCA GAC CCA GTC AAC AAC AAT GCA TGG TCA TAT

210 A D H L A D P V N N N A W S Y

C-terminal

676 GCC ACC AAC TTT GTT CCC GGA AAA CAC CAT CAC CAT CAC CAT TAA

225 A T N F V P G K H H H H H H Stop

His_6-tag

7.4 Spectra deconvolution:

To decovolute the spectra from donor dye labelled samples, the dye emission of labelled apoprotein was directly used for fitting the dye emission of each spectra. Because the spectra were slightly distorted, small adjustments were required to avoid over subtracting spectra. For the acceptor dye, because of the overlapping of Chl *a* emission at far red region and dye emission, the spectra were first fitted at Chl emission and the subtracted this part to get dye contribution. All the spectra had more or less distortion around the maximal emission of Chl *a*.

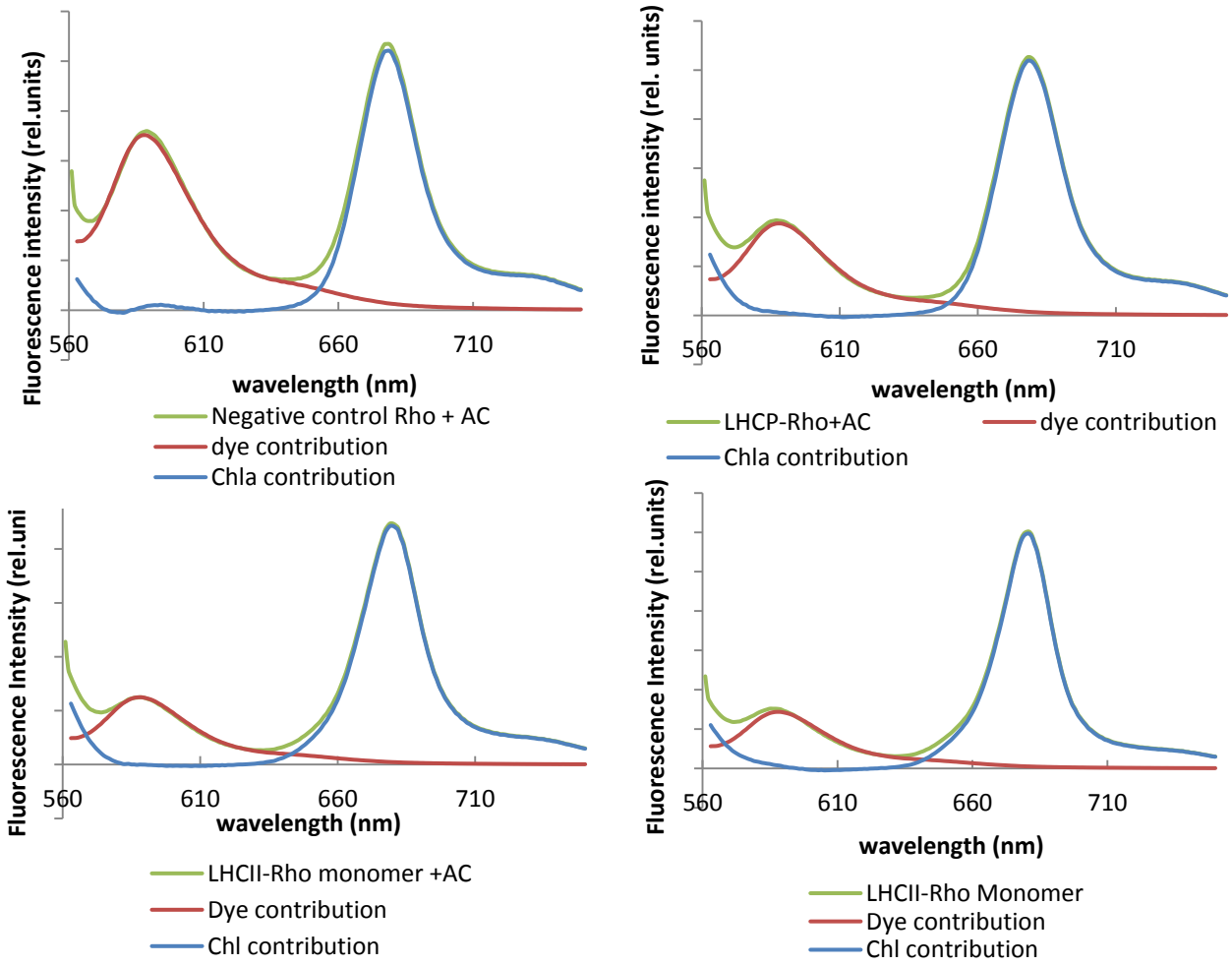

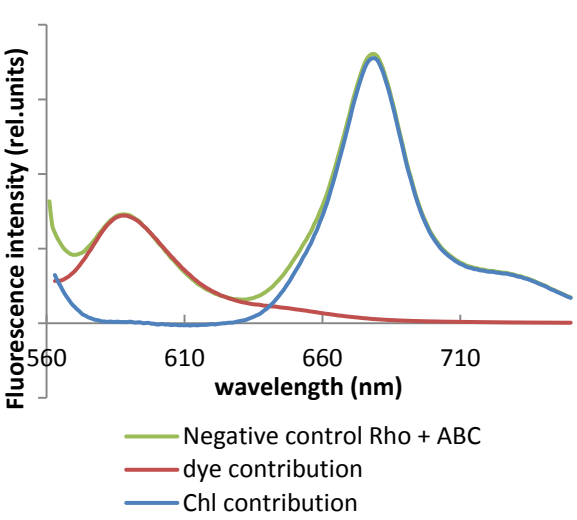
Fluorescence intensity (rel.units)
560
610
660
710
wavelength (nm)
Negative control Rho + ABC
dye contribution
Chl contribution

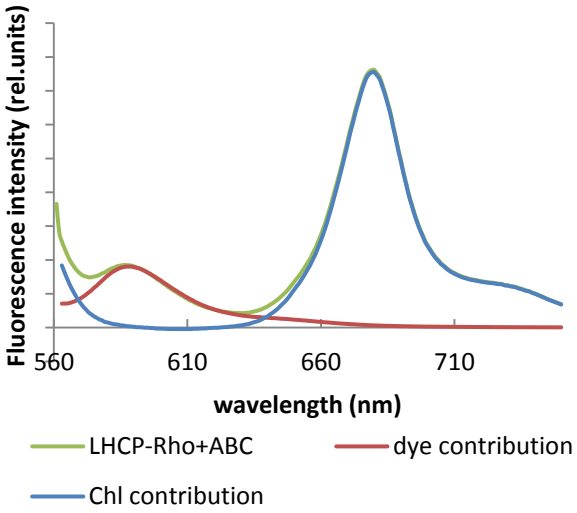
Fluorescence intensity (rel.units)
560
610
660
710
wavelength (nm)
LHCP-Rho+ABC
dye contribution
Chl contribution

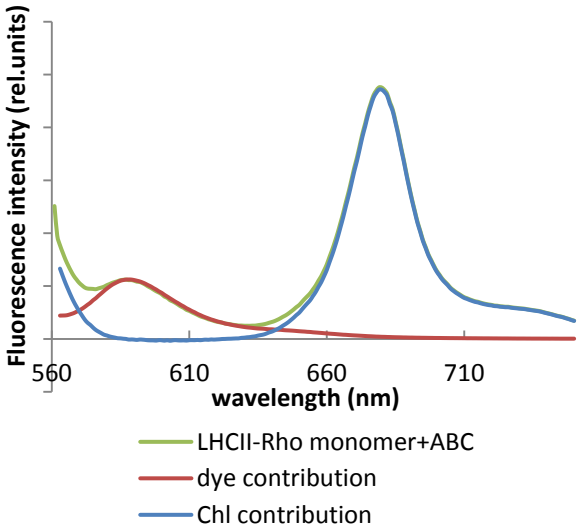
Fluorescence intensity (rel.units)
560
610
660
710
wavelength (nm)
LHCII-Rho monomer+ABC
dye contribution
Chl contribution

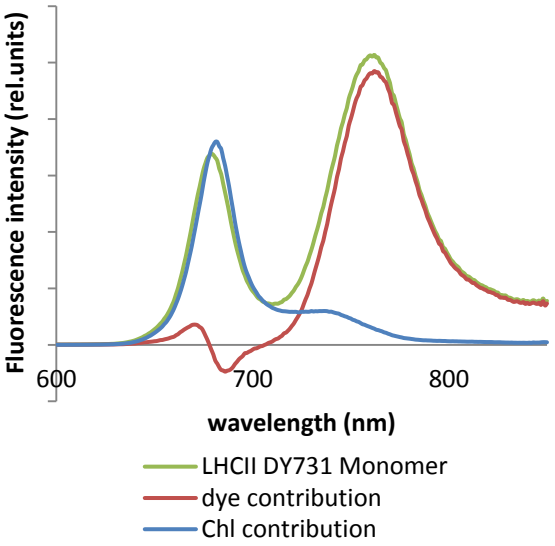
Fluorescence intensity (rel.units)
600
700
800
wavelength (nm)
LHCII DY731 Monomer
dye contribution
Chl contribution

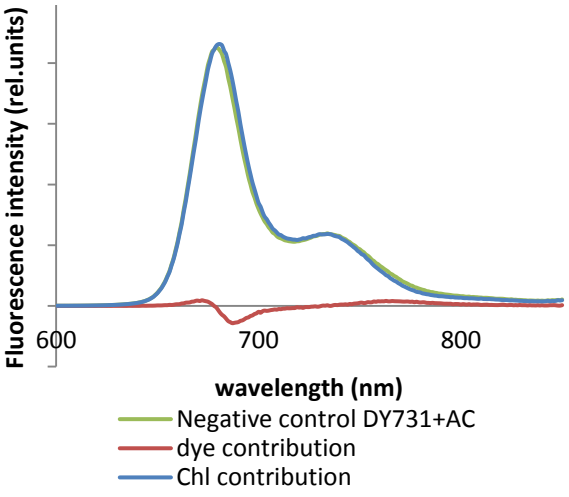
Fluorescence intensity (rel.units)
600
700
800
wavelength (nm)
Negative control DY731+AC
dye contribution
Chl contribution

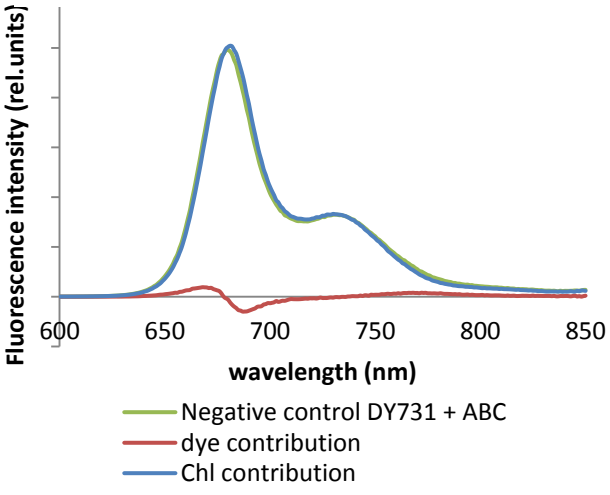
Fluorescence intensity (rel.units)
600
650
700
750
800
850
wavelength (nm)
Negative control DY731 + ABC
dye contribution
Chl contribution

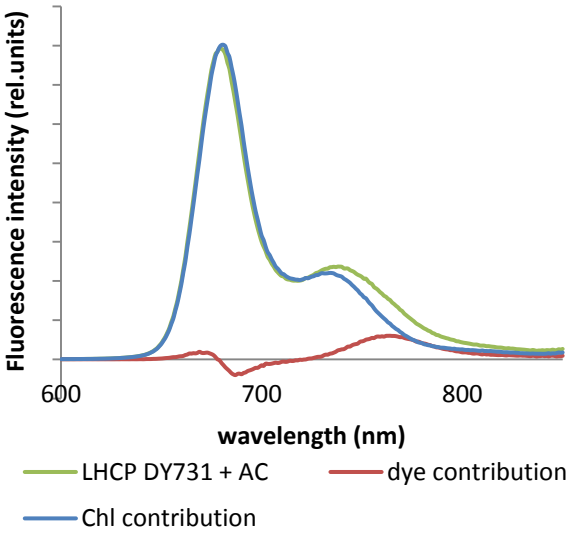
Fluorescence intensity (rel.units)
600
700
800
wavelength (nm)
LHCP DY731 + AC
dye contribution
Chl contribution

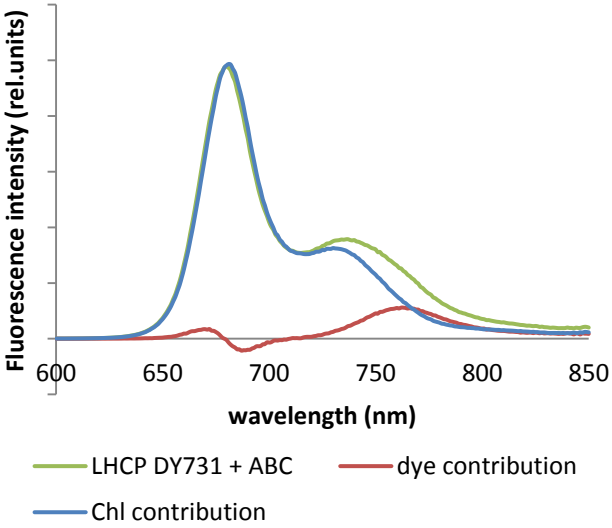
Fluorescence intensity (rel.units)
600
650
700
750
800
850
wavelength (nm)
LHCP DY731 + ABC
dye contribution
Chl contribution

Reference

Adamska I. (1997) ELIPs-light-induced stress proteins, Physiologia. Plantarum. 100; 794-805.

Agarwal, S. K. (2005) Advanced biophysics. APH Publishing Corporation, New Delhi.

Allen, J. F., Forsberg, J. (2001) Molecular recognition in thylakoid structure and function. Trends Plant Sci., 6: 317-326.

Amster R.L. (1969) A spectroscopic investigation of aggregations in chlorophyll solutions. Photochem Photobiol. 9(4):331-338.

Anderson JM, Aro E-M (1994) Grana stacking and protection of photosystem II in thylakoid membranes of higher plant leaves under sustained high irradiance: an hypothesis. Photosynth Res 41:315-326.

Barros, T., Kühlbrandt, W. (2009) Crystallisation, structure and function of plant Light-Harvesting Complex II, Biochim. Biophys. Acta, 1787:753-772.

Bassi, R., Sandonà, D. & Croce, R. (1997) Novel aspects of chlorophyll a/b proteins. Physiol. Plant. 100:769-779.

Bender A. (2004) Konformationsanalyse und Lipidbindung am rekombinanten Lichtsammlerprotein LHCIIb höherer Pflanzen. Dissertation am Fachbereich Biologie, Johannes Gutenberg-Universität Mainz.

Biswas R., Kühne H., Brudvig G. W., Gopalan V. (2001) Use of EPR spectroscopy to study macromulecular structure and function. Science Progress. 84(1):45-68.

Block H., Maertens B., Spriestersbach A., Brinker N., Kubicek J., Fabis R., Labahn J., Schäfer F. (2009) . Immobilized-metal affinity chromatography (IMAC): a review. Methods Enzymol. 463:439-473.

Boekema, E.J. Hankamer B., Bald D.,. Kruip J,. Nield J, Boonstra, A.F.. Barber J,. Rögner M. (1995) Supramolecular structure of the photosystem II complex from green plants and cyanobacteria. Proc. Natl. Acad. Sci. USA. 92:175-179.

Boggasch S. (2006) Immobilisierung von rekombinantem Haupt-Lichtsammlerkomplex LHCIIb in Liposomen, an Affinitätsmaterialien und Nanokristallen - biochemische und einzelmolekülspektroskopische Untersuchungen. Dissertation am Fachbereich Biologie, Johannes Gutenberg-Universität Mainz.

Bolanos-Garcia V.M., Davies O.R. (2006) Structural analysis and classification of native proteins from E. coli commonly co-purified by immobilised metal affinity chromatography. Biochim Biophys Acta. 1760(9):1304-1313.

Booth, P. J. and Paulsen, H. (1996). Assembly of light-harvesting chlorophyll *a/b* complex *in vitro*: time-resolved fluorescence measurements. Biochemistry. 35(16):5103-5108.

Broyde S. B. And Brody S. S. (1967) Emission spectra of Chlorophyll-a in polar and nonpolar solvents. J. Chem. Phys. 46:3334-3340.

Broglie R., Bellemare G., Bartlett S. G., Chua N. H., Cashmore A. R. (1981) Cloned DNA sequences complementary to mRNAs encoding precursors to the small subunit of ribulose-1,5-bisphosphate carboxylase and a chlorophyll a/b binding polypeptide, Proc. Natl. Acad. Sci. USA. 78:7304-7308.

Caffarri S, Croce R, Cattivelli L, Bassi R. (2004) A look within LHCII: differential analysis of the Lhcb1-3 complexes building the major trimeric antenna complex of higher-plant photosynthesis. Biochemistry, 43(29):9467-9476.

Cain, P.; Holdermann, I.; Sinning, I.; Johnson, A. E.; Robinson, C. (2011): Binding of chloroplast signal recognition particle to a thylakoid membrane protein substrate in aqueous solution and delineation of the cpSRP43-substrate interaction domain. Biochem J. 437 (1):149-155.

Carpenter E.P., Beis K., Cameron A.D., Iwata S. (2008) Overcoming the challenges of membrane protein crystallography. Current Opinion in Structural Biology 18 (5):581-586.

Carraro U., Doria D., Rizzi C., Sandri M. (1994) A new two-step precipitation method removes free-SDS and thiol reagents from diluted solutions, and then allows recovery and quantitation of proteins. Biochem Biophys Res Commun. 200(2):916-24.

Cashmore, A. R. (1984). Structure and expression of a pea nuclear gene encoding a chlorophyll *a/b*-binding polypeptide. Proc. Natl. Acad. Sci. USA. 81:2960-2964.

Camm E. L., Green B. R. (2004) How the chlorophyll-proteins got their names, Photosynth Res. 80 (2004):189-196.

Chow W. S., Miller C., Anderson J. M (1991) Surface charges, the heterogeneous lateral distribution of the two photosystems, and thylakoid stacking. Biochim Biophys Acta 1057:69-77.

Connelly JP, Müller MG, Hucke M, Gatzen G, Mullineaux CW, Ruban AV, Horton P. (1997) Ultrafast spectroscopy of trimeric light harvesting complex II from higher plants. J Phys Chem, 101:1902−1909.

Coruzzi G., Broglie R., Cashmore A., Chua N. H. (1983) Nucleotide sequences of two pea cDNA clones encoding the small subunit of ribulose 1,5-bisphosphate carboxylase and the major chlorophyll a/b-binding thylakoid polypeptide, J. Biol. Chem. 258:1399-1402.

Dall'Osto L., Lico C., Alric J., Giuliano G., Havaux M., Bassi R. (2006) Lutein is needed for efficient chlorophyll triplet quenching in the major LHCII antenna complex of higher plants and effective photoprotection in vivo under strong light. BMC Plant Biol. 6: 32.

Daum B. Nicastro D. Austin J. McIntosh J. R. and Kühlbrandt W. (2010) Arrangement of Photosystem II and ATP Synthase in Chloroplast Membranes of Spinach and Pea. Plant Cell. 22(4):1299-1312.

Dietz, C. (2008) Konformationsuntersuchungen am rekombinanten LHCII mittels NMR- und EPR-Spektroskopie. Diplomarbeit am Fachbereich Biologie, Johannes Gutenberg-Universität Mainz.

Dietz, C. (2012). Structural analysis of the major lightharvesting complex II by electron paramagnetic resonance (EPR): comparison between monomers and trimers. Dissertation am Fachbereich Biologie, Johannes Gutenberg-Universität Mainz.

Drescher M. (2012) "EPR in Protein Science" in. EPR Spectroscopy: Applications in Chemistry and Biology. Topics in Current Chemistry Volume 321:91-119.

Dockter C. (2009) Untersuchung der Struktur und Assemblierung des Lichtsammelkomplexes II höherer Pflanzen mittels elektronenparamagnetischer Resonanz (EPR). Dissertation am Fachbereich Biologie, Johannes Gutenberg-Universität Mainz.

Dockter C., Volkov A., Bauer C., Polyhach Y., Joly-Lopez Z., Jeschke G., Paulsen H. (2009) Refolding of the integral membrane protein light-harvesting complex II monitored by pulse EPR. Proc. Natl. Acad. Sci. USA. 106:18485-18490.

Dockter C., Müller A. H., Dietz C., Volkov A., Polyhach Y., Jeschke G., and Paulsen H. (2011) Rigid Core and Flexible Terminus. J. Biol. Chem. 287(4):2915-2925.

Ducruet J.M., Peeva V., Havaux M. (2007) Chlorophyll thermofluorescence and thermoluminescence as complementary tools for the study of temperature stress in plants. Photosynth Res. 93(1-3):159-171.

Dudkowiaka A., Nakamuraa C., Araib T., Miyake J. (1998) Interactions of chlorophyll a with synthesized peptide in aqueous solution. J. Photochem. Photobiol. B. Biol. 45(1):43-50.

Fanucci G. E., Lee J. Y., and Cafiso D. S. (2003) Specroscopic evidence that osmolytes used in crystallization buffers inhibit a conformation change in a membrane protein. Biochemistry, 42:13106-13112.

Fehr. N. (2014) Struktur- und Faltungsuntersuchungen am majoren Lichtsammelkomplex II mittels Elektronen-Paramagnetischer-Resonanz (EPR). Dissertation am Fachbereich Biologie, Johannes Gutenberg-Universität Mainz.

Garavito R.M., Ferguson-Miller S. (2001) Detergents as tools in membrane biochemistry. J. Biol. Chem. 276:32403-32406.

Georgakopoulou S., van der Zwan G., Bassi R., van Grondelle R., van Amerongen H., Croce R. (2007) Understanding the changes in the circular dichroism of light harvesting complex II upon varying its pigment composition and organization. Biochem. 46(16):4745-4754.

Gradinaru CC, Özdemir S, Gülen D, van Stokkum IHM, van Grondelle R, van Amerongen H. (1998) The flow of excitation energy in LHCII monomers: Implications for the structural model of the major plant antenna. Biophys J. 75:3064-3077.

Greenfield. N.J. (2006) Using circular dichroism spectra to estimate protein secondary structure. Nat Protoc. 1(6):2876-2890.

Gundlach K., Werwie M., Wiegand S., Paulsen H. (2009) Filling the "green gap" of the major light-harvesting chlorophyll a/b complex by covalent attachment of Rhodamine Red. Biochimica et Biophysica Acta. 1787:1499-1504

Henry R. L. (2010) SRP: adapting to life in the chloroplast. Nature Structural & Molecular Biology 17:676-677.

High, S., Henry R, Mould R.M., Valent Q., Meacock S., Cline K., Gray J.C., Luirink J. (1997) Chloroplast SRP54 interacts with a specific subset of thylakoid precursor proteins. J. Biol. Chem. 272:11622-11628

Hobe, S., Fey, H., Rogl, H., and Paulsen, H. (2003). Determination of relative chlorophyll binding affinities in the major light-harvesting chlorophyll a/b complex. J. Biol. Chem., 278(8):5912-5919..

Hobe, S., Niemeier, H., Bender, A., and Paulsen, H. (2000). Carotenoid binding sites in lhciib. relative affinities towards major xanthophylls of higher plants. Eur. J. Biol. Chem., 267(2):616-624.

Hobe, S., Prytulla, S., K•uhlbrandt, W., and Paulsen, H. (1994). Trimerization and crystallization of reconstituted light-harvesting chlorophyll *a/b* complex. EMBO J., 13(15):3423-3429.

Hochuli, E., Bannwarth, W., Dobeli, H., Gentz, R., Stuber, D., (1988) Genetic approach to facilitate purification of recombinant proteins with a novel metal chelate adsorbent. Bio-Technology, 6:1321-1325.

Hoober J.K., Eggink L.L. (2001) A potential role of chlorophylls b and c in assembly of light-harvesting complexes. FEBS Lett. 489(1):1-3.

Horn, R. (2004a). Early steps in the assembly of light-harvesting chlorophyll *a/b* complex: time resolved uorescence measurements. J. Biol. Chem. 279(43):44400-44406.

Horn, R. (2004b). Zeitaufgel•oste Messung der Faltung und Pigmentbindung des Lichtsammlerproteins LHCIIb anhand verschiedener spektroskopischer Monitore: Dissertation am Johannes Gutenberg Universit ät Mainz.

Horn, R., Grundmann, G., and Paulsen, H. (2007). Consecutive binding of chlorophylls a and b during the assembly in vitro of light-harvesting chlorophyll-a/b protein (lhciib). J. Mol. Biol. 366(3):1045-1054.

Horn, R. and Paulsen, H. (2002). Folding in vitro of light-harvesting chlorophyll a/b protein is coupled with pigment binding. J. Mol. Biol. 318(2):547-556.

Horton P., Ruban A.V., Rees D., Pascal A. A., Noctor G., Young A. J. (1991) Control of the light-harvesting function of chloroplast membranes by aggregation of the LHCII chlorophyll-protein complex. FEBS Lett. 292:1-4.

Horton P, Wentworth M., Ruban A.V. (2005) Control of the light harvesting function of chloroplast membranes: the LHCII-aggregation model for non-photochemical quenching. FEBS Lett. 579:4201-4206.

Jahns P., Holzwarth A. R. (2012) The role of the xanthophyll cycle and of lutein in photoprotection of photosystem II. Biochim.Biophys Acta. 1817(1):182-193.

Jansson, S. (1994) The light-harvesting chlorophyll a/b-binding proteins. Biochim.Biophys Acta, 1184:1-19.

Jansson, S. (1999) A guide to the Lhc genes and their relatives in Arabidopsis. Trends in Plant Science, 4:236-240.

Jansson S, Pichersky E, Bassi R, Green BR, Ikeuchi M, Melis A, Simpson DJ, Spangfort M, Staehelin LA, Thornber JP (1992) A nomenclature for the genes encoding the chlorophyll alb-binding proteins of higher plants. Plant Mo1. Biol. Rep. 10:242-253.

Jeschke, G. (2012). Deer distance measurements on proteins. Annu. Rev. Phys. Chem. 63(1):419-446.

Jeschke G., Bender A., Schweikardt T., Panek G., Decker H. and Paulsen H. (2005) Localization of the N-terminal domain in light-harvesting chlorophyll a/b protein by EPR measurements. J Biol. Chem. 280:18623-18630.

Jeschke, G., Panek, G., Godt, A., Bender, A., and Paulsen, H. (2004). Data analysis procedures for pulse eldor measurements of broad distance distributions. Appl. Magn. Reson., 26(1-2):223-244.

Jeschke G. and Polyhach Y. (2007). Distance measurements on spin-labelled biomacromolecules by pulsed electron paramagnetic resonance. Phys. Chem. Chem. Phys. 9(16):1895.

Kalituho L., Rech J., Jahns P. (2007) The role of specific xanthophylls in light utilization. Planta. 225:423-439.

Kelly S. M., Jess T. J., Price N. C. (2005) How to study proteins by circular dichroism. Biochim.Biophys Acta. 1751:119 – 139.

Kessler, F., and Schnell, D. (2009) Chloroplast biogenesis: diversity and regulation of the protein import apparatus. Curr. Opin. Cell Biol. 21:494-500.

Kim S., Sandusky P., Bowlby N. R., Aebersold R., Green B. R., Vlahakis S., Yocum C. F., Pichersky E. (1992) Characterization of a spinach psbS cDNA encoding the 22 kDa protein of photosystem II. FEBS Lett. 314:67-71.

Kleima FJ, Gradinaru CC, Calkoen F, van Stokkum IHM, van Grondelle R, van Amerongen H. (1997) Energy transfer in LHC II monomers at 77K studied by subpicosecond transient absorption spectroscopy. Biochemistry 36:15262−15268

Kleima F.J., Hobe S, Calkoen F, Urbanus M.L., Peterman E. J. G., van Grondelle R., Paulsen H., and van Amerongen H. (1999) Decreasing the Chlorophyll a/b Ratio in Reconstituted LHCII: Structural and Functional Consequences. Biochemistry. 38:6587-6596.

Kleima F.J., Hobe S, Calkoen F, Urbanus M.L., Peterman E. J. G., van Grondelle R., Paulsen H., and van Amerongen H. (1998) Spectroscopic Characterization of Reconstituted LHCII Which Contains Mainly CHL B and Xanthophylls. Photosynthesis: Mechanisms and Effects. 259-264

Kosemund, K. (1999) Die Biogenese von Chlorophyll-*a*/*b*-bindenden Lichtsammelkomplexen: Topographie des Apoproteins bei der Thylakoidinsertion. Dissertation am Fachbereich Biologie, Johannes Gutenberg-Universität Mainz.

Kouřil R, Dekker JP, Boekema EJ. (2012) Supramolecular organization of photosystem II in green plants.Biochim Biophys Acta. 1817(1):2-12.

Kühlbrandt, W., Wang, D. N., and Fujiyoshi, Y. (1994). Atomic model of plant light-harvesting complex by electron crystallography. Nature, 367(6464):614-621.

Kung, S.D., Thornber, J.P., Wildman, S.G. (1972) Nuclear DNA codes for the photosystem II chlorophyll-protein of chloroplast membranes. FEBS Lett. 24:185-188.

Linnanto J., Martiskainen J., Lehtovuori V., Ihalainen J., Kananavicius R., Barbato R., Korppi-Tommola J. (2006) Excitation energy transfer in the LHC-II trimer: a model based on the new 2.72 Å structure. Photosynth Res. 87(3):267-279.

Liu, Z., Yan, H., Kuang, T., Zhuang, J., Bui, L., Chang, W. (2004) Crystal structure of spinach major light-harvesting complex at 2.72 Å resolution. Nature. 428:287-292.

MatsuoK., Yonehara R. and Gekko K. (2005) Improved Estimation of the Secondary Structures of Proteins by Vacuum-Ultraviolet Circular Dichroism Spectroscopy. J. Biochem. 138:79-88.

Meyer G., Kloppstech K. (1984) A rapidly light-induced chloroplast protein with a high turnover coded for by pea nuclear DNA, Eur. J. Biochem. 138:201-207.

Minagawa J. Takahashi Y. (2004) Structure, function and assembly of Photosystem II and its light-harvesting proteins. Photosynth. Res. 82:241-263.

Minagawa J. (2011) State transitions--the molecular remodeling of photosynthetic supercomplexes that controls energy flow in the chloroplast. Biochim Biophys Acta. 1807(8):897-905.

Mohanty P, Vani B, Prakash S (2002) Elevated temperature treatment induced alteration in thylakoid membrane organization and energy distribution between the two photosystems in *Pisum sativum* Z Naturforsch 57:836-842.

Montaville P., Jamin N. (2010) Determination of Membrane Protein Structures Using Solution and Solid-State NMR. Membrane Protein Structure Determination. Methods in Molecular Biology. 654:261-282.

Moore, M., Goforth, R. L., Mori, H. Henry, R. (2003). Functional interaction of chloroplast SRP/FtsY with the ALB3 translocase in thylakoids: substrate not required. J. Cell Biol. 162, 1245-1254.

Mozzo M., Dall'Osto L., Hienerwadel R., Bassi R., Croce R. (2008) Photoprotection in the antenna complexes of photosystem II — role of individual xanthophylls in chlorophyll triplet quenching. J Biol Chem. 283:6184-6192.

Müller P., Li X.P., and Niyogi K. K. (2001) Non-Photochemical Quenching. A Response to Excess Light Energy. Plant Physiol 125:1558-1566.

Murray D.L., and Kohorn B.D., (1991) Chloroplasts of Arabidopsis thaliana homozygous for the ch-1 locus lack chlorophyll b, lack stable LHCPII and have stacked thylakoids. Plant Mol. Biol. 16(1):71-79.

Nellaepalli S., Mekala N.R., Zsiros O., Mohanty P., Subramanyam R. (2011) Moderate heat stress induces state transitions in Arabidopsis thaliana. Biochim Biophys Acta. 1807(9):1177-84

Niyogi K.K., Grossman A.R. and Björkman O. (1998) Arabidopsis Mutants Define a Central Role for the Xanthophyll Cycle in the Regulation of Photosynthetic Energy Conversion. The Plant Cell. 10(7):1121-1134.

Novoderezhkin V., Palacios M.A., van Amerongen H., van Grondelle R. (2005). Excitation dynamics in the LHCII complex of higher plants: modeling based on the 2.72 Angstrom crystal structure. J Phys Chem. B. 109(20):10493-10504.

Nußberger, S., Dörr, K., Wang, D. N., Kühlbrandt, W. (1993) Lipid-protein interactions in crystals of plant light-harvesting complex. J. Mol. Biol. 234:347-356.

Paulsen, H., Finkenzeller, B., and K•uhlein, N. (1993). Pigments induce folding of light-harvesting chlorophyll a/b-binding protein. Eur. J. Biol. Chem., 215(3):809-816.

Paulsen, H. and Hobe, S. (1992). Pigment-binding properties of mutant light-harvesting chlorophyll-a/b-binding protein. Eur. J. Biol. Chem. 205(1):71-76.

Paulsen, H., Rümler, U., and Rüdiger, W. (1990) Reconstitution of pigment-containing complexes from light-harvesting chlorophyll a/b-binding protein overexpressed in E. coli. Planta 181:204-211.

Peter G.F., Thornber J.P. (1991) Biochemical composition and organization of higher plant photosystem II light-harvesting pigment-proteins. J Biol Chem. 266(25):16745-16754.

Peterman E.J.G., Dukker F.M., van Grondelle R., van Amerongen H. (1995) Chlorophyll a and carotenoid triplet states in light-harvesting complex II of higher plants. Biophys J., 69:2670-2678.

Peterman E.J.G., Gradinaru C.C., Calkoen F., Borst J.C., van Grondelle R., van Amerongen H. (1997) Xanthophylls in light-harvesting complex II of higher plants: light harvesting and triplet quenching. Biochem. 36:12208-12215.

Plumley, F. G., Schmidt, G. W. (1987) Reconstitution of chlorophyll a/b light-harvesting complexes: Xanthophyll-dependent assembly and energy transfer. Proc. Natl. Acad. Sci. USA, 84:146-150.

Pool M.R. (2005) Signal recognition particles in chloroplasts, bacteria, yeast and mammals. Mol. Membr. Biol., 22:3-15.

Raghavendra, A. S. (1998).Photosynthesis: A comprehensive treatise. Cambridge, U.K: Cambridge University Press.

Reed J, Reed TA. (1997) A set of constructed type spectra for the practical estimation of peptide secondary structure from circular dichroism. Anal. Biochem. 254:36-40.

Reinsberg, D., Booth, P. J., Jegerschöld, C., Khoo, B. J., Paulsen, H. (2000). Folding, assembly, and stability of the major light-harvesting complex of higher plants, LHCII, in the presence of native lipids. Biochemistry, 39:14305-14313.

Reinsberg, D., Ottmann, K., Booth, P. J. Paulsen, H. (2001). Effects of chlorophyll a, chlorophyll b, and xanthophylls on the in vitro assembly kinetics of the major light-harvesting chlorophyll a/b complex, LHCIIb. J. Mol. Biol. 308:59-67.

Remelli R, Varotto C, Sandon áD, Croce R, Bassi R. (1999) Chlorophyll binding to monomeric light-harvesting complex: a mutational analysis of chromophore-binding residues. J Biol Chem. 274:33510-33521.

Rochaix J.D.(2011) Reprint of: Regulation of photosynthetic electron transport. Biochim Biophys Acta. 1807(8):878-886.

Ruban A.V., Lee P.J., Wentworth M., Young, A.J., Horton P. (1999). Determination of the stoichiometry and strength of binding of xanthophylls to the photosystem II light-harvesting complexes. J Biol Chem. 274:10458-10465.

Rüdiger W. (1987) Chlorophyll Synthetase and its Implication for Regulation of Chlorophyll Biosynthesis. Progress in Photosynthesis Research. 4:461-467.

Sá-Pereira P., Duarte J., Costa-Ferreira M. (2000) Electroelution as a simple and fast protein purification method: isolation of an extracellular xylanase from Bacillus sp. CCMI 966. Enzyme Microb Technol. 27(1-2):95-99.

Schmidt H.H., Genschel J., Haas R., Manns M.P. (1997) Preparative electrophoresis: an improved method for the isolation of human recombinant apolipoprotein A-I. Biotechniques 23:778-779

Scholes, G. D. Fleming, G. R. (2005).Energy transfer in photosynthesis. Adv. Chem. Phys. 132:57-129.

Scholes G.D.,Fleming G.R.,Olaya-Castro A.,van Grondelle R. (2011) Lessons from nature about solar light harvesting. Nat Chem. 3(10):763-774.

Schünemann D. (2004) Structure and function of the chloroplast signal recognition particle. Curr Genet. 44: 295-304.

Seddon A.M., Curnow P., Booth P.J. (2004) Membrane proteins, lipids and detergents: not just a soap opera. Biochim. Biophys. Acta. 1666 (1-2), 3:105-117.

Soll J, Schultz G., Rudiger W., Benz J. (1983) Hydrogenation of geranylgeraniol: two pathways exits in spinach chloroplasts. Plant Physiol. 71:849-854.

Soll, J., and Schleiff, E. (2004) Protein import into chloroplasts. Nat. Rev. Mol. Cell Biol. 5:198-208.

Sreerama, N. & Woody, R. W. (1993). A self-consistent method for the analysis of protein secondary structure from circular dichroism. Anal. Biochem. 209:32-44.

Sreerama N. and Woody R. W. (2004) Computation and analysis of protein circular dichroism spectra. Methods Enzymol. 383:318-351.

Sreerama N. and Woody R. W. (2000) Estimation of Protein Secondary Structure from Circular Dichroism Spectra: Comparison of CONTIN, SELCON, and CDSSTR Methods with an Expanded Reference Set. Anal. Biochem. 287:252-260.

Standfuss, J., Kühlbrandt, W. (2004) The three isoforms of the light-harvesting complex II. Spectroscopic features, trimer formation, and functional roles. J. Biol. Chem. 279(35):36884-36891.

Standfuss, R., van Scheltinga, A. C. T., Lamborghini, M., Kühlbrandt, W. (2005). Mechanisms of photoprotection and non-photochemical quenching in pea light-harvesting complex at 2.5 Å resolution. EMBO J. 24:919-928.

Stengel, K. F., Holdermann, I., Cain, P., Robinson, C., Wild, K., and Sinning, I. (2008) Structural basis for specific substrate recognition by the chloroplast signal recognition particle protein cpSRP43. Science 321:253-256.

Suzuki H., Terada T. (1988) Removal of dodecyl sulfate from protein solution. Anal Biochem. 172(1):259-263.

Takaichi S and Mimuro M (1998) Distribution and geometric isomerism of neoxanthin in oxygenic phototrophs: 9'- cis, a sole molecular form. Plant Cell Physiol. 39(9):968-977.

Tanaka, A., Ito, H., Tanaka, R., Tanaka, N. K., Yoshida, K. Okada, K. (1998). Chlorophyll a oxygenase (CAO) is involved in chlorophyll b formation from chlorophyll a. Proc. Natl Acad. Sci. USA. 95:12719-12723.

Tanaka, R. Tanaka, A. (2005). Effects of chlorophyllide a oxygenase overexpression on light acclimation in Arabidopsis thaliana. Photosynth. Res. 85:327-340.

Tanaka R., Tanaka A. (2007) .Tetrapyrrole Biosynthesis in Higher Plants. Annu. Rev. Plant Biol. 58:321-346.

Tanaka Y., Tanaka A. and Tsuji H. (1993) Effects of 5-Aminolevulinic Acid on the Accumulation of Chlorophyll b and Apoproteins of the Light-Harvesting Chlorophyll *a/b*-Protein Complex of Photosystem II. Plant Cell Physiol. 34(3):465-472.

Thornber J.P. (1995) Thirty years of fun with antenna pigment-proteins and photochemical reaction centers: A tribute to the people who have influenced my career. Photosynth Res.. 44(1-2):3-22.

Trémolières A., Dubacq J. P., Ambard-Bretteville F., RÈmy R. (1981) Lipid composition of chlorophyl-protein complexes: specific enrichment in trans-hexadecenoic acid of an oligomeric form of light-harvesting chlorophyll *a/b* protein, FEBS Lett. 130:27-31.

Trinkunas G, Connelly JP, Müller MG, Valkunas L, Holzwarth AR. (1997) Model for the excitation dynamics in the light-harvesting complex II from higher plants. J Phys Chem B, 101:7313−7320

Tu C.J., Peterson E.C., Henry R., Hoffman N.E. (2000) The L18 domain of light-harvesting chlorophyll proteins binds to chloroplast signal recognition particle 43. J Biol Chem. 275(18):13187-13190.

Ueda E.K.M., Gout P.W., Morganti L. (2003) Current and prospective applications of metal ion-protein binding. Journal of Chromatography A. 988(1):1-23.

Uehara K., Mimuro M., Fujita Y. and Tanaka M. (1988) Spectral analysis of Chlorophyll *a* aggregates in the presence of water-soluble macromolecules. Photochem Photobiol. 48(6): 725-732.

Visser HM, Kleima FJ, van Stokkum IHM, van Grondelle R, van Amerongen H. (1996) Probing the many energy-transfer processes in the photosynthetic lightharvesting complex II at 77 K using energy-selective sub-picosecond transient absorption spectroscopy. Chem Phys. 210: 297−312

Vladkova R. (2000) Chlorophyll a Self-assembly in Polar Solvent-Water Mixtures. Photochem Photobiol., 71(1):71-83.

Volkov, A., Dockter, C., Bund, T., Paulsen, H., and Jeschke, G. (2009). Pulsed epr determination of water accessibility to spin-labeled amino acid residues in lhciib. Biophys. J., 96(3):1124-1141.

Wedel N., Klein R., Ljungberg U., Andersson B., Herrmann R. G. (1992) The single-copy gene psbS codes for a phylogenetically intriguing 22 kDa polypeptide of photosystem II, FEBS Lett. 314:61-66.

Werwie, M., Xu, X., Haase, M., Basche, T., and Paulsen, H. (2012). Bio serves nano: Biological light-harvesting complex as energy donor for semiconductor quantum dots. Langmuir, 28(13):5810-5818.

Wientjes E., Drop B, Kouřil R, Boekema EJ, Croce R. (2013) During state 1 to state 2 transition in Arabidopsis thaliana, the photosystem II supercomplex gets phosphorylated but does not disassemble. J Biol. Chem. 288(46):32821-32826.

Whitmarsh J., Govindjee (1999) "The Photosynthetic Process". In "Concepts in Photobiology: Photosynthesis and Photomorphogenesis", Narosa Publishers, New Delhi and Kluwer Academic,Dordrecht.

Whitmore L, Wallace B.A. (2007) Protein secondary structure analyses from circular dichroism spectroscopy: Methods and reference databases. Biopolymers. 89(5):392-400.

Yamamoto H.Y. (1985) Xanthophyll cycles. Methods Enzymol. 110:303-312.

Yamamoto H.Y., Bugos R.C., Hieber A.D. (1999) Biochemistry and Molecular Biology of the Xanthophyll Cycle. The Photochemistry of Carotenoids Advances in Photosynthesis and Respiration. 8:293-303.

Yamamoto H.Y., Nakayama TOM, Chichester CO. (1962) Studies on the light and dark interconversions of leaf xanthophylls. Arch Biochem Biophys 97:168-173.

Yang C.H., Horn R. Paulsen H. (2003) The Light-Harvesting Chlorophyll *a*/*b* Complex Can Be Reconstituted *in Vitro* from Its Completely Unfolded Apoprotein. Biochemistry. 42:4527-4533.

Yang, C., Kosemund K., Cornet C., and Paulsen H. (1999) Exchange of Pigment-Binding Amino Acids in Light-Harvesting Chlorophyll a/b Protein. Biochemistry. 38:16205-16213.

Yang D., Paulsen H., Andersson B. (2000) The N-terminal domain of the light-harvesting chlorophyll a/b-binding protein complex (LHCII) is essential for its acclimative proteolysis. FEBS Lett. 466(2-3):385-388

Young C. L., Britton Z. T.,. Robinson A. S. (2012) Recombinant protein expression and purification: A comprehensive review of affinity tags and microbial applications. Biotechnology Journal. 7(5):620-634.

Zhang Y., Liu C., Liu S., Shen Y., Kuang T. Yang C. (2008) Structural stability and properties of three isoforms of the major light-harvesting chlorophyll a/b complexes of photosystem II. Biochim. Biophys. Acta 1777:479-487.